

NAM

Numerical evaluation of the seismic response of the main typologies of non-masonry (non-URM) buildings that are found within the Groningen region

Report on structural modelling of non-URM buildings – v2 risk model update

Helen Crowley, Federica Bianchi, Daniele Cicola, Roberto Nascimbene

Eucentre

(European Centre for Training and Research in Earthquake Engineering)

Date October 2015

Editors Jan van Elk & Dirk Doornhof

General Introduction

Much work has been done to understand the seismic response of Unreinforced Masonry (URM) buildings. This report describes the modelling of selected non-URM index buildings. The seismic response of a selection of cast-in-place reinforced concrete buildings, pre-cast concrete buildings, timber frame buildings and steel frame buildings is modelled.

The models have been used for the preparation of the fragility curves (Version 2) for non-URM buildings (Ref. 1). These fragility curves have been used for the Risk Assessment of November 2015 (Ref. 2).

References

1. Development of v2 fragility and consequence functions for the Groningen Field, H. Crowley, R. Pinho, B. Polidoro, P. Stafford, October 2015.
2. Hazard and Risk Assessment for Induced Seismicity in Groningen Interim Update November 2015, Nederlandse Aardolie Maatschappij BV (Jan van Elk and Dirk Doornhof, eds), 1st November 2015.



NAM

Title	Numerical evaluation of the seismic response of the main typologies of non-masonry (non-URM) buildings that are found within the Groningen region Report on structural modelling of non-URM buildings – v2 risk model update	Date	October 2015
		Initiator	NAM
Autor(s)	Helen Crowley, Federica Bianchi, Daniele Cicola, Roberto Nascimbene	Editors	Jan van Elk and Dirk Doornhof
Organisation	Eucentre, Pavia (European Centre for Training and Research in Earthquake Engineering)	Organisation	NAM
Place in the Study and Data Acquisition Plan	<p><u>Study Theme:</u> Building Fragility</p> <p><u>Comment:</u> Much work has been done to understand the seismic response of Unreinforced Masonry (URM) buildings. This report describes the modelling of selected non-URM index buildings. The seismic response of a selection of cast-in-place reinforced concrete buildings, pre-cast concrete buildings, timber frame buildings and steel frame buildings is modelled. The models have been used for the preparation of the fragility curves (Version 2) for non-URM buildings (Ref. 1). These fragility curves have been used for the Risk Assessment of November 2015 (Ref. 2).</p>		
Directly linked research	(1) Building material properties (2) Development of Fragility Curves for building Typologies (3) Risk Assessment		
Used data	Building Material properties		
Associated organisation	NAM		
Assurance	Eucentre		

D2

DELIVERABLE

Project Information

Project Title: **Numerical evaluation of the seismic response of the main typologies of non-masonry (non-URM) buildings that are found within the Groningen region**

Project Start: 12th May 2014

Duration: 24 months

Technical Point of Contact: Rui Pinho
rui.pinho@mosayk.it

Business Point of Contact: Roberto Nascimbene
roberto.nascimbene@mosayk.it

Deliverable Information

Deliverable Title: **Report on structural modelling of non-URM buildings – v2 risk model update**

Data of Issue: 22nd October 2015

Editor(s): Helen Crowley, Federica Bianchi, Daniele Cicola, Roberto Nascimbene

Reviewer: Rui Pinho

REVISION: **v2 Risk Model Update**

Table of Contents

Introduction	5
1 Cast-in-Place RC Residential Terraced Buildings (REST-RC-A)	7
1.1 General description and structural configuration.....	7
1.2 Modelling assumptions.....	8
1.3 Numerical analyses and results	9
2 Precast RC Residential Terraced Buildings (REST-RC-B).....	11
2.1 General description and structural configuration for index building #1	11
2.2 Modelling assumptions for index building #1	13
2.3 Numerical analyses and results for index building #1	16
2.4 General description and structural configuration for index building #2	19
2.5 Modelling assumptions for index building #2	21
2.6 Numerical analyses and results for index building #2	24
2.7 Summary of the Test and FE numerical results on Precast Panels	26
2.8 Calibrated index building.....	28
3 Cast-in-Place RC Residential Apartment Buildings with ≤ 4 storeys (RESA-RC-A-L4S)....	32
3.1 General description and structural configuration.....	32
3.2 Modelling assumptions.....	34
3.3 Numerical analyses and results	35
4 Timber Frame Residential Detached Buildings (RESD-W-A)	37
4.1 General description and structural configuration.....	37
4.2 Modelling assumptions.....	39
4.3 Numerical analyses and results	40
5 Steel Frame Industrial Buildings (AGRI/INDU/COML-S-B/A)	43
5.1 General description and structural configuration.....	43
5.2 Modelling assumptions.....	45
5.3 Numerical analyses and results	47
6 Timber Agricultural Barns with URM walls (AGRI/INDU/COML-W-A)	51
6.1 General description and structural configuration.....	51
6.2 Modelling assumptions.....	54
6.3 Numerical analyses and results	55
7 Glulam Portal Frame Buildings with Steel Stability Bracing (AGRI/INDU/COML-W-B1)	60
7.1 General description and structural configuration.....	60

7.2	Modelling assumptions.....	61
7.3	Numerical analyses and results	62
8	Glulam Portal Frame Buildings with URM Stability Walls (AGRI/INDU/COML-W-B2) ...	64
8.1	General description and structural configuration.....	64
8.2	Modelling assumptions.....	64
8.3	Numerical analyses and results	65
9	Precast RC Portal Frame Industrial Buildings (AGRI/INDU/COML-RC-B1)	67
9.1	General description and structural configuration.....	67
9.2	Modelling assumptions.....	68
9.3	Numerical analyses and results	69
10	Cast-in-Place RC Portal Frame Industrial Buildings (AGRI/INDU/COML-RC-A)	71
10.1	General description and structural configuration.....	71
10.2	Modelling assumptions.....	71
10.3	Numerical analyses and results	72
11	Steel Moment Frame Commercial Buildings (COMO-S-B-L4S)	74
11.1	General description and structural configuration.....	74
11.2	Modelling assumptions.....	75
11.3	Numerical analyses and results	77
	Conclusions	80
	References.....	81

Introduction

In the Groningen gas field, according to the application of the v1 inference rules to the building and population exposure model¹, 12% of the building stock is comprised of non-masonry (non-URM) buildings (that are constructed from either reinforced concrete, steel or timber), where a third of the population live/work in these structures. This implies that the structural modelling of these structures, in addition to those constructed in masonry, is necessary in order to obtain a complete picture of the level of seismic risk to which the population in the Groningen gas field is exposed.

This report is an updated version of Mosayk deliverable D2, and has been produced to provide an update summary of the final results of the non-URM structural modelling activities that have been directly used in the v2 fragility functions (Crowley et al., 2015), which in turn have been used in the v2 risk assessment of the Groningen field. The v2 fragility functions make use of capacity curves (i.e. curves representing the lateral capacity of single degree of freedom (DOF) systems), which have been obtained by transformation of the pushover curves presented herein.

In the v2 exposure model, 31 non-URM building typologies have been identified and an attempt has been made to obtain and cover as many of these typologies as possible within the timeframe available. Each typology has been represented with one or more index buildings, which are specific examples of real (or realistic) buildings. The structural details (i.e. structural drawings, connection details, material properties) for 18 real buildings from the Groningen region have been provided by Arup² and the models for 7 of these real Groningen buildings have been used for the v2 fragility functions, and are described herein. In addition, 5 models have been developed based on information regarding typical construction practices provided by the local Groningen engineers. A summary of all the non-URM building models that are described in this report is provided in the table below.

Summary of v2 non-URM building models

Chapter	Building Typology	Description	Comments
1	REST-RC-A	Cast-in-Place RC Residential Terraced Buildings	Based on typical construction practice
2	REST-RC-B	Precast RC Residential Terraced Buildings	Real building in Groningen, 4-units
			Real building in Groningen, 7-units
3	RESA-RC-A-L4S	Cast-in-Place RC Residential Apartment Buildings with <= 4-storeys	Real building in Groningen, 4-storeys
4	RESD-W-A	Timber Frame Residential Detached Buildings	Real building in Groningen
5	AGRI/INDU/COML-S-B (& A)	Steel frame industrial building with light roof (bracing in one direction (longitudinal), moment frame in the other direction (transverse))	Real building in Groningen

¹ Internal NAM report “Exposure model v1 – updated typologies and inference rules”

² Index buildings and info from: Gerben de Vries, Jerome Pauwels, Rob Bakker, Hinke Wijbenga, Beatriz Zapico Blanco, Johan Pool, Martin Schaaphok, Han Krijgsman

Chapter	Building Typology	Description	Comments
6	AGRI/INDU/ COML-W-A	Agricultural barn with wooden trussed roof and URM façade walls	Real building in Groningen
7	AGRI/INDU/ COML-W-B1	Glulam portal frame with steel stability bracing in other direction	Based on typical construction practice
8	AGRI/INDU/ COML-W-B2	Glulam portal frame with URM infill walls for stability in the other direction	Based on typical construction practice
9	AGRI/INDU/ COML-RC-A	Cast-in-place RC industrial portal frame with light steel roof	Based on typical construction practice
10	AGRI/INDU/ COML-RC-B1	Precast RC portal frames in parallel with roof beams connected to columns with steel dowels, light steel roof	Based on typical construction practice
11	COMO-S-B- L4S	Steel moment frame, less than or equal to 4 storeys, with concrete slab floor/roof	Real building in Groningen

Nonlinear static analysis of each the structural models described in the table above has been carried out in order to directly provide input for the capacity curves for the fragility modelling (Crowley et al., 2015), as described in Chapters 1 to 11 of this report.

As stated in the introduction of the Mosayk deliverable (D1), the software which has been adopted for the majority of the non-URM modelling is SeismoStruct (Seismosoft, 2015), an award-winning, extensively quality-checked and internationally validated Finite Elements program able to accurately predict the large displacement behaviour of space frames under static or dynamic loading (e.g. earthquake strong motion), taking into account both geometric nonlinearities and material inelasticity. Another Finite Elements code, MidasFEA (MIDAS, 2010), has been employed for the detailed shell elements modelling, and the wall building structures have been modelled with Extreme Loading for Structures (ASI, 2010), a commercial structural-analysis software based on the applied element method (AEM) (Meguro and Tagel-Din, 2000; Tagel-Din and Meguro, 2000a and 2000b). This software was judged to provide a more reliable estimation of the shear capacity of these structures.

1 Cast-in-Place RC Residential Terraced Buildings (REST-RC-A)

1.1 General description and structural configuration

This building typology comprises residential terraced, reinforced concrete (RC), cast-in-place (CIP) *tunnel form* (“tunnelgietsbouw” in Dutch) buildings (within which unreinforced walls may also be present). An index building for this typology has not yet been made available, but it has been possible to construct a model based on the input provided by local engineers.

Figure 1.1 shows the tunnel shaped formwork that are used to construct this typology. The walls and floor are cast at the same time and stability is taken care of by means of the portal frame.

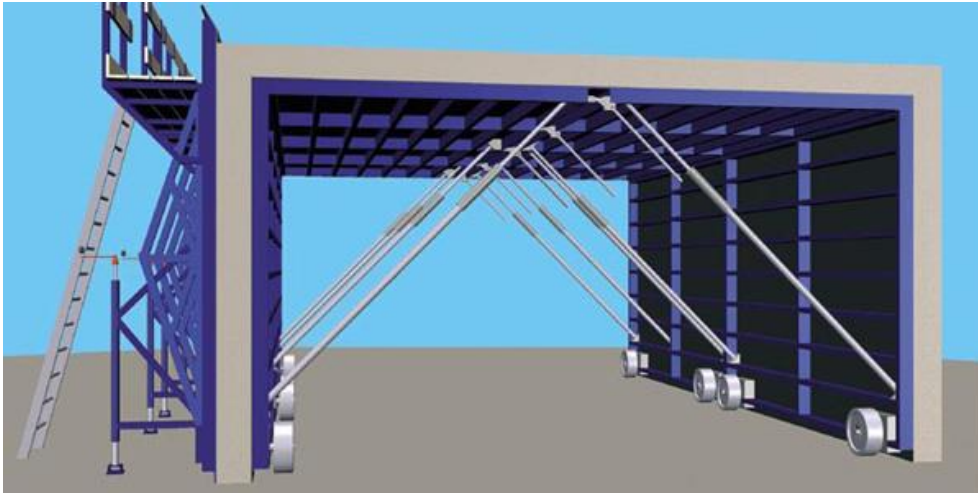


Figure 1.1: “Tunnelgietsbouw” construction technique

According to local engineers, the following construction details may be assumed:

- Typical dimensions: party walls 0.25 m, floor 0.21-0.23 m, inner leaf gable wall 0.17 m.
- Front and back façade are cavity walls; timber, precast concrete or masonry plus outer leaf masonry. These should not affect the structural performance as they are not infill to the reinforced concrete frame. However, the out-of-plane failure of the outer leaf masonry façade walls is of relevance and will need to be considered in the risk assessment using the model described in §1.4.
- The most common concrete grade used for this structure is C25/35, but higher grades (e.g. C35/45) may also be used.
- The reinforcing steel is formed by a wire mesh, with grade FeB500 steel. The reinforcing ratios used in these structures are similar to those of precast terraced buildings (i.e. around 0.2-0.4% for the party walls).
- Figure 1.2 presents the variation in geometry of terraced buildings in the Netherlands, which can be used to define the wall depth and spacing of the walls.

A 2-unit index building has been produced in Extreme Loading for Structures (ASI, 2010) based on the above input, with a standard storey height of 2.9 m and the geometrical details summarised in Table 1.1. The modelling assumptions for this index building are further described in the next section.

Table 1.1: RC cast-in-place terraced building with 2 units – Geometrical details of structural elements

Storey	External wall	Internal Wall	Slab
2	8 m x 0.17 m (54 ϕ 12)	8 m x 0.25 m (54 ϕ 12)	8 m x 6.25 m x 0.22 m (54 ϕ 12)
1	8 m x 0.17 m (54 ϕ 12)	8 m x 0.25 m (54 ϕ 12)	8 m x 6.25 m x 0.22 m (54 ϕ 12)

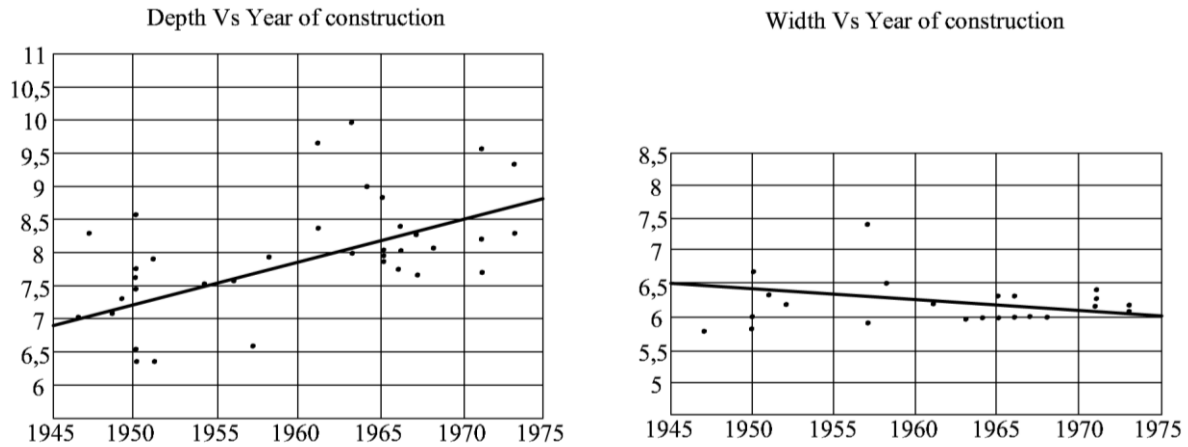


Figure 1.2: Variation of wall depth (left) and spacing (right) of terraced housing in the Netherlands (adapted from figure supplied by Arup)

1.2 Modelling assumptions

The structure has been modelled with Extreme Loading for Structures, ELS (ASI, 2010), introduced previously. The default material models were used.

Materials

The mean material properties for concrete and steel are listed below:

- Concrete C25/35: $f_c = 33$ MPa; $f_t = 3.3$ MPa
- Steel FeB500: $f_y = 575$ MPa

Loads

The superimposed dead and live loads have been applied to the structure by increasing the mass of each floor. The upper floor also includes the weight of the roof. Loads in addition to the self-weight are taken as 100% permanent load plus 30% live load, based on the values given in Table 1.2.

Table 1.2: RC cast-in-place terraced building – assumed loads (in addition to self-weight)

Type of load	Typical level [kN/m ²]	Roof [kN/m ²]
Permanent Load	3.0	2.0
Live Load	2.0	-

Other modelling assumptions

The building is assumed to be fixed at the base.

A screenshot of the 2 units RC cast-in-place terraced model is presented in the following figure.

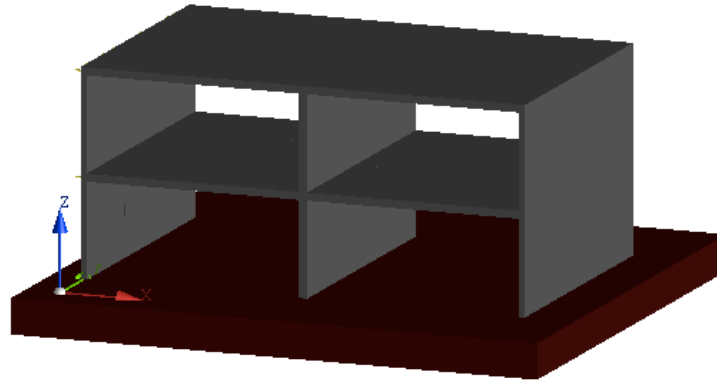


Figure 1.3: Screenshot of the ELS model of the REST-RC-A index building

1.3 Numerical analyses and results

Eigenvalue analysis

An eigenvalue analysis has been undertaken as an initial check of the model. The first mode period was found to be 0.37 s in the longitudinal direction and 0.046 s in the transverse direction.

Pushover analyses

Given the simplicity of the structure, conventional pushover analysis using a triangular loading profile has been undertaken in each direction. The pushover curve in the longitudinal direction is provided in Figure 1.4.

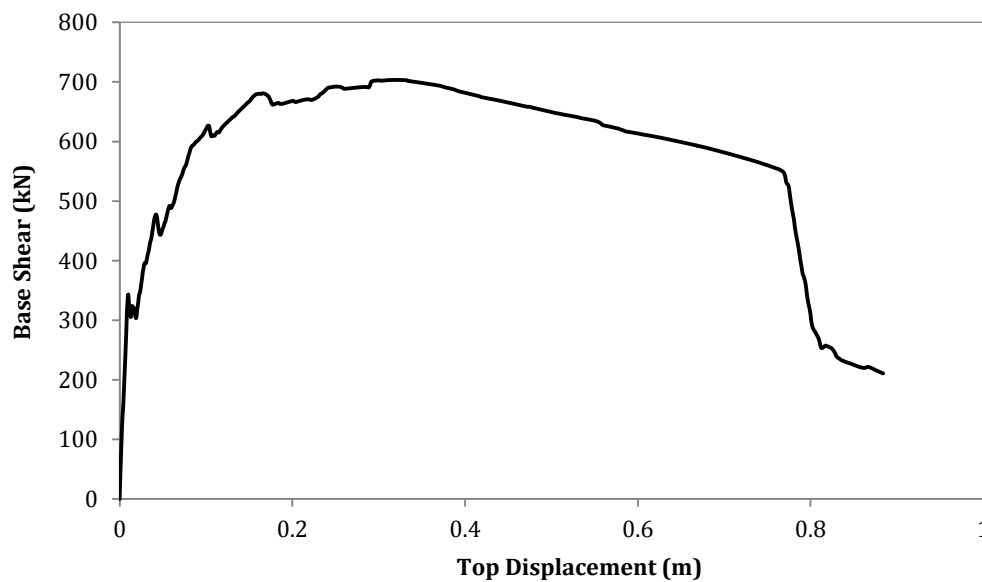


Figure 1.4: Pushover curve in the longitudinal direction

The pushover curve in the transverse direction is provided in Figure 1.5.

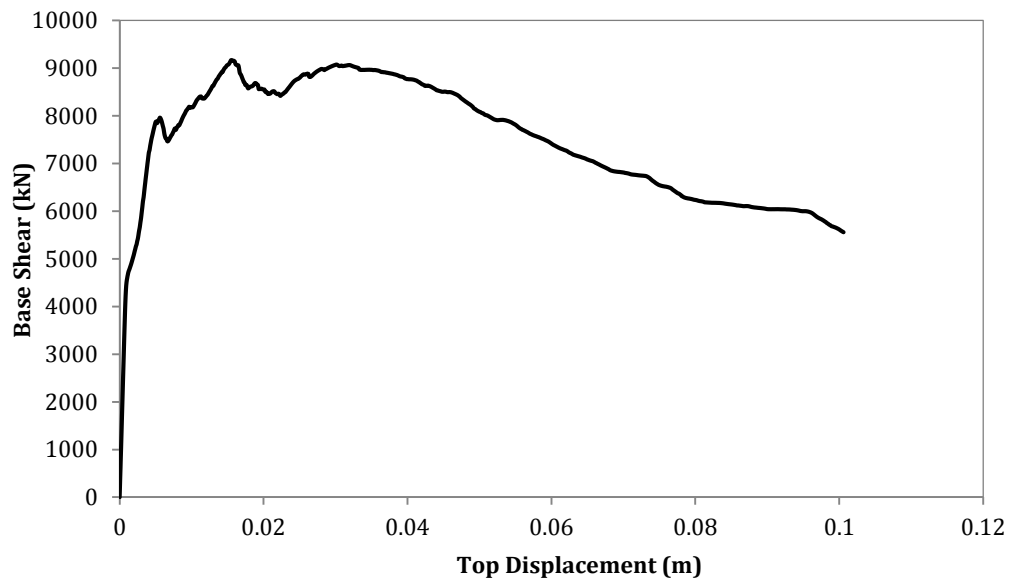


Figure 1.5: Pushover curve in the transverse direction

A SeismoStruct (Seismosoft, 2015) model was also developed for this structure (see Version 1 of the present report), and shear failure was predicted to occur at much lower displacements, based on Eurocode 8 (CEN, 2005) formulae. The ELS model does not fail in shear until much higher levels of displacement, and given the conservativeness of code equations, it was deemed to provide a more reliable representation of the collapse capacity of these structures. However, the amount of reinforcement (longitudinal and transverse) that has been assumed in the walls and slabs will need to be verified as part of the future developments, to ensure they are not being overestimated.

2 Precast RC Residential Terraced Buildings (REST-RC-B)

For the precast, reinforced concrete (RC), residential terraced building typologies, 2 different index buildings (4- and 7-units) have been analysed. These will be called, respectively, building #1 and building #2 in the following paragraphs.

2.1 General description and structural configuration for index building #1

Index building #1 represents a real 4-unit precast terraced structure located in the village of Loppersum (Figure 2.1).



Figure 2.1: Precast RC residential terraced building with 4 units (Google Street View)

The precast RC terraced building typologies are constructed with precast floors, precast party/gable walls and precast walls in the longitudinal direction. The precast walls are erected first and shored up by steel diagonal members; subsequently, the floor is settled on the walls and supported by steel bars that connect the first with the second-storey wall, through the floor (see Figure 2.2).



Figure 2.2: Precast RC residential terraced building – construction practices for precast panels

According to local engineers, the following construction details may be assumed:

- Typical dimensions: party walls 0.25 m, floor 0.21-0.23 m, inner leaf gable wall 0.12-0.15 m.
- Front and back façade are cavity walls; the additional masonry outer leaf should not affect the structural performance, as it is not infill to the reinforced concrete frame. However, the out-of-plane failure of these façade walls is of relevance and will need to be considered in the risk assessment using the model already described in §1.4.

- The most common concrete grade used for these structures is C35/45.
- The reinforcing steel is formed by a wire mesh, with grade FeB500 steel. The reinforcing ratios used in these structures are similar to those of cast-in-place residential terraced buildings (i.e. around 0.2-0.4% for the party walls).
- The most common precast floors are hollow-core sections.

The building (Figure 2.3) is 27.2 m long and 10 m wide at the ground level with a smaller width of 8.8 m at the upper floor.

A 4-unit index building model has thus been produced based on the available structural drawings and aforementioned assumptions, with a storey height of 2.5 m and the geometrical details summarised in the following tables, i.e. precast walls (longitudinal direction) and precast party/gable walls (transverse direction). All the element sections have been defined as reinforced concrete rectangular sections in the adopted software.

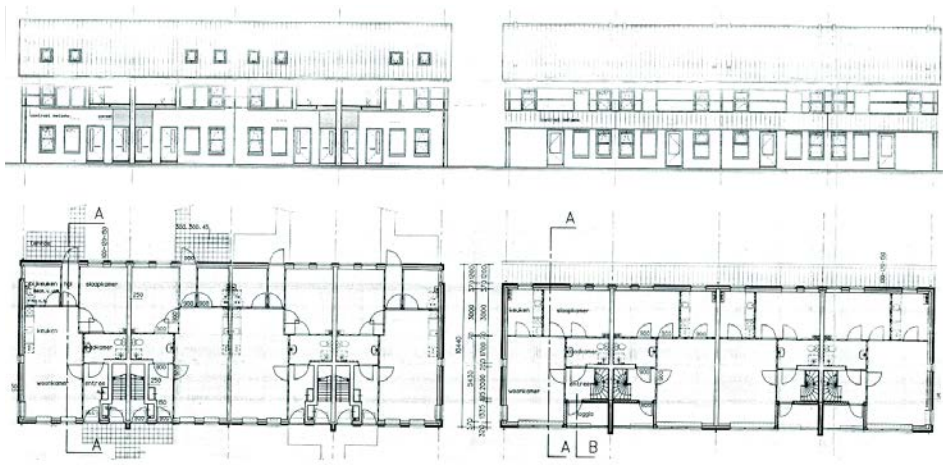


Figure 2.3: Precast RC residential terraced building with 4 units - drawings

Although an irregular internal disposition of structural walls is displayed in the drawings above, the precast wall sections can be divided into external and internal sections, considering the different thicknesses and focusing on the primary parallel transverse walls. A double layer welded reinforcement mesh is used and the number of reinforcement bars summarized in Table 2.1 represents the total amount of bars in the section.

Table 2.1: Precast RC residential terraced building with 4 units – Geometrical details for walls in transverse direction

Storey	External wall	Internal Wall
2	9.7 m x 0.125 m (60 ϕ 12)	9.7 m x 0.25 m (60 ϕ 12)
1	9.7 m x 0.125 m (60 ϕ 12)	9.7 m x 0.25 m (60 ϕ 12)

The longitudinal walls are comprised of eight vertical and three horizontal structural elements, as shown in Figure 2.4 and described in Table 2.2. The elements comprising the central walls of the structure, thus placed in the middle of the longitudinal direction of the terraced house, are also described in Table 2.2. The structure has a 0.05 m solid concrete slab placed on the horizontal hollow-core floor panels. The roof is constructed with a RC slab and the foundation system consists of precast foundation beams, supported on piles. A double layer welded mesh is again used, and the number of reinforcement bars summarized in Table 2.2 represents the total bars in the section.

Table 2.2: Precast RC residential terraced building with 4 units – Geometrical details for walls in longitudinal direction

Storey	Vertical 1	Vertical 2	Vertical 3	Vertical 4	Vertical 5	Vertical 6	Vertical 7	Vertical 8
2	0.9x0.125 (8 ϕ 12)		0.47x0.125 (6 ϕ 12)		0.47x0.125 (6 ϕ 12)	0.755x0.125 (8 ϕ 12)	2.25x0.125 (20 ϕ 12)	0.7x0.125 (8 ϕ 12)
1	0.9x0.125 (8 ϕ 12)	0.58x0.125 (6 ϕ 12)	0.47x0.125 (6 ϕ 12)	2.45x0.125 (22 ϕ 12)	0.47x0.125 (6 ϕ 12)			0.7x0.125 (8 ϕ 12)

Storey	Horizontal 1	Horizontal 2
2	0.57x0.125 (6 ϕ 12)	0.16x0.125 (4 ϕ 12)
1	0.57x0.125 (6 ϕ 12)	0.16x0.125 (4 ϕ 12)

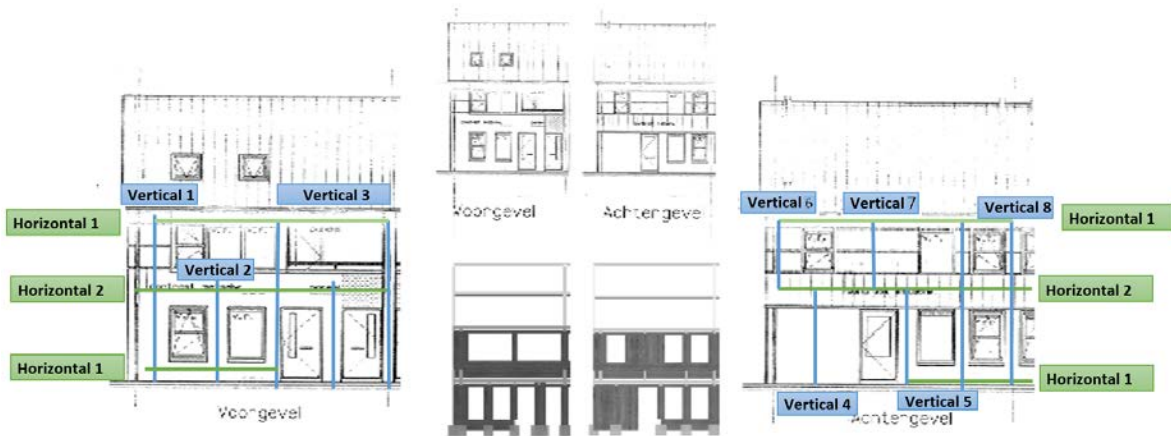


Figure 2.4: Precast RC residential terraced building with 4 units – Example of façade layout

2.2 Modelling assumptions for index building #1

The structure has been modelled with force-based fibre-elements (infrmFB) with 5 integration sections with the structural analysis package SeismoStruct (Seismosoft, 2015). A total of 150 section fibres have been defined, which are used in equilibrium computations carried out at each of the element’s integration sections.

In order to better calibrate the use of equivalent frame elements to model precast panels with openings for windows and doors, subassemblies of the terraced house have been modelled with three-dimensional finite elements using the MidasFEA (MIDAS, 2010) software. Three panels have been modelled, and static pushover analyses have been executed using both SeismoStruct and MidasFEA (see Figure 2.5). Based on the comparison of these pushover analyses, it has been necessary to modify the material properties of the SeismoStruct frame element model, such that similar pushover curves are obtained.

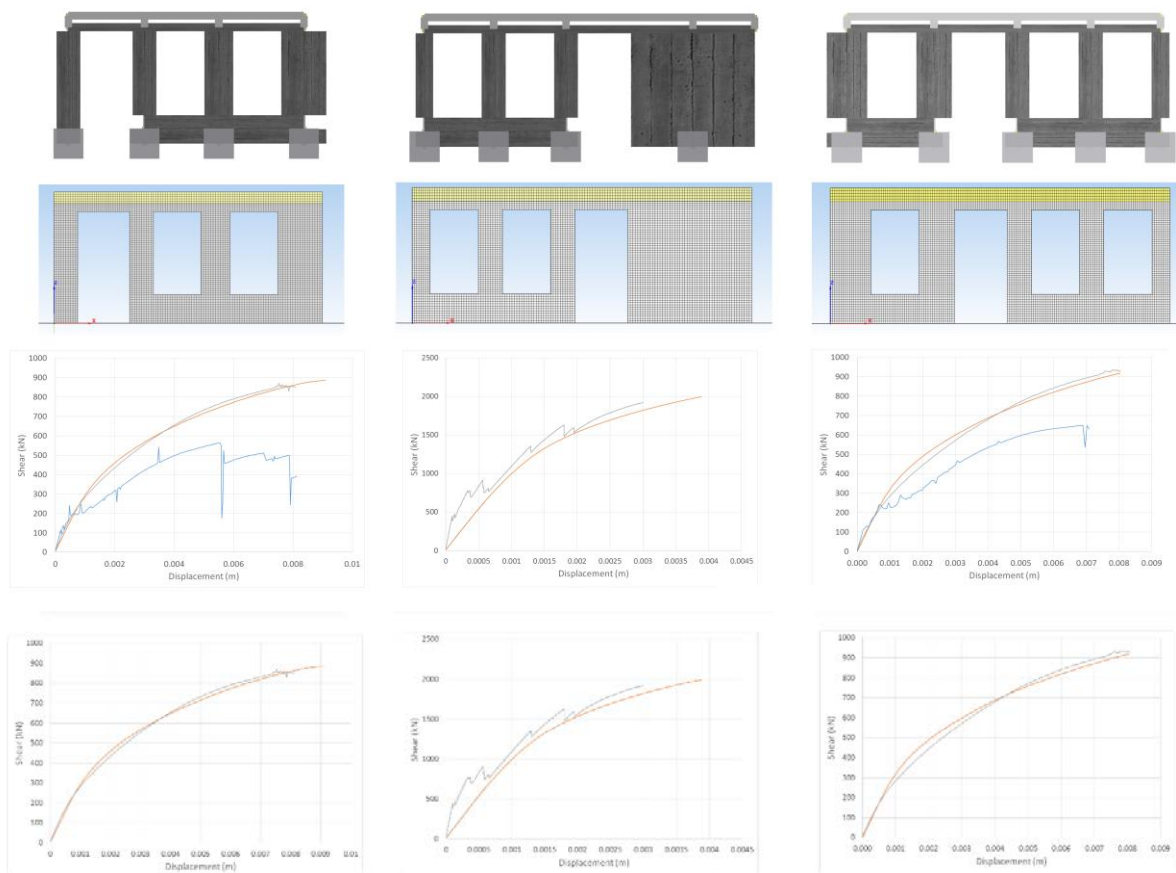


Figure 2.5: Precast RC residential terraced building with 4 units – Panels calibration and pushover curves before (top) and after (bottom) material calibration in SeismoStruct

Materials

For panel number 1 and number 3 the *Chang Mander nonlinear concrete* and *Menegotto-Pinto steel* models have been employed for defining the concrete and steel material parameters, respectively.

The post-calibration material properties for each constitutive model are as follows:

- Concrete: $f_c = 30$ MPa; $f_t = 3.0$ MPa; $\epsilon_c = 0.005$ m/m, $\epsilon_t = 0.007$ m/m, $\gamma = 24$ kN/m³;
- Steel: $E_s = 200$ GPa; $f_y = 600$ MPa; $\mu = 0.02$.

For panel number 2 the *Mander et al. nonlinear concrete* and *Menegotto-Pinto steel* models have been employed for defining the concrete and the steel material, respectively.

The post-calibration material properties for each constitutive model are as follows:

- Concrete: $f_c = 43$ MPa; $f_t = 3.2$ MPa; $\epsilon_c = 0.002$ m/m, $E_c = 34000$ MPa, $\gamma = 24$ kN/m³;
- Steel: $E_s = 200$ GPa; $f_y = 600$ MPa; $\mu = 0.02$.

Loads

The loads have been applied to the structure as lumped masses. The assumed values for a typical level and for the roof are summarized in Table 2.3.

Table 2.3: Precast RC residential terraced building with 4 units – Permanent loads

Type of load	Typical level Hollow-core [kN/m ²]	Typical level Solid slab [kN/m ²]	Roof [kN/m ²]
Dead Load	4	6.75	2
Live Load	2.0	2.0	0
Partition walls	0.5	0.5	-
Finishing	1.5	1.5	2

The upper floor includes the half weight of the roof, while the other half is applied to the roof elements. Loads in addition to the self-weight are taken as 100% permanent load plus 30% live load.

Other modelling assumptions

The precast roof has been modelled through an elastic frame element with the following properties: $EA = 1.0E+010$ [kN]; EI (axis2) = $1.0E+009$ [kNm²]; EI (axis3) = $1.0E+008$ [kNm²]; $GJ = 1.0E+008$ [kNm²].

The slabs have been modelled by introducing a rigid diaphragm in the X-Y plane for each floor level.

As these structures simply rest on the foundations, springs have been added at the base of each node to model the effect of friction. The springs have been modelled using symmetric bilinear link elements, with the yield force calculated as a function of the axial load and the friction coefficient, which has been taken to vary between 20% and 40%.

Further, because of the uncertainty concerning the presence of connections at the base of the precast walls, two different modelling assumptions have been investigated. In the first case the assumption is made that the panels are not connected to each other, and the springs under each wall have been defined separately (this model will be called “without connection of panels” in the following paragraphs), whilst in the second case the panels have been assumed to be connected and the same properties have been used for all the springs, calibrated using the wall with the highest axial load (this model will be called “with connection of panels”).

Performance criteria have been set in order to model progressive collapse of the structure due to strength degradation. As stated for REST-RC-A index building, the shear capacity of each element has been calculated automatically by the software. In order to avoid excessive conservatism in the estimation of the shear capacity, all partial safety factors have been set to 1, though it is noted that the formulae may still provide conservative estimates of shear failure. A residual strength of 20% is assigned to the element when shear capacity is reached (to allow for the influence of aggregate interlock).

A screenshot of the model of the precast RC terraced building with 4 units is presented in Figure 2.6.

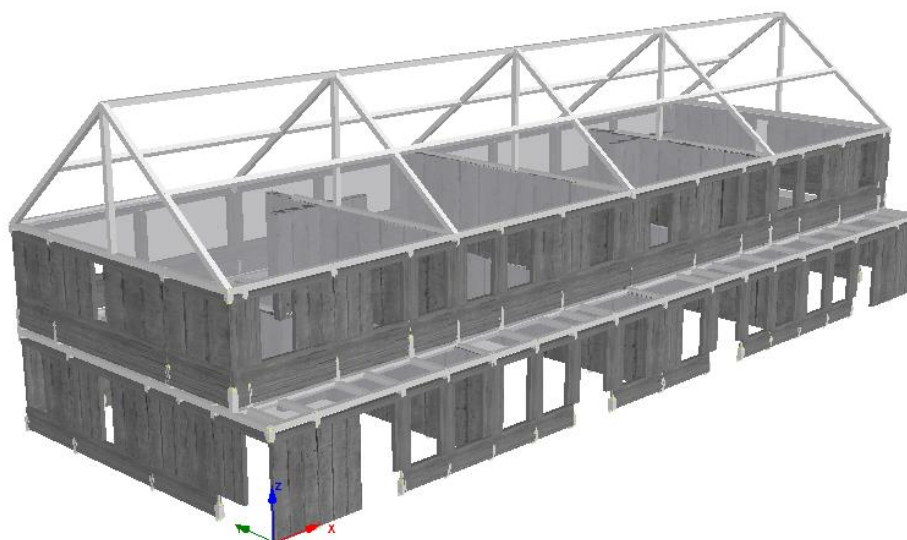


Figure 2.6: Screenshot of the SeismoStruct model of the four-unit REST-RC-B index building

2.3 Numerical analyses and results for index building #1

As described previously, four different modelling cases have been investigated to cover the response variation due to friction coefficient and the presence (or not) of connection of panels, as summarized in Table 2.4.

Table 2.4: Precast RC residential terraced building with 4 units – Analysis cases

ANALYSES CASES	Friction Coefficient 20%	Friction Coefficient 40%
Without connection of panels	Without connection of panels_20%	Without connection of panels_40%
With connection of panels	With connection of panels_20%	With connection of panels_40%

Eigenvalue analysis

An eigenvalue analysis has been undertaken as an initial check of the models; the results are displayed in Table 2.5.

Table 2.5: Precast RC residential terraced building with 4 units – Results from eigenvalues analyses

EIGENVALUES	First Longitudinal		First Transverse	
	Friction Coeff. 20%	Friction Coeff. 40%	Friction Coeff. 20%	Friction Coeff. 40%
Without connection of panels	0.233 s	0.172 s	0.212 s	0.156 s
With connection of panels	0.101 s	0.076 s	0.098 s	0.070 s

Pushover analyses and sensitivity studies

Given the complexity introduced into the models by adding springs at the base to model the friction between the structure and the foundation, it was felt to be pertinent to use both force-based conventional pushover analyses as well as displacement-based adaptive pushover analyses (Antoniou and Pinho, 2004) for the nonlinear static analysis.

Conventional pushover analyses have been undertaken using a triangular loading profile. For what concerns the adaptive pushover, the lateral load distribution (which starts as a uniform distribution of displacements initially set equal to 0.1 m) is not kept constant but is rather continuously updated during the analysis, according to the modal shapes and participation factors derived by eigenvalue analysis carried out at each analysis step. Hence, this kind of analysis method accounts for the softening of the structure, its period elongation, and the modification of the inertia forces due to spectral amplification. Figure 2.7 shows the site-specific spectrum which has been considered for the spectral amplification; this spectrum was based on the Groningen v0 hazard disaggregation and ground-motion prediction equation.

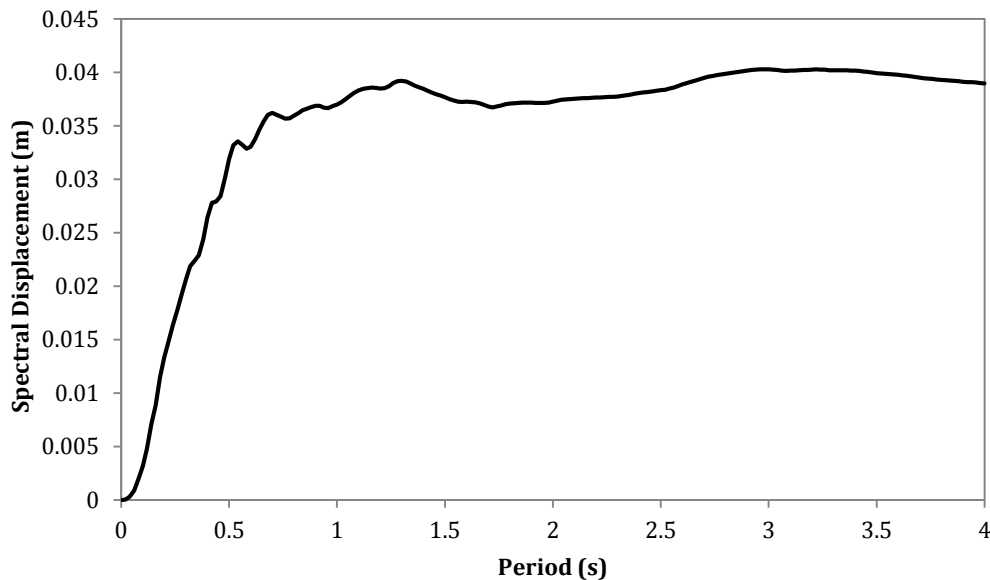


Figure 2.7: Displacement spectrum

Similar results were obtained with both the conventional and adaptive pushover analyses, but numerical instabilities arose with the use of the conventional pushover in the transverse direction.

The deformed shape at ultimate displacement for the longitudinal direction is shown in Figure 2.8, which shows that collapse occurs due to the shear failure of the longitudinal wall elements for the models “with connection of panels” (Figure 2.8b), for the case of friction coefficient equal to 40%, whilst the models “without connections of panels” seem to be able to slide significantly, before the shear failure of few transverse walls occurs (Figure 2.8a).

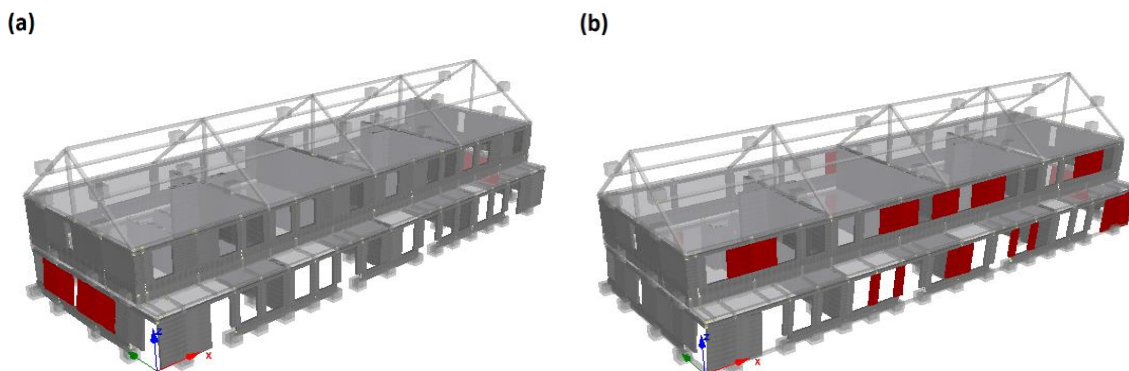


Figure 2.8: Precast RC residential terraced building with 4 units - Deformed shape at ultimate displacement and elements that reach their shear capacity (longitudinal direction)

The pushover curves in the longitudinal direction are provided in Figure 2.9. The change of friction coefficient has a larger influence on the case “with connection of panels”, allowing the structure to resist a larger base shear. Less influence of the friction coefficient is noted for the case “without connection of panels”; the structure presents a similar ultimate displacement for the different analysed cases.

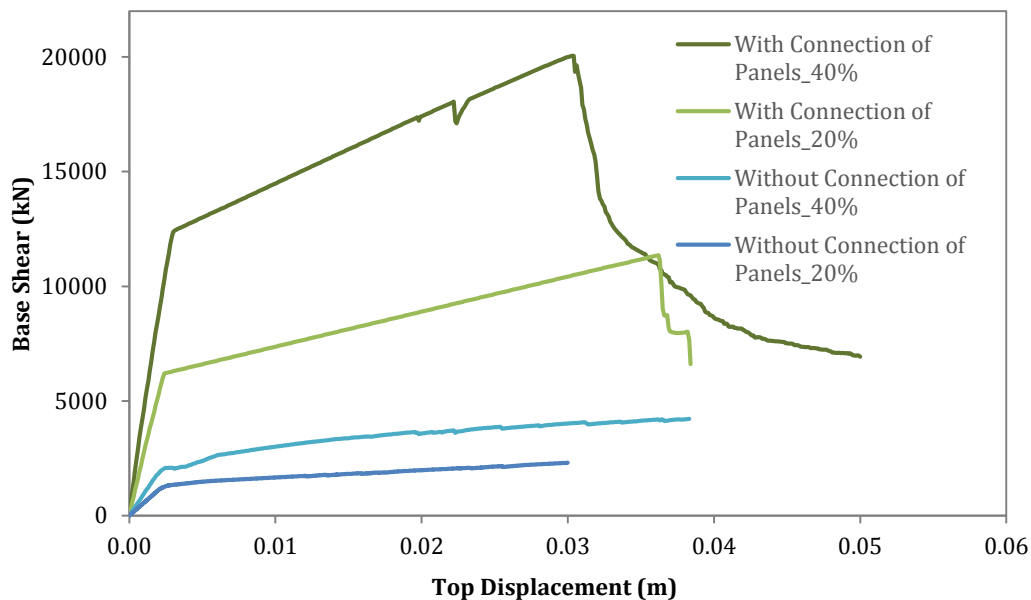


Figure 2.9: Precast RC residential terraced building with 4 units – Pushover curves (longitudinal direction)

For what concerns the transverse direction, the deformed shape at ultimate displacement is shown in Figure 2.10. In this direction the connection of panels and the friction coefficient do not affect the behaviour of the structure and sliding until unseating is likely to occur for all the models.

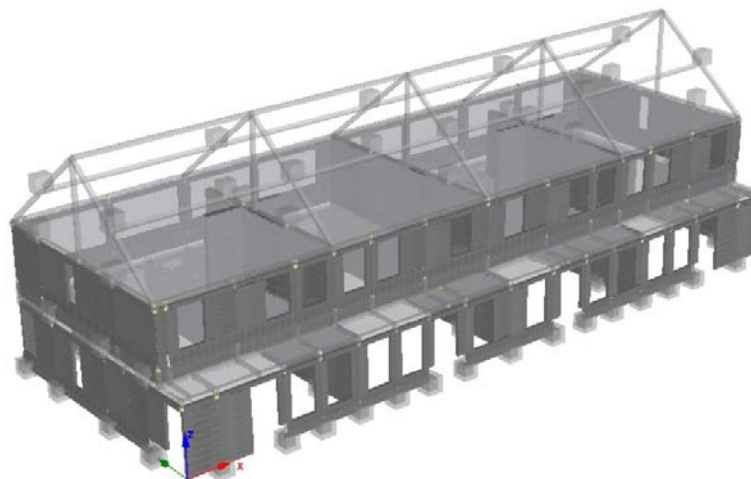


Figure 2.10: Precast RC residential terraced building with 4 units – Deformed shape at ultimate displacement (transverse direction)

The pushover curves in the transverse direction are provided in Figure 2.11.

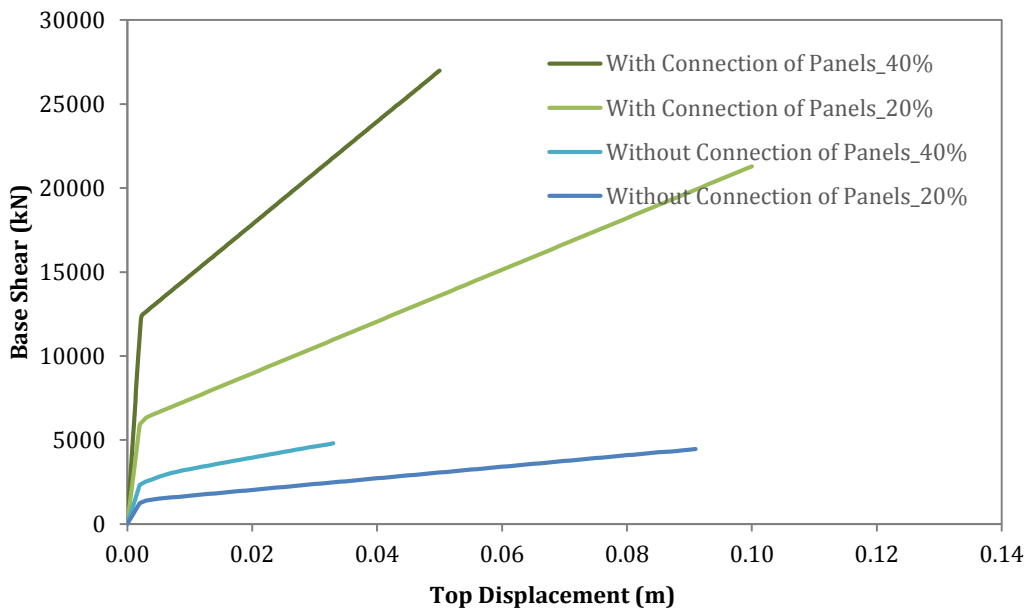


Figure 2.11: Precast RC residential terraced building with 4 units – Pushover curves (transverse direction)

In accordance with the ultimate deformed shape, the curves show that the panels slip before significant shear failure occurs. Higher values of base shear capacity are obtained compared to the longitudinal direction.

2.4 General description and structural configuration for index building #2

The second index building that has been modelled for the precast RC terraced building typology is a 7-unit real building. The architectural model that was provided by Arup for this structure is shown in Figure 2.12.

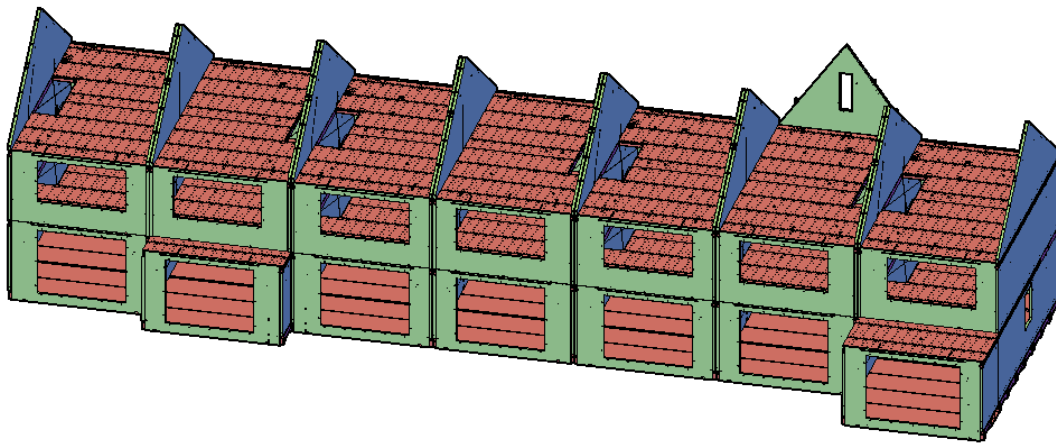


Figure 2.12: Precast RC residential terraced building with 7 units

The same construction details and assumptions described previously in §2.1 for the 4-unit building also apply to this structure.

Although the building has an asymmetrical shape, the largest dimensions in plan are 37.8 m length and 11.5 m width at the ground level with a smaller width of 9.1 m at the upper floor.

A 7-unit index building has thus been produced based on the structural drawings that were available, with a storey height of 2.7 m and the geometrical details summarised in Table 2.6, i.e. precast walls (longitudinal direction) and precast party/gable walls (transverse direction). All the element sections have been defined as reinforced concrete rectangular sections.

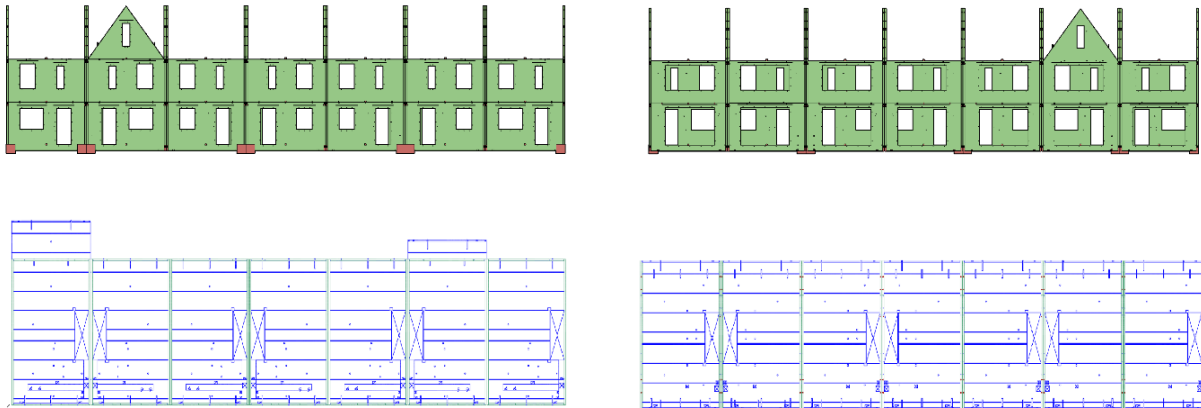


Figure 2.13: Precast RC residential terraced building with 7 units – drawings (plan and frontal views)

Along the transverse direction, precast wall sections can be divided into external and internal ones, considering the different thickness and focusing on the primary parallel transverse walls. A double layer welded reinforced mesh is used and the number of reinforcement bars summarized in Table 2.7 represents the total amount of bars in the section.

Table 2.6: Precast RC residential terraced building with 7 units – Geometrical details for walls in transverse direction

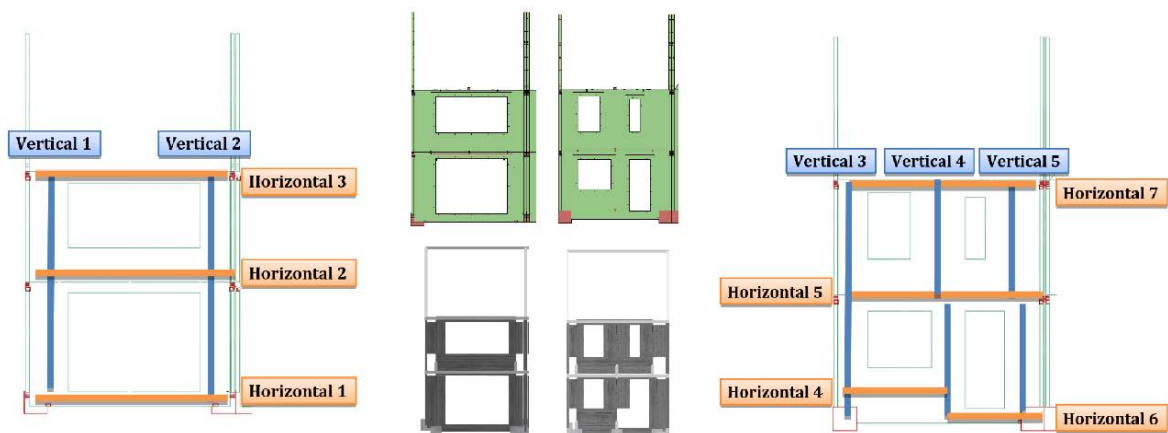
Storey	External wall	Internal Wall
2	9.1 m x 0.1 m (58 ϕ 12)	9.1 m x 0.2 m (58 ϕ 12)
1	9.1 m x 0.1 m (58 ϕ 12)	9.1 m x 0.2 m (58 ϕ 12)

The longitudinal front walls are comprised of two vertical and three horizontal structural elements, while the longitudinal back walls are comprised of three vertical and three horizontal structural elements, as shown in the figure and table below. The elements comprising the central RC precast walls of the structure, thus placed in the middle of the longitudinal direction of the terraced house, are also described in the following table. The structure has a 0.05 m solid concrete topping on top of the horizontal hollow-core floor panels. The roof is a precast RC slab and the foundation system consists of precast foundation beams, supported on piles. Again, a double layer welded mesh is used in the longitudinal wall elements and the number of reinforcement bars summarized in Table 2.7 represents the total bars in the section.

Table 2.7: Precast RC residential terraced building with 7 units – Geometrical details for walls in longitudinal direction

Storey	Vertical 1	Vertical 2	Vertical 3	Vertical 4	Vertical 5
2	0.994x0.09 (8 ϕ 12)	0.774x0.09 (8 ϕ 12)	0.774x0.09 (8 ϕ 12)		0.891x0.09 (8 ϕ 12)
1	0.994x0.09 (8 ϕ 12)	0.774x0.09 (8 ϕ 12)	0.774x0.09 (8 ϕ 12)	1.409x0.09 (12 ϕ 12)	1.379x0.09 (12 ϕ 12)

Storey	Horizontal 1	Horizontal 2	Horizontal 3	Horizontal 4	Horizontal 5	Horizontal 6	Horizontal 7
2		0.894x0.09 (8 ϕ 12)	0.3x0.09 (4 ϕ 12)		0.894x0.09 (8 ϕ 12)		0.3x0.09 (4 ϕ 12)
1	0.367x0.09 (6 ϕ 12)			1.399x0.09 (12 ϕ 12)		0.367x0.09 (6 ϕ 12)	


Figure 2.14: Precast RC residential terraced building with 7 units – Example of façade layout

2.5 Modelling assumptions for index building #2

As for the modelling of building #1, the structure has been modelled with force-based fibre-elements (infrmFB) with 5 integration sections (each with 150 section fibres) with the structural analysis package SeismoStruct (Seismosoft, 2015).

As in the case of the terraced building with 4-units, for three of the panels a calibration exercise has been performed using MidasFEA (MIDAS, 2010). The same static pushover analyses have been executed both on SeismoStruct and MidasFEA (see Figure 2.15), and the material properties of the SeismoStruct model have been modified accordingly.

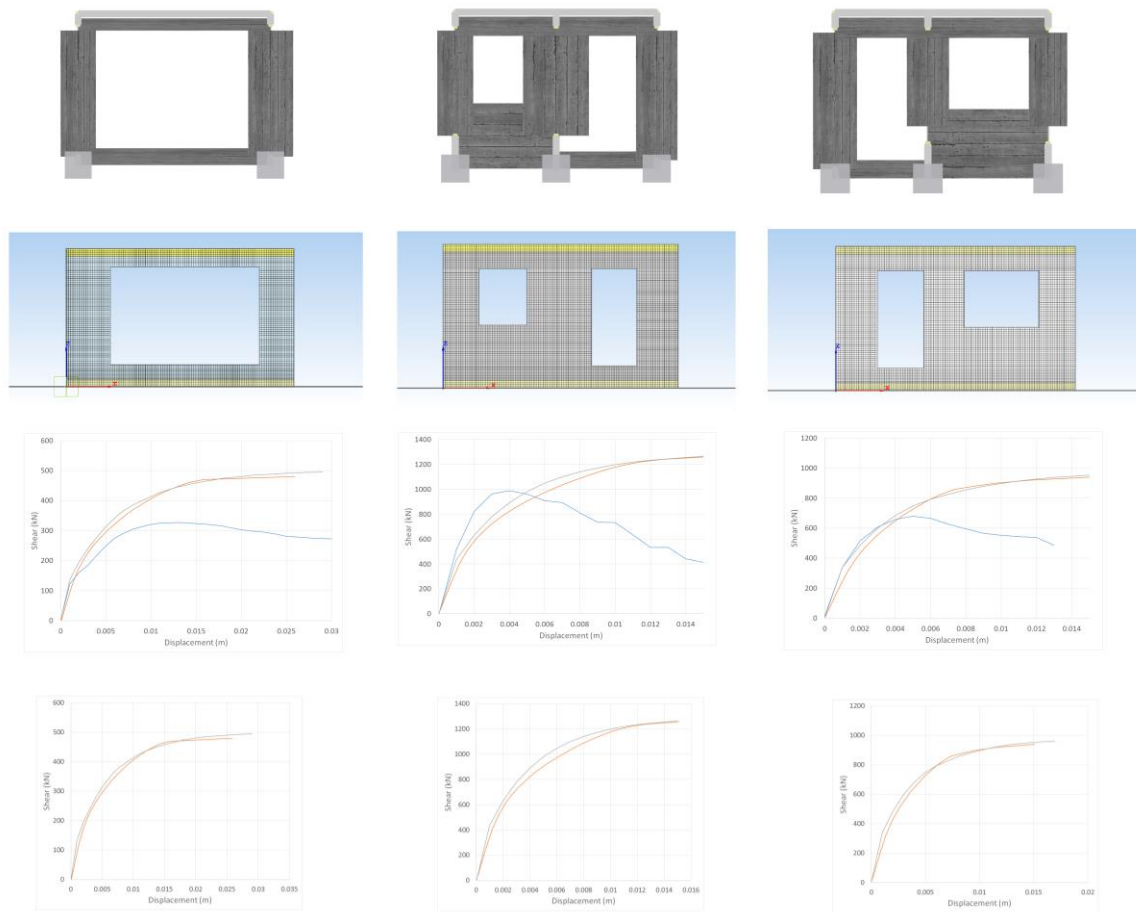


Figure 2.15: Precast RC residential terraced building with 7 units – Panels calibration and pushover curves before (top) and after (bottom) material calibration in SeismoStruct

Materials

For all panels the *Chang Mander nonlinear concrete* and *Menegotto-Pinto steel* models have been employed for the concrete and steel materials, respectively. The post-calibration material properties for each constitutive model are listed below:

- Concrete: $f_c = 48 \text{ MPa}$; $f_t = 2.5 \text{ MPa}$; $\epsilon_c = 0.01 \text{ m/m}$, $\epsilon_t = 0.01 \text{ m/m}$, $\gamma = 24 \text{ kN/m}^3$;
- Steel: $E_s = 210 \text{ GPa}$; $f_y = 600 \text{ MPa}$; $\mu = 0.04$.

Loads

The loads have been applied to the structure as lumped masses. The assumed values for a typical level and for the roof are summarized in Table 2.8.

Table 2.8: Precast RC residential terraced building with 7 units – Permanent loads

Type of load	Typical level (hollow-core) [kN/m ²]	Roof [kN/m ²]
Dead Load	4	2
Live Load	2.0	0
Partition walls	0.5	-
Finishing	1.5	2

The upper floor includes the weight of the roof. The assumed loads (in addition to the self-weight) are taken as 100% permanent load plus 30% live load.

Other modelling assumptions

The precast roof has been modelled through an elastic frame element with the following properties: $EA = 1.0E+010$ [kN]; EI (axis2) = $1.0E+009$ [kNm²]; EI (axis3) = $1.0E+008$ [kNm²]; $GJ = 1.0E+008$ [kNm²].

The slabs at each floor level have been modelled by introducing a rigid diaphragm in the X-Y plane.

In order to take into account the effects of friction at the base of the walls, the same modelling assumptions introduced for the 4-unit structure (see §2.2) have been done. Hence, nonlinear springs have been employed at the base nodes of each wall panel, as shown in Figure 2.17 (blue “cubes”), using symmetric bilinear link elements in both translational directions, considering a friction force equal to the axial load multiplied by the friction coefficient (taken as 20% and 40%, respectively).

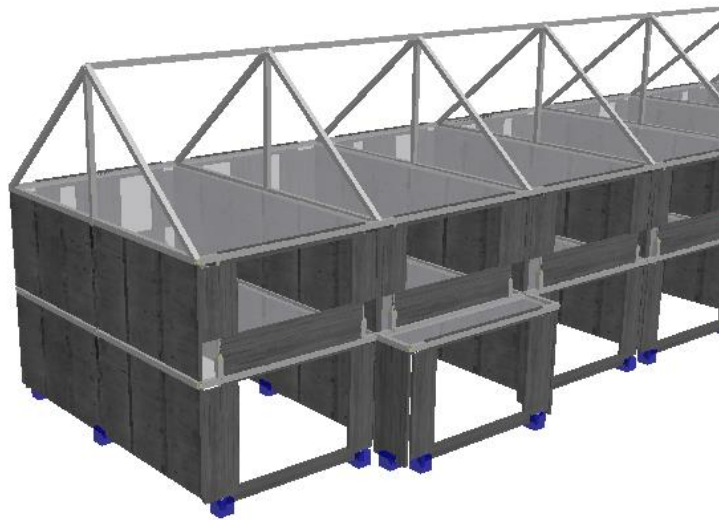


Figure 2.16: Screenshot of the SeismoStruct model of the seven-unit REST-RC-B index building with nonlinear springs at the base of the wall panels

Performance criteria have been set in order to model progressive collapse due to strength degradation using the previously reported assumptions (see §2.2).

A screenshot of the model of the precast RC terraced building with 7 units model is presented in Figure 2.17.

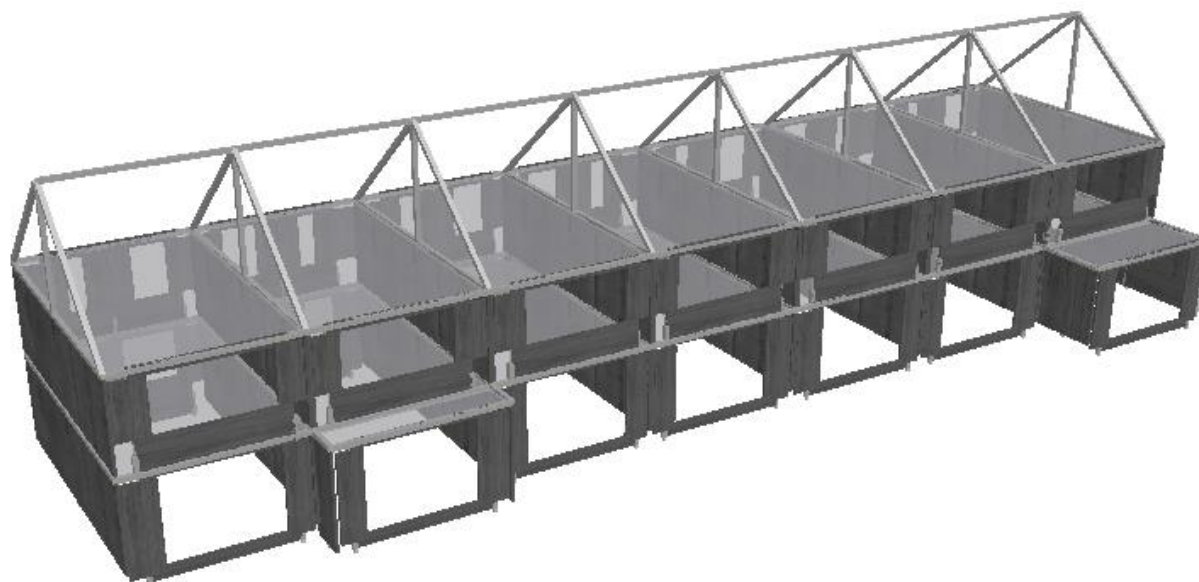


Figure 2.17: Screenshot of the SeismoStruct model of the seven-unit REST-RC-B index building

2.6 Numerical analyses and results for index building #2

Also for this index building four different modelling cases have been investigated to cover the variation due to friction coefficient and the presence (or not) of connection of panels, as summarized in Table 2.9.

Table 2.9: Precast RC residential terraced building with 7 units – Analyses cases

ANALYSES CASES	Friction Coefficient 20%	Friction Coefficient 40%
Without connection of panels	Without connection of panels_20%	Without connection of panels_40%
With connection of panels	With connection of panels_20%	With connection of panels_40%

Eigenvalue analyses

An eigenvalue analysis has been undertaken as an initial check of the models and the results are displayed in Table 2.10.

Table 2.10: Precast RC residential terraced building with 7 units – Eigenvalues analyses

EIGENVALUES	First Longitudinal		First Transverse	
	Friction Coeff. 20%	Friction Coeff. 40%	Friction Coeff. 20%	Friction Coeff. 40%
Without connection of panels	0.273 s	0.221 s	0.216 s	0.155 s
With connection of panels	0.109 s	0.091 s	0.088 s	0.063 s

Pushover analyses and sensitivity studies

As discussed for the 4-unit model, for each analysis case presented in Table 2.9, a force-based conventional pushover analysis has been undertaken using a triangular loading profile. In addition, displacement-based adaptive pushover analyses have also been undertaken. Similar

results were obtained with both the conventional and adaptive pushover analyses, but numerical instabilities arose with the use of the conventional pushover in the transverse direction.

The deformed shape at ultimate displacement for longitudinal direction is shown in Figure 2.18, which shows that collapse occurs due to the unseating of the walls for the model “without connection of panels” (Figure 2.18a). On the other hand, in the cases “with connection of panels” (Figure 2.18b) the collapse occurs due to the shear failure of the longitudinal walls.

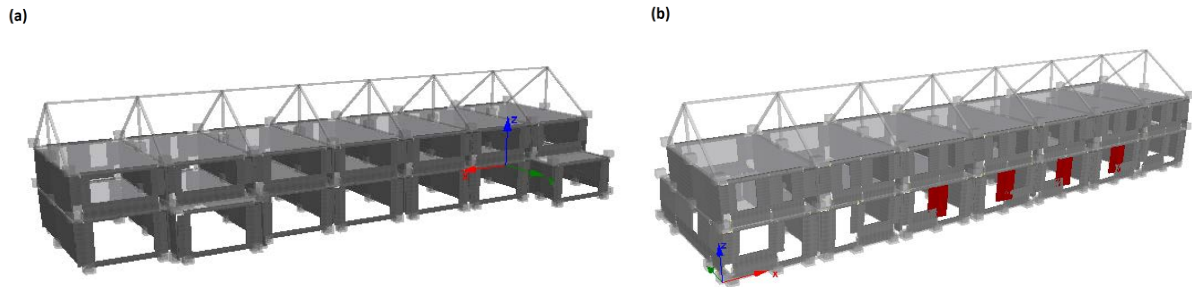


Figure 2.18: Precast RC residential terraced building with 7 units – Deformed shape at ultimate displacement and elements that reaches its shear capacity (longitudinal direction)

The “pushover curves in the longitudinal direction are provided in Figure 2.19. For this structure, the change of friction coefficient has a minimal influence on the pushover curves, at least in terms of base shear capacity, both with and without connection of panels.

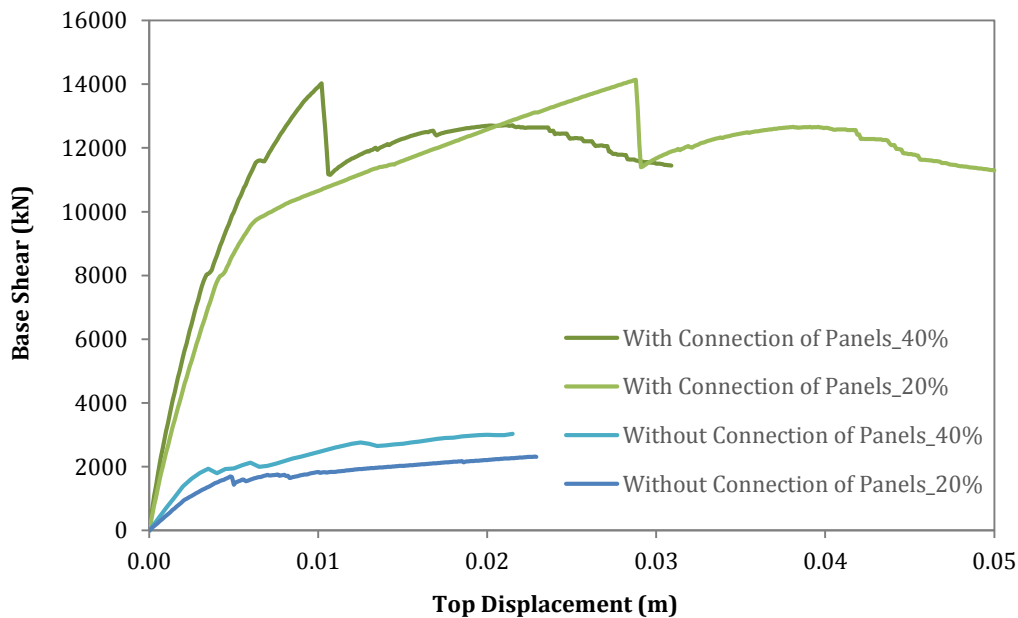


Figure 2.19: Precast RC residential terraced building with 7 units – ‘Original’ pushover curves in the longitudinal direction

With the connection of panels, the structure collapses due to shear failure. On the other hand, without the connection of panels, both 20% and 40% friction cases feature failure due to unseating of walls.

For what concerns the transverse direction, the deformed shape at ultimate displacement is shown in Figure 2.20. This figure shows that collapse occurs due to the shear failure of all the transverse walls at the base of the structure for the models “with connection of panels” (Figure 2.20b) and for both friction coefficients, whilst for the models “without connection of panels”

(Figure 2.20a) this occurs at larger displacements, activating the shear failure of few longitudinal walls in the case of 20% of friction coefficient and also an external transverse wall for friction equal to 40%.

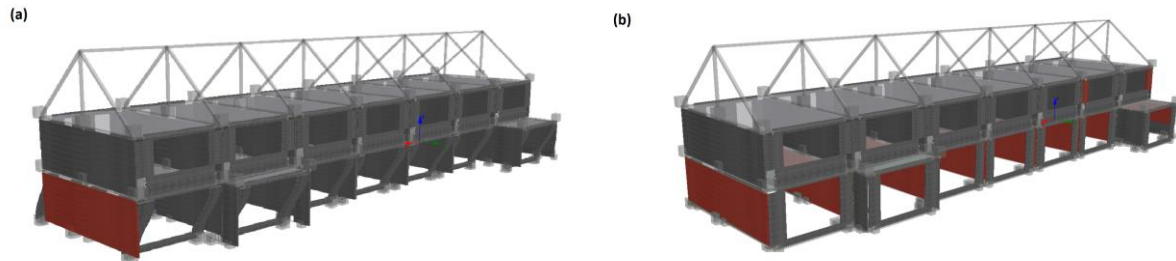


Figure 2.20: Precast RC residential terraced building with 7 units – Deformed shape at ultimate displacement and elements that reaches its shear capacity (transverse direction)

The pushover curves in the transverse direction are provided in Figure 2.21. On the one hand, in accordance with the ultimate deformed shape, for 20% and 40% friction without foundation beam the curves show that the panels slip reaches higher displacements, but shear failure does eventually occur. On the other hand, when the connection of panels is considered, the structure collapses reaching the shear capacity of the transverse precast walls at moderate displacements. Higher values of the base shear capacity are obtained compared to the longitudinal direction.

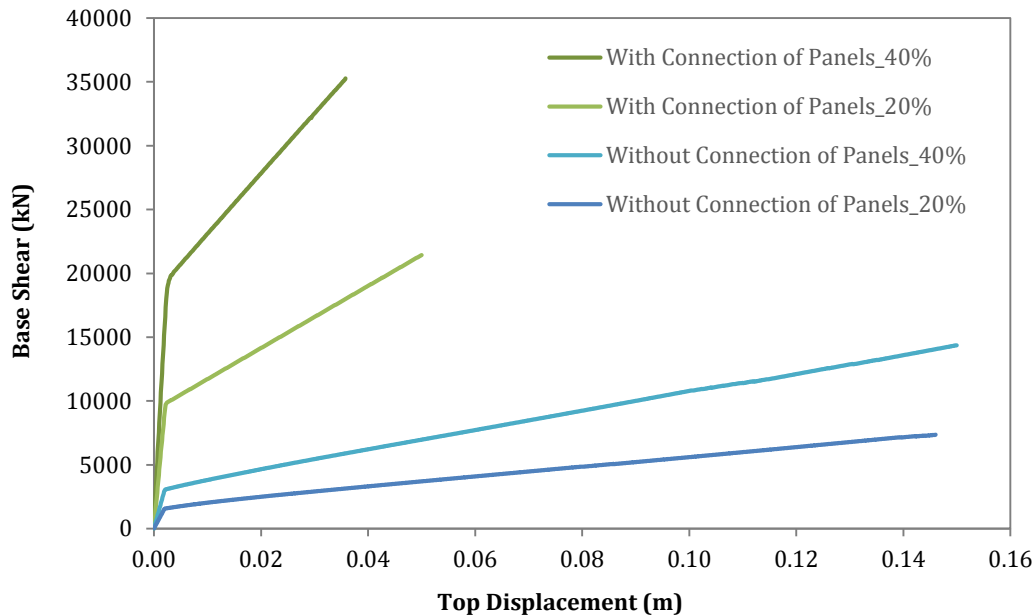


Figure 2.21: Precast RC residential terraced building with 7 units – Pushover curves (transverse direction)

2.7 Summary of the Test and FE numerical results on Precast Panels

At the Eucentre laboratory of Pavia (Italy) several specimens have been prepared and tested in order to reproduce the wall-to-wall and wall-to-foundation connection systems that are used in precast terraced houses typical of Dutch building practice. Figure 2.22 shows an example of specimen which has been constructed and set up in the laboratory (see EUCENTRE, 2015 for more details).



Figure 2.22: Example of specimen of precast panel tested at the Eucentre laboratory of Pavia (Italy)

To simulate the experimental behaviour of these specimens, an equivalent mechanical model, consisting of a set of vertical fibre wall elements in combination with rigid links and nonlinear shear-flexural springs, was constructed in SeismoStruct and a series of geometrically and materially nonlinear FE simulations were performed in order to validate the numerical approach proposed.

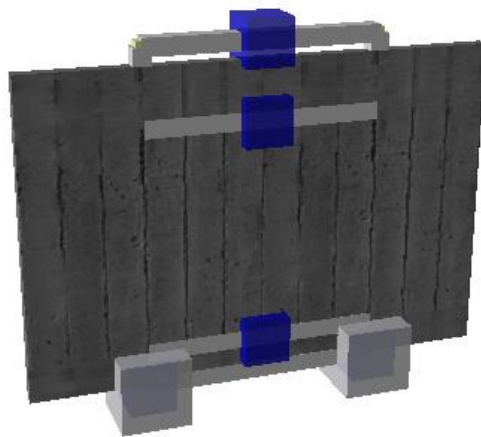


Figure 2.23: Screenshot of the SeismoStruct model of the calibrated precast panel

Figure 2.24 shows the direct comparison between experimental (cyclic) and numerical (monotonic) base shear-top displacement curves to quantify the effectiveness of FE predictions for a particular specimen (i.e. with thickness of 20mm, highest axial load and no openings).

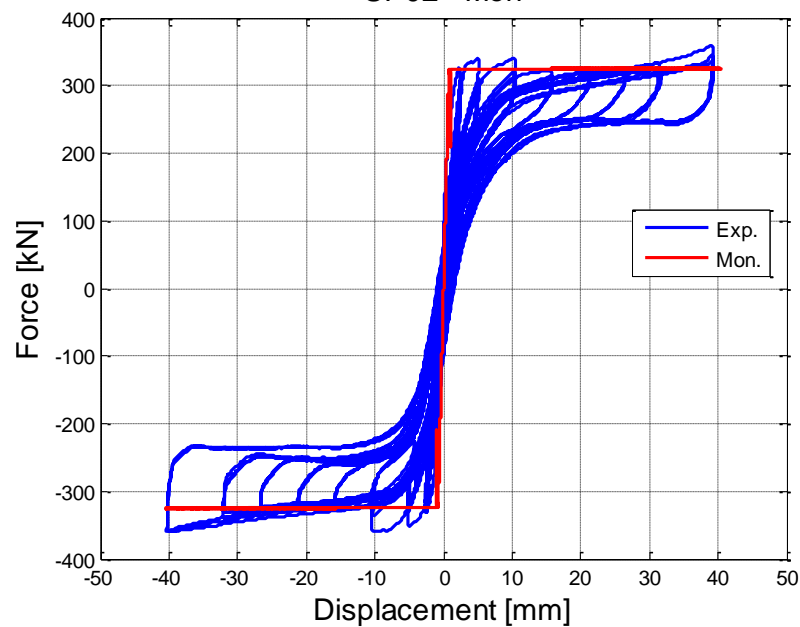


Figure 2.24: Comparison between numerical (monotonic) and experimental (cyclic) results on a precast panel

2.8 Calibrated index building

Modelling Assumptions

Given that the connections between panels are only provided to prevent out-of-plane failure and are unlikely to provide significant shear resistance, only the model “without connections” has been taken into account in the calibration phase.

Based on the calibration of the precast panel model using the laboratory test results as described in the previous section, an updated model has been developed using one unit of the seven-unit REST-RC-B index building (described previously in § 2.5).

The material properties, loads, and modelling assumptions made on the precast roof (i.e. elastic frame elements) and the floor slabs (i.e. rigid diaphragms) remain unchanged. Instead, the nonlinear springs have been updated based on the experimental results, and new nonlinear springs have been added at the base nodes of the wall panels of first floor level and between adjacent panels, as shown in Figure 2.25 (blue “cubes”).



Figure 2.25: Screenshot of the SeismoStruct model of the calibrated one-unit REST-RC-B index building with nonlinear springs at the base of the wall panels and between adjacent panels

The springs at the base of the panels have been introduced in order to model the in-plane (rocking) and the out-of-plane resistance of the walls, as well as the sliding resistance. For what concerns the friction coefficient, and on the basis of the laboratory tests, it has been taken equal to 0.6 (60%) for axial loads lower than 300 kN and 0.4 (40%) in all other cases.

Performance criteria have been set in order to model progressive collapse due to strength degradation using the previously reported assumptions (see §2.2).

Pushover analyses

Displacement-based adaptive pushover analyses have been undertaken and the final pushover curves in each direction are provided in Figure 2.26 and Figure 2.27, respectively.

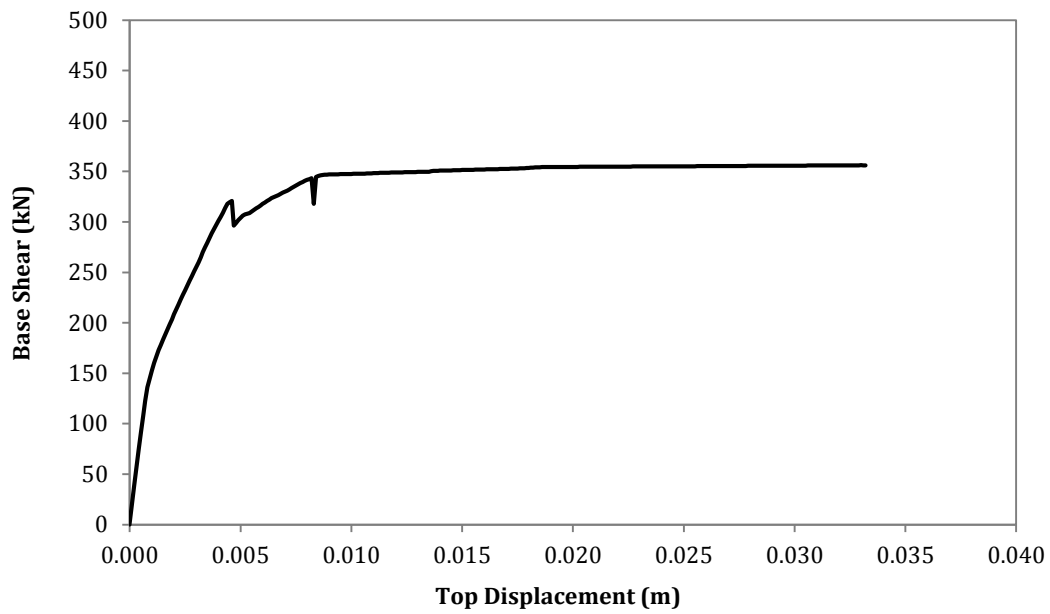


Figure 2.26: Pushover curves for calibrated precast RC residential terraced building (longitudinal direction)

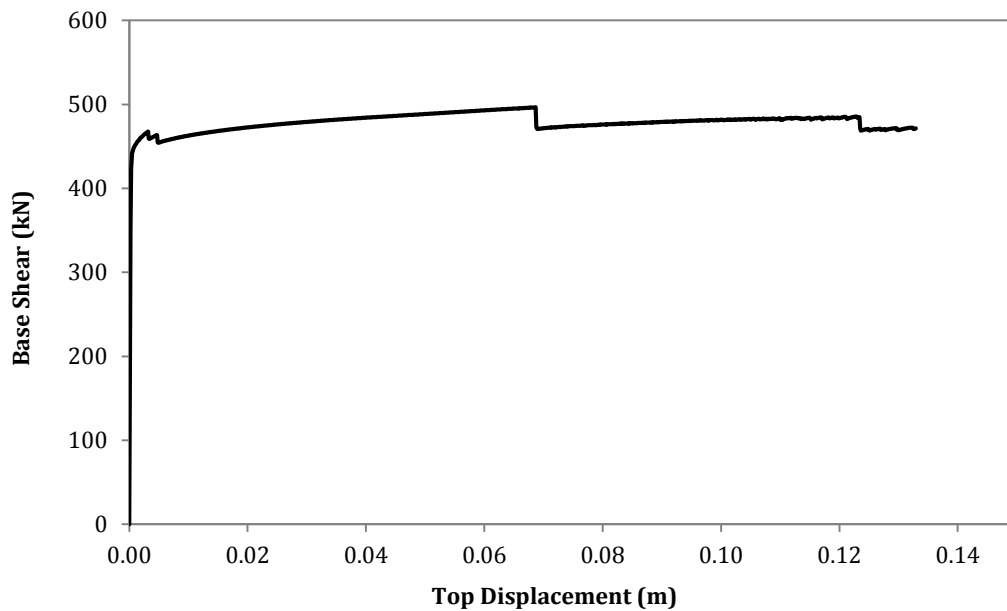


Figure 2.27: Pushover curves for calibrated precast RC residential terraced building (transverse direction)

The deformed shape at ultimate displacement and the shear failures for both longitudinal and transverse directions are shown in Figure 2.28.

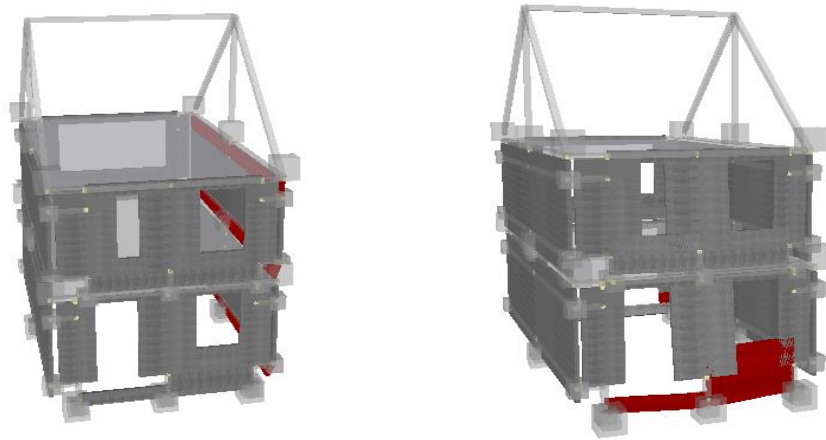


Figure 2.28: Calibrated one-unit REST-RC-B index building – Deformed shape at ultimate displacement and elements that reaches its shear capacity (longitudinal (left) and transverse (right) direction)

3 Cast-in-Place RC Residential Apartment Buildings with ≤ 4 storeys (RESA-RC-A-L4S)

3.1 General description and structural configuration

A real 4-storey cast-in-place reinforced concrete *tunnel form* residential apartment building with less than or equal to 4 storeys (Figure 3.1) has been modelled.



Figure 3.1: Cast-in-place RC residential apartment building with ≤ 4 storeys (Google Street View)

This building presents a V-shape configuration in plan, but only a rectangular portion of it, indicated in red in Figure 3.7, has been modelled. The main structural system is made up of shear walls (which are the primary lateral load resisting and vertical load carrying members) and flat slabs having approximately the same thickness (25 cm for the walls along the transverse direction and 30 cm for the slabs of the main floors), whilst the walls along the longitudinal direction are thinner (16 cm) and the roof is 24 cm thick.

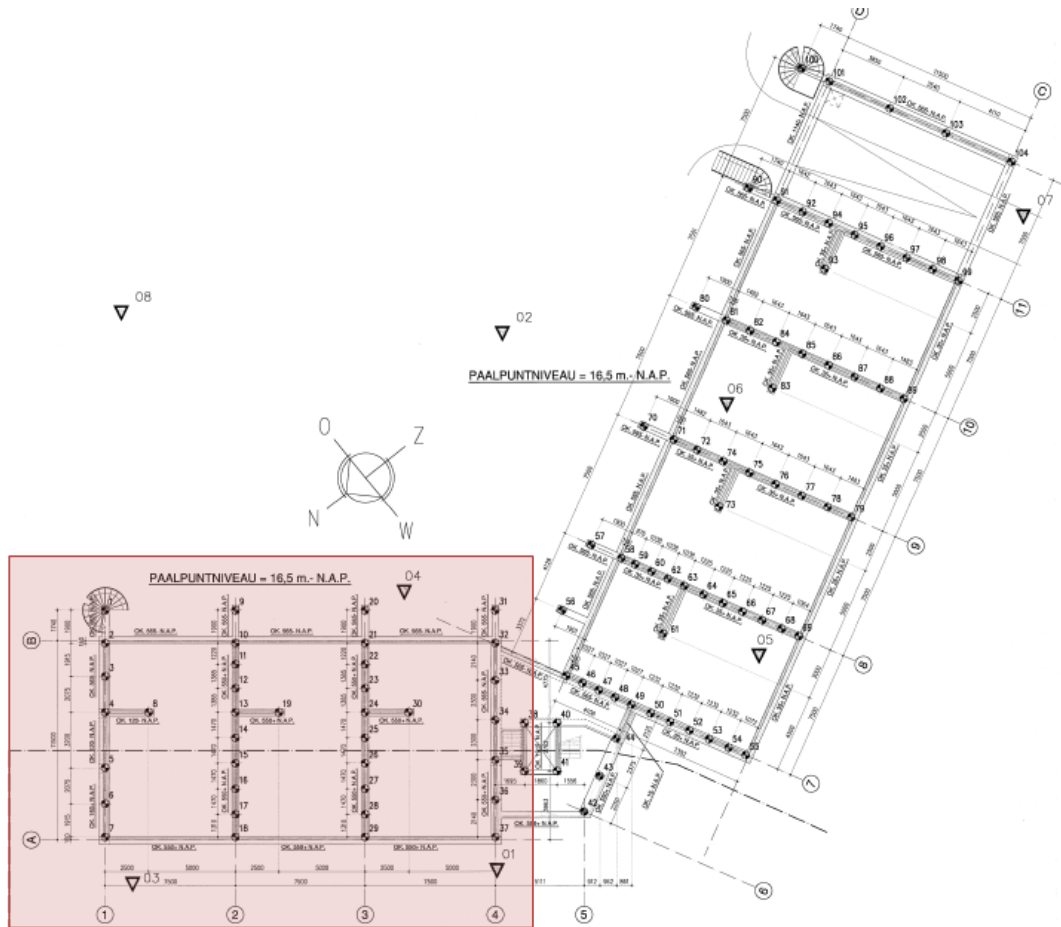


Figure 3.2: Cast-in-place RC residential apartment building with <= 4 storeys – Plan configuration

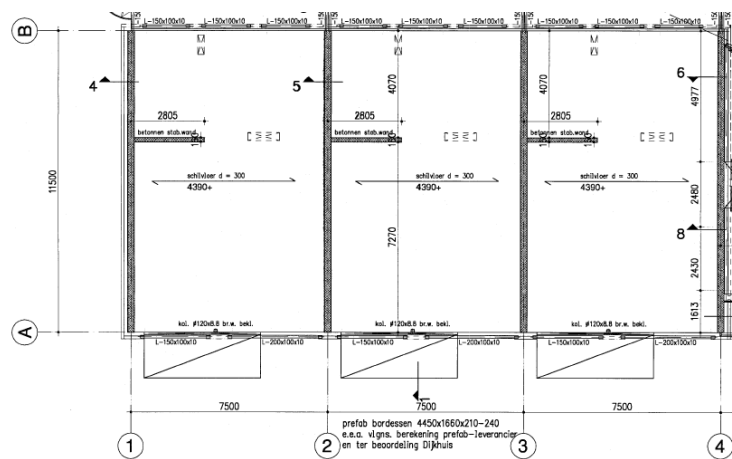


Figure 3.3: Cast-in-place RC residential apartment building with <= 4 storeys – Plan view of a main floor

The selected portion of the building measures 22.5 m in the longitudinal direction and 11.5 m in the transverse direction, respectively, excluding the balconies and an exterior walkway (consisting of a prefabricated slab supported by steel columns).

As shown in Figure 3.8, the longer walls are oriented in the transverse direction and are spaced at 7.5 m, whilst in the longitudinal direction there are only three shorter walls that may resist the lateral loads. Figure 3.4 shows the section views of the exterior wall in the transverse direction.

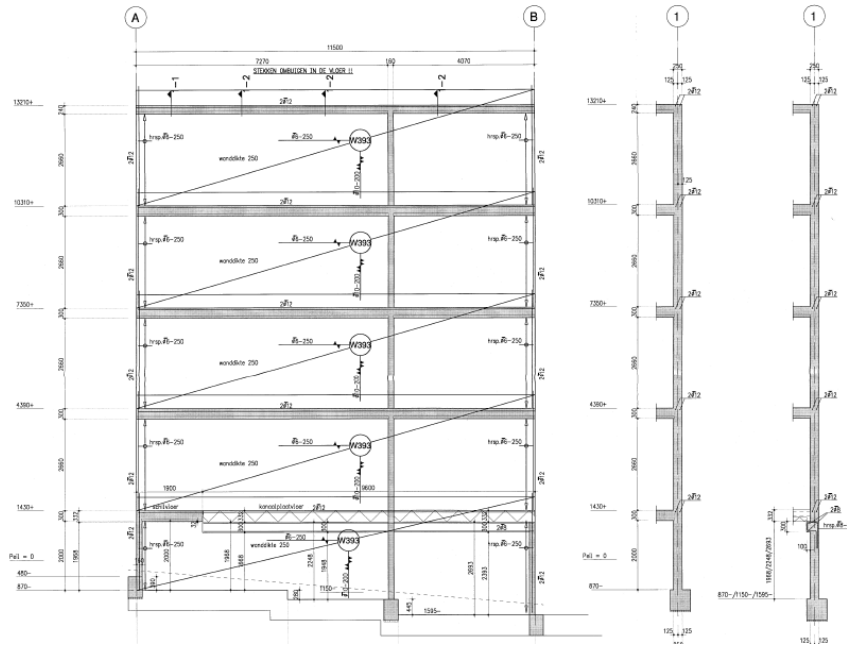


Figure 3.4: Cast-in-place RC residential apartment building with <= 4 storeys – Section view (exterior wall)

3.2 Modelling assumptions

In order to evaluate the 3D nonlinear seismic response of this RC residential apartment building, a structural model (slightly modified with respect to the original configuration, so as to render it symmetric, as shown in Figure 3.5) has been created using Extreme Loading for Structures (ELS).

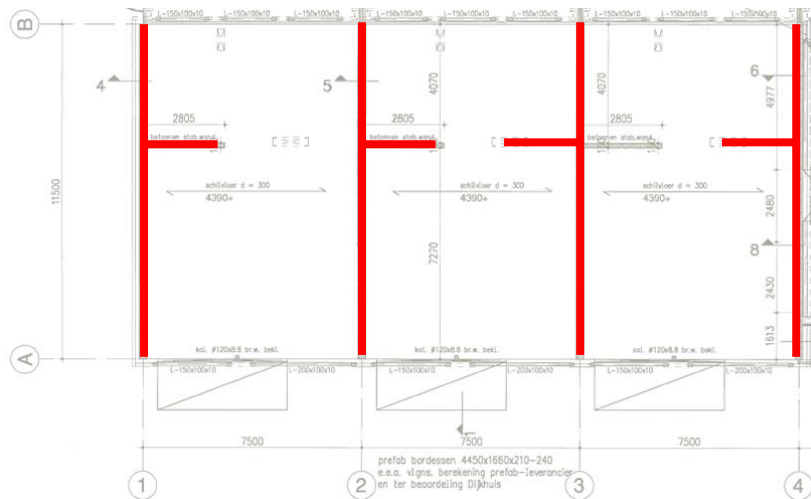


Figure 3.5: Cast-in-place RC residential apartment building with <= 4 storeys – Plan view of the modified configuration (in red the modelled walls)

Materials

The C20/25 concrete material has been modelled with a mean value of 28 MPa for the compressive strength. The mean yield strength of the FeB500 steel has been judged to be 575 MPa for both structural walls and slabs (based on a normal distribution and coefficient of variation of 8.5%).

Loads

Loads in addition to the self-weight for a typical floor level and for the roof have been computed proportionally to the slabs tributary areas and have been taken as 100% permanent load plus 30% live load, based on the values given in Table 3.1, and have been applied to the structural model as increased masses of each floor.

Table 3.1: Cast-in-place RC residential apartment building with ≤ 4 storeys – Loads (in addition to self-weight)

Type of load	Typical level [kN/m ²]	Roof [kN/m ²]
Permanent Load	2.0	1.0
Live Load	1.75	-

Other modelling assumptions

All the base nodes have been assumed to be fully restrained.

A screenshot of the model of the second cast-in-place RC residential apartment building with less than or equal to 4-storeys model is presented in Figure 3.6.

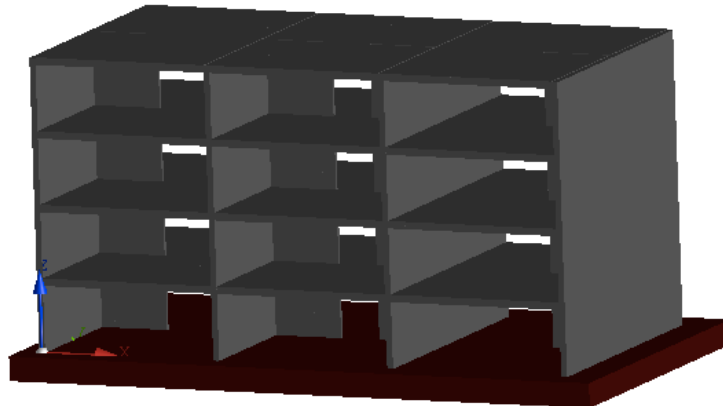


Figure 3.6: Screenshot of the ELS model of the RESA-RC-A-L4S

3.3 Numerical analyses and results

Eigenvalue analysis

An eigenvalue analysis has been undertaken as an initial check of the model and in order to determine the fundamental periods of vibration of the structure. The first mode period has been found to be 0.21 s in the longitudinal direction and 0.08 s in the transverse direction, respectively.

Pushover analyses

Conventional pushover analyses have been undertaken in each direction using a triangular load profile, with the loads applied at the barometric centre of the slab. The pushover curves in the longitudinal as well as in the transverse direction is provided in Figure 3.7 and Figure 3.8 respectively.

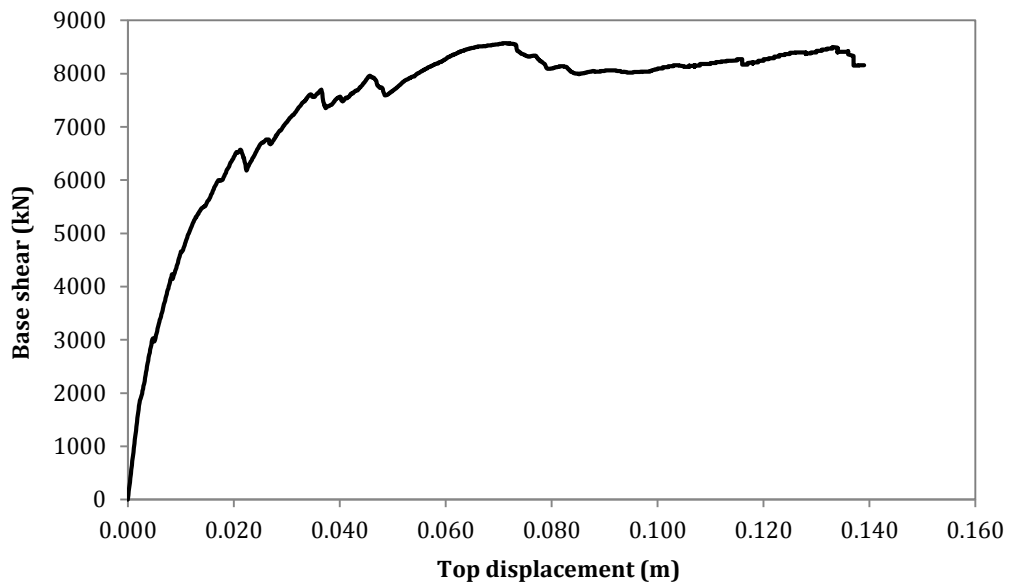


Figure 3.7: Cast-in-place RC residential apartment building with ≤ 4 storeys - Pushover curves in the longitudinal direction

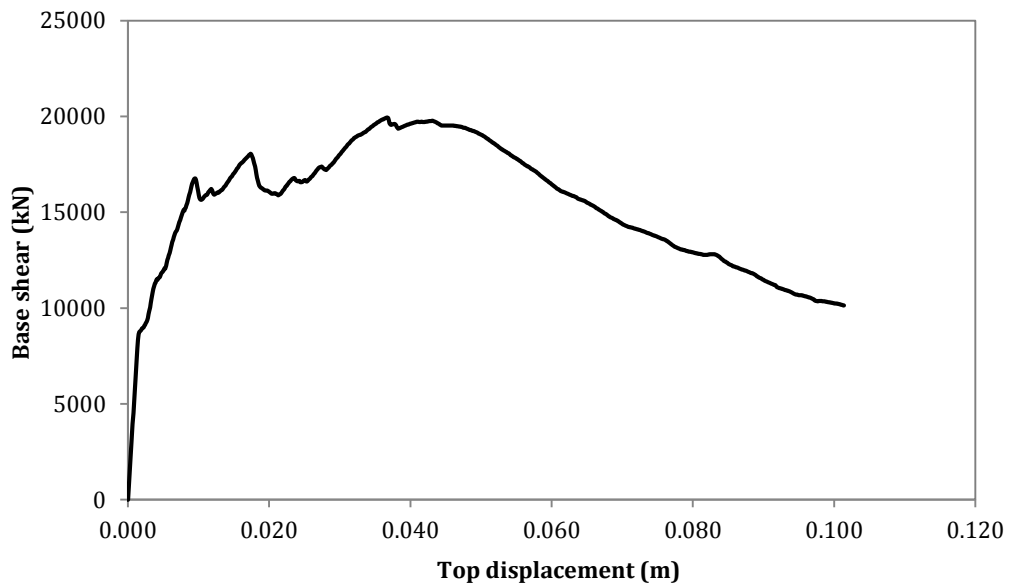


Figure 3.8: Cast-in-place RC residential apartment building with ≤ 4 storeys - Pushover curves in the transverse direction

4 Timber Frame Residential Detached Buildings (RESD-W-A)

4.1 General description and structural configuration

This building typology comprises residential detached, timber frame buildings, characterised by an internal load-bearing timber frame and an outer brick façade. Figure 4.1 shows the external view of the timber frame house in the Groningen region that has been modelled herein.



Figure 4.1: Timber Frame Residential Detached House – External view (Google Street View)

The structure has a square plan, 8.7 m on each side, with a brick garage attached to one corner of the house; it has a timber hipped roof, with a chimney on the top (approximately 7 m above the ground). The following figure shows the plan and section views of the house.

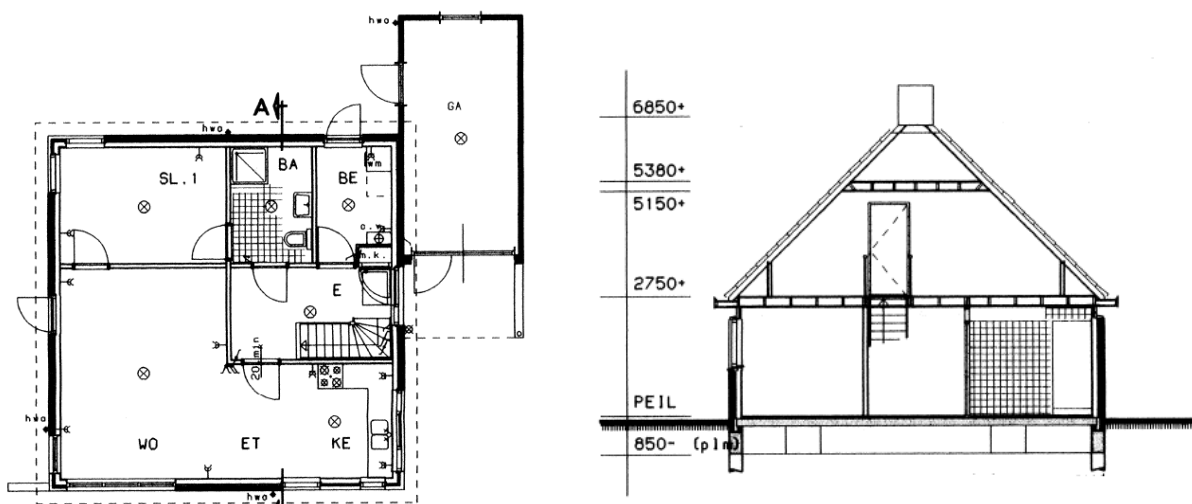


Figure 4.2: Timber Frame Residential Detached House – Plan view (left) and section view (right)

The details of a typical timber frame wall panel are shown in Figure 4.3. In particular, for an external wall, it is typically constructed as follows:

- 12.5 mm plasterboard + vapour resistant foil;
- 120 mm isolation;
- 46X121 mm stud, 600 mm centre to centre;
- 12.5 mm green sheet;
- 100 mm cavity;
- brick external cladding.

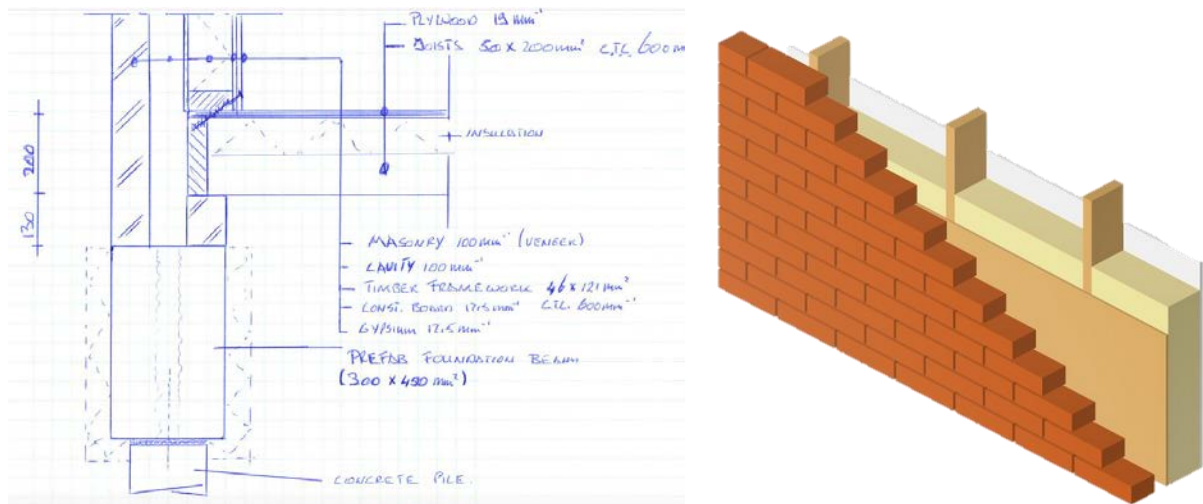


Figure 4.3: Timber Frame Residential Detached House - Typical wall details

For the internal wall, the side of the studs is reduced (46 x 71 mm, 600 mm centre to centre), the isolation is 60 mm width and the 12.5 mm of plasterboard is placed on both sides. The studs adjacent to an opening (see e.g. Figure 4.4) have a section which is twice the normal one, since they support a greater share of the load. Several horizontal elements link the structure, whilst top and bottom plates are provided along the full length of the wall (except at door openings).



Figure 4.4: Timber Frame Residential Detached House - Detail of studs adjacent to a window opening

The timber floor, as shown in Figure 4.5, consists of:

- 3 timber bearers 90 x 300 mm;
- 46 x 146 timber joists, 600 mm centre to centre;
- 19 mm plywood.

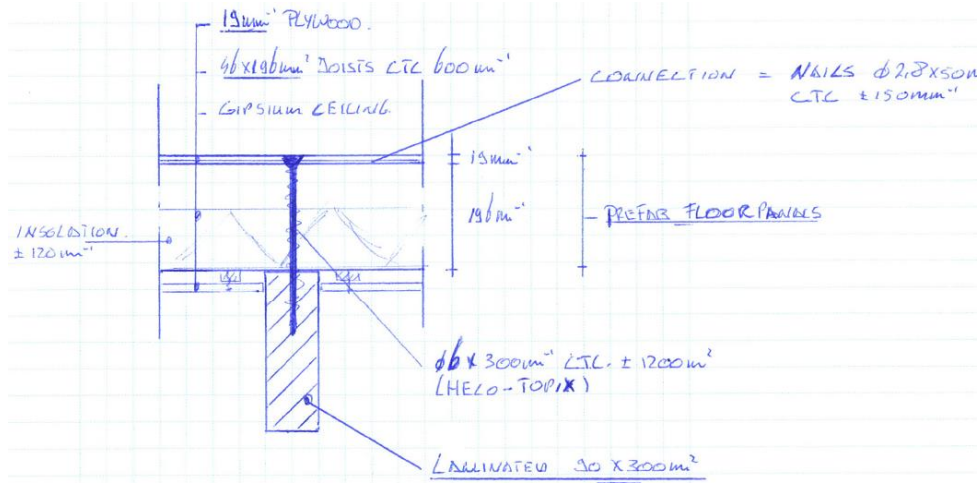


Figure 4.5: Timber Frame Residential Detached House – Typical timber floor section

4.2 Modelling assumptions

In order to evaluate the 3D nonlinear seismic response of the timber frame house, a model has been created using the FE analysis package SeismoStruct (Seismosoft, 2015), in which the structural frame has been modelled through the use of elastic elements, and nonlinear links are employed to represent the behaviour at the base of each stud.

Only the timber frame (vertical and horizontal elements, floor and roof) has been modelled, since the outer leaf of masonry does not bear the weight of the floor or roof; hence the model has a square plan (the brick garage is not considered because it is disconnected from the structure).

Materials

Since all the timber elements have been modelled with elastic frame elements, the only relevant parameters for the material are the modulus of elasticity and the specific weight, assumed as 9.5 GPa and 3.9 kN/m³, respectively.

Loads

The loads have been applied to the structure as lumped masses. Loads in addition to the self-weight for the floor, the attic and the roof are taken as 100% permanent load plus 30% live load, based on the values given below.

Table 4.1: Timber Frame Residential Detached House – assumed loads (in addition to self-weight)

Type of load	Floor [kN/m ²]	Attic [kN/m ²]	Roof [kN/m ²]
Permanent Load	0.35	0.25	0.5
Live Load	2.0	0.5	-

Other elements which have not been modelled, such as the chimney, the plasterboard of the wall and the inner wall of the first floor, have been considered though lumped masses.

Due to the absence of a rigid diaphragm, the location of the lumped masses of the floor and roof is not irrelevant. In order to understand how the structure redistributes the weight, a static analysis has been performed, loading the floor with uniform distributed mass; the masses of the floor were then lumped at the top of those studs with a larger base reaction from the static analysis.

Other modelling assumptions

Springs, modelled with multi-linear link elements, are defined at the base of the structure as the timber frame simply rests on the foundation beams. It is assumed that the studs slide indefinitely in three directions (two for the corner studs), with only friction resisting the motion. In the direction outwards of the structure, after 120 mm of sliding the stud loses its support because of the cavity between the frame and the outer façade. The link does not permit rotations to occur, since it is believed that the presence of the plasterboard panels prohibits the overturning of the studs.

A static analysis has been performed, with the model fixed at the base, in order to obtain the base reaction for each stud, and its axial load is then multiplied by 0.5 (assumed coefficient of friction for wood-wood) in order to define the lateral resistance force for each link element situated under each stud.

A screenshot of the model is presented in the following figure.

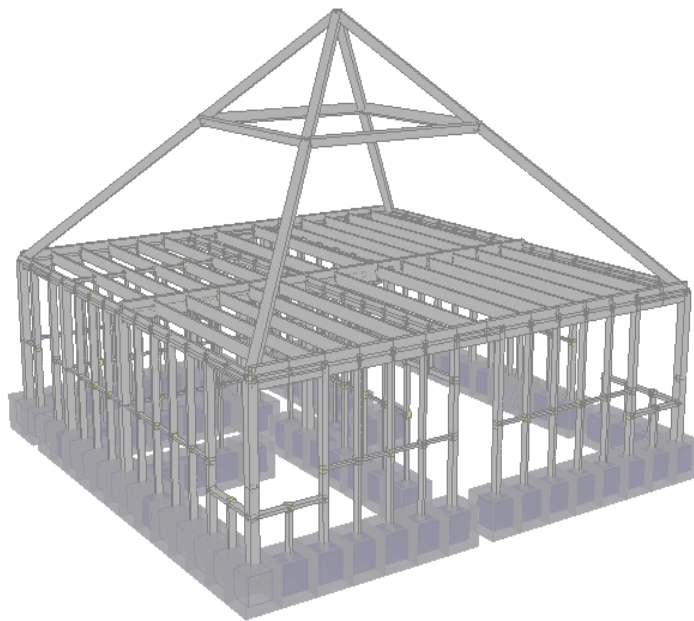


Figure 4.6: Screenshot of the SeismoStruct model of the RESD-W-A index building

4.3 Numerical analyses and results

Eigenvalue analysis

An eigenvalue analysis has been undertaken as an initial check of the model. The first mode period was found to be 0.71 s (with 76% modal mass) in the transverse direction and 0.61 s (with 89% modal mass) in the longitudinal direction.

Given that the periods of vibration for this structure seemed high for a single storey model, a second model has been developed considering also the stiffness contribution of the plasterboard panels. They have been modelled using two equivalent struts for each panel. With this assumption, the system has a higher stiffness, leading to a period of 0.21 s (with 72% modal mass) in the longitudinal direction and 0.18 s (with 42% modal mass) in the transverse direction.

Pushover analyses and sensitivity studies

Given the simplicity of the structure, a conventional force-based pushover analysis has been performed in each direction (longitudinal and transverse), assuming the top node of the roof as the control node. A distribution of forces proportional to the masses and the height has been considered.

A comparison of the pushover curves obtained for the longitudinal direction, with and without the plasterboard panels, is shown in Figure 4.7.

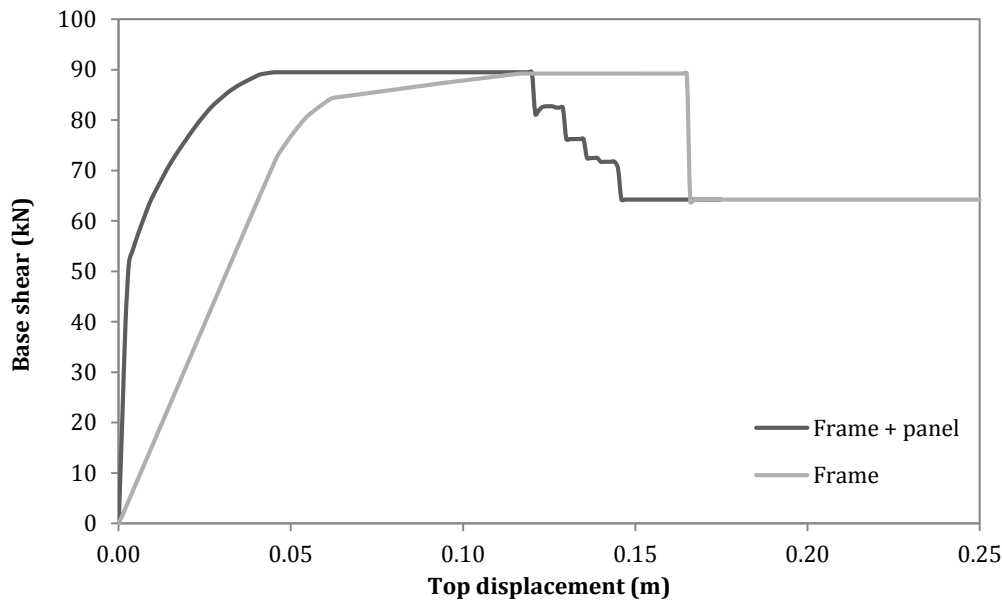


Figure 4.7: Pushover curves in the longitudinal direction for the RESD-W-A index building

When the plateau of the curve is reached, it means that all the links under the structure are activated and are providing the maximum resistance to prevent sliding; the drop in the curve represents the loss of support of some studs.

The same maximum and residual base shear is obtained in the two cases, because the springs under the structure are defined in the same way, using the axial load obtained from a static analysis; however, the initial stiffness and the ultimate displacement are different when the contribution of the panels is considered.

The presence of the equivalent struts (to represent the plasterboard panels) makes the structure much stiffer and so the springs are activated at lower global displacements, and subsequently sliding and unseating of the studs happens earlier in the analysis. The residual base shear after unseating is due to the springs which do not unseat (as they move inside the house).

The pushover curves for the transverse direction are shown in Figure 4.8.

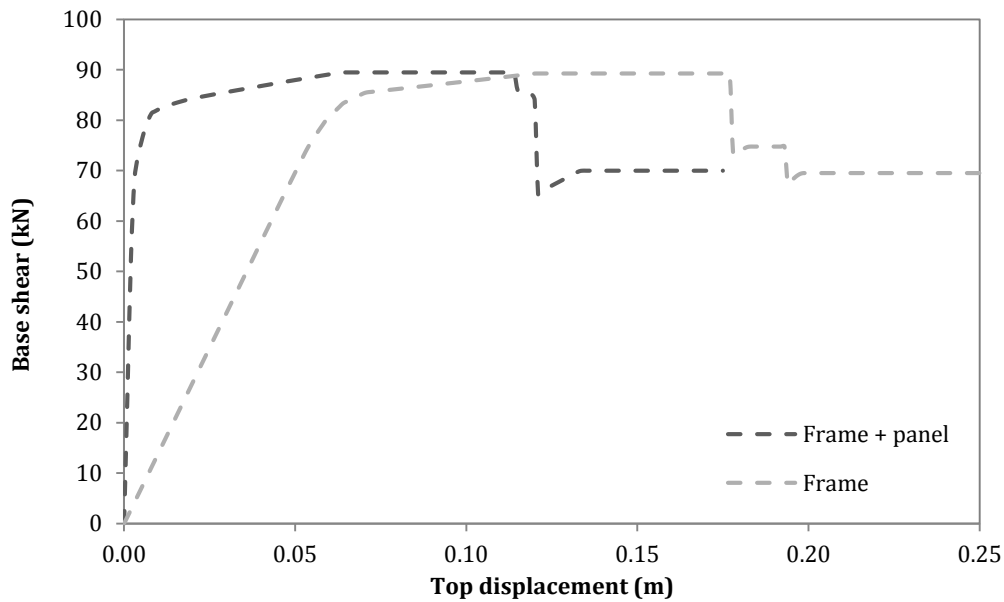


Figure 4.8: Pushover curves in the transverse direction for the RESD-W-A index building

As already mentioned for the longitudinal direction, the same base shear is reached with and without the plasterboard, but the change of stiffness due to the modelling of the panels produces a different behaviour of the structure above the springs, and the unseating of the studs occurs earlier when compared with the model without the equivalent struts.

Figure 4.9 presents a comparison between pushover curves in the longitudinal and transverse directions for the structure modelled without the stiffness contribution of the panels. The curves are very similar, since the structure is almost symmetrical; the maximum base shear is identical since the spring provides the same resistance in both direction (based on its axial load), the residual strength is different because the studs that unseat are not the same in both directions.

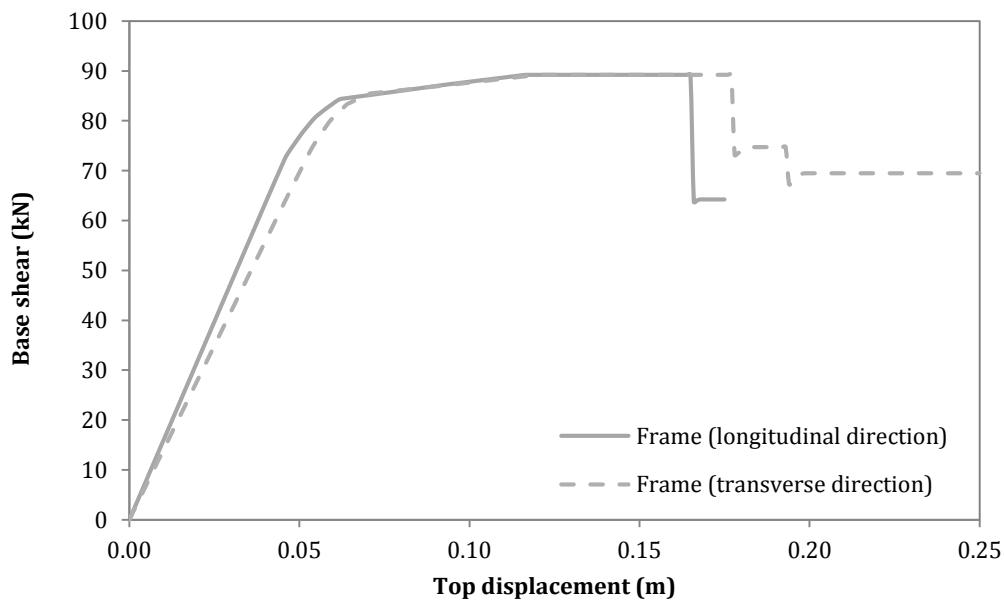


Figure 4.9: Pushover curves comparison for the RESD-W-A index building

5 Steel Frame Industrial Buildings (AGRI/INDU/COML-S-B/A)

5.1 General description and structural configuration

Within the agricultural, industrial and commercial/recreational (large opening) usage category there are two steel portal frame buildings typologies, AGRI/INDU/COML-S-B and AGRI/INDU/COML-S-A, which have braces in one or both directions, respectively. A single storey real industrial index building with braces in one direction (see Figure 5.1) has been modelled, and used for both typologies (as it is assumed that the typology with bracing in both directions can be represented by the braced direction of this building). The index building has five steel portal frames along the longitudinal direction and steel braced frames in the transverse direction.



Figure 5.1: AGRI/INDU/COML-S-B – external view

The structure plan dimensions are 20 m and 15 m in longitudinal and transverse directions, respectively, as shown in Figure 5.2.

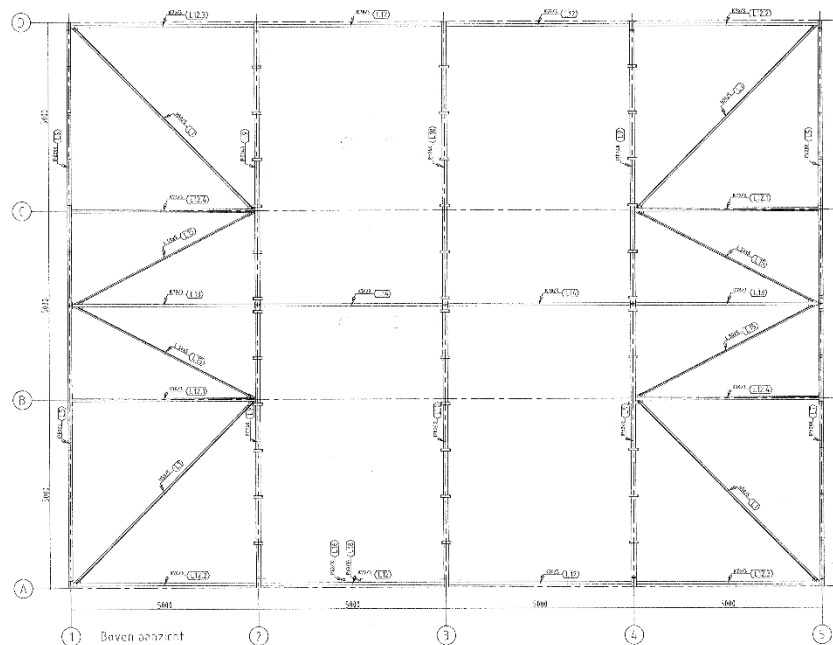


Figure 5.2: Plan view of AGRI/INDU/COML-S-B/A

The total height of the structure is 6.53 m (top of the roof). The height of the outer columns is 3.8 m, while the height of the inner columns is 5.62 m, as shown in Figure 5.3 and Figure 5.4.

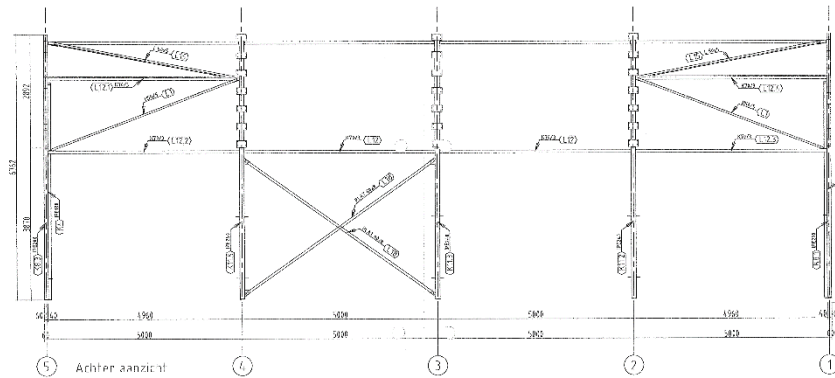


Figure 5.3: Lateral view of AGRI/INDU/COML-S-B/A

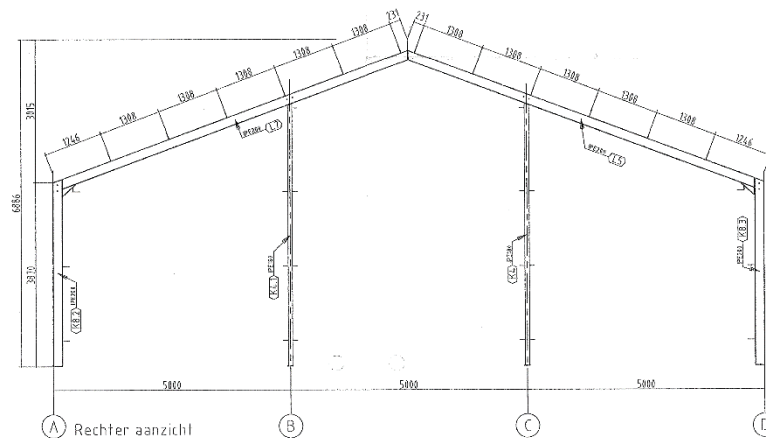


Figure 5.4: Front view of AGRI/INDU/COML-S-B/A

The portal frames are orthogonally connected through lateral members (rectangular hollow sections of 70x70x3 mm). Concentric lateral braces (rectangular plates of 60x6 mm) and roof braces (L-shape sections of 50x50x3 mm) have been used for defining the steel braces in the transverse direction, as shown in Figure 5.5.

The geometrical details of the structural elements (i.e. columns and beams) are given in the table below.

Table 5.1: One-storey steel frame – geometrical details of beams and columns for AGRI/INDU/COML-S-B/A

Portal	Columns	Beams
1 - 5	IPE 180, IPE 200	IPE 200
2 - 3 - 4	IPE 240	IPE 240

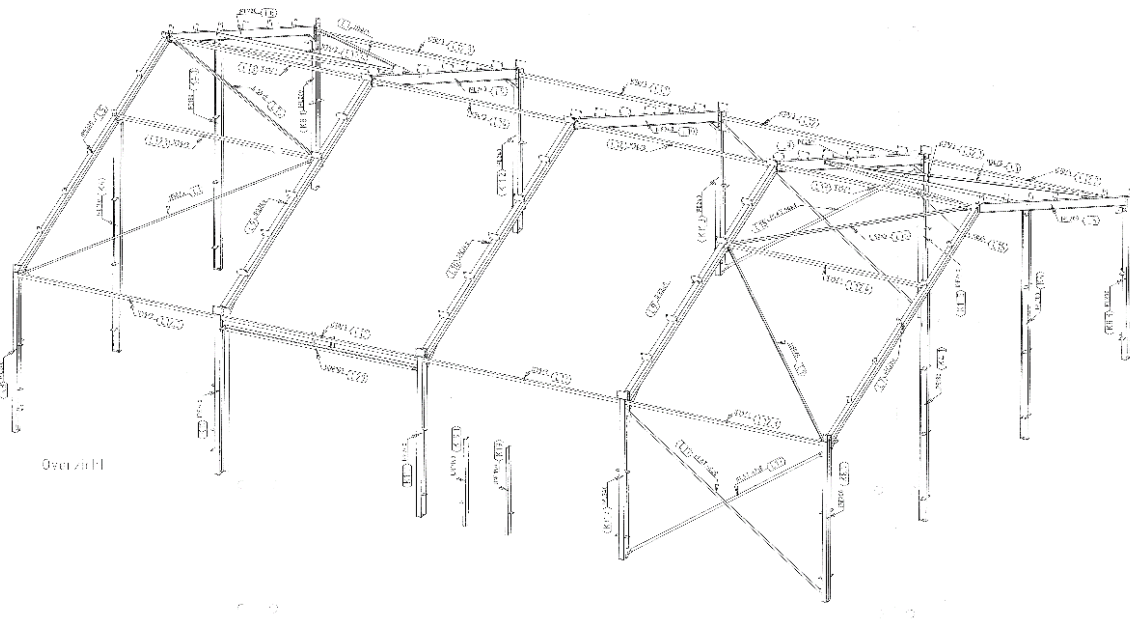


Figure 5.5: 3D View of AGRI/INDU/COML-S-B/A

5.2 Modelling assumptions

The structure has been modelled in the structural analysis package SeismoStruct (Seismosoft, 2015) using steel structural elements. The columns, beams and bracing have been modelled using 3D force-based inelastic fibre-elements (infrmFB) with 5 integration sections with 150 section fibres. The lateral members, which connect each portal frames along the longitudinal direction, are characterised by rectangular hollow sections (rhs), and have been modelled through elastic frame elements.

Materials

A *bilinear* model has been used to define the steel material properties using the parameters listed in Table 5.2.

Table 5.2: Bilinear model steel material parameters

PARAMETERS	Columns and Beams
E (GPa)	200
f_y (MPa)	270
μ	0.1
γ (kN/m ³)	78

Loads

The vertical loads assigned for the portal frame have been applied to each beam as permanent loads in terms of forces in the Z direction. Loads in addition to the self-weight for the roof are taken as 100% permanent load, based on the values given in Table 5.3. The roof of the structure is not flat and hence live loads (due to the presence of occupants) have not been considered.

Table 5.3: One storey steel building – applied permanent loads (in addition to self-weight)

Load	Permanent Load [kN/m ²]	Live Load [kN/m ²]	Inter-column Length [m]	Total Distributed Load [kN/m]	
				Internal Frame	External Frame
Roof	0.5	0	5	2.5	1.25

Other modelling assumptions

Some sensitivity analyses have been carried out to understand the influence of local buckling, connection flexibility, connection of the rhs lateral sections (either pinned or fixed) and connection failure.

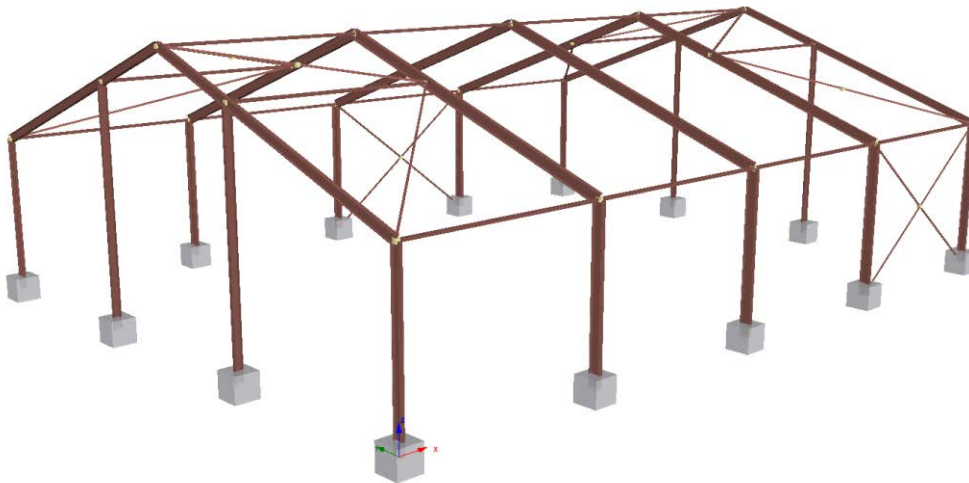


Figure 5.6: Screenshot of the SeismoStruct model of the AGRI/INDU/COML-S-B/A index building

The various modelling assumptions for this index building are reported below:

- Semi-rigid springs were added to model the joints of the portal frame and the base connections. The properties of these springs were assigned typical semi-rigid moment-rotation relationships (for the beam-column connections a yield moment of 60 MPa and yield rotation of 10^{-3} rad was defined; for the base connections these values were 100 MPa and 10^{-3} rad, respectively).
- Moment releases were used to model the pinned connections of the lateral rectangular hollow sections.
- Buckling has been modelled following recommendations of Uriz et al. (2008), wherein imperfections have been introduced at the mid-point of each compression strut of the lateral bays. These imperfections have been modelled by dividing the element into two beam-column elements and moving the node of one with respect to the other by 0.075% of the free brace length.
- Connection failure has been modelled by setting the ultimate rotation of the springs to 0.1 rad (using a multi-linear model for the semi-rigid springs).
- Performance criteria have been used in order to estimate the ultimate displacement capacity; the ultimate rotation capacity of each element has been set as 8 times the yielding rotation capacity following the recommendations of Eurocode 8 Part 3 (CEN, 2005).

5.3 Numerical analyses and results

Eigenvalue analysis

An eigenvalue analysis has been undertaken as an initial check of the model. The first mode period was found to be 0.45 s (with 32% modal mass) in the transverse direction and 0.43 s (with 57% modal mass) in the longitudinal direction.

Pushover analyses and sensitivity studies

Given the simplicity of the structure, a conventional force-based pushover analysis using a uniform loading profile has been undertaken in each direction.

A comparison of the pushover curves under different assumptions is shown in Figure 5.7 where it is possible to see how the local buckling has a large influence on the base shear capacity. This is because the resistance capacity of the structure in the longitudinal direction arrives from the braced frame. Having pinned lateral beams slightly decreases further the strength and stiffness, whilst the influence of modelling the ultimate rotation of the connections is minimal. The first ultimate rotation capacity is reached after 0.5 m of top displacement.

Given that local buckling affects the performance of the structure, and it is more realistic to include it in the structural model, the pushover curves with buckling will be used for the fragility model (see Figure 5.8). This pushover curve is also based on semi-rigid connections and pinned lateral beams, given that these are also more realistic assumptions, albeit with less impact on the global response.

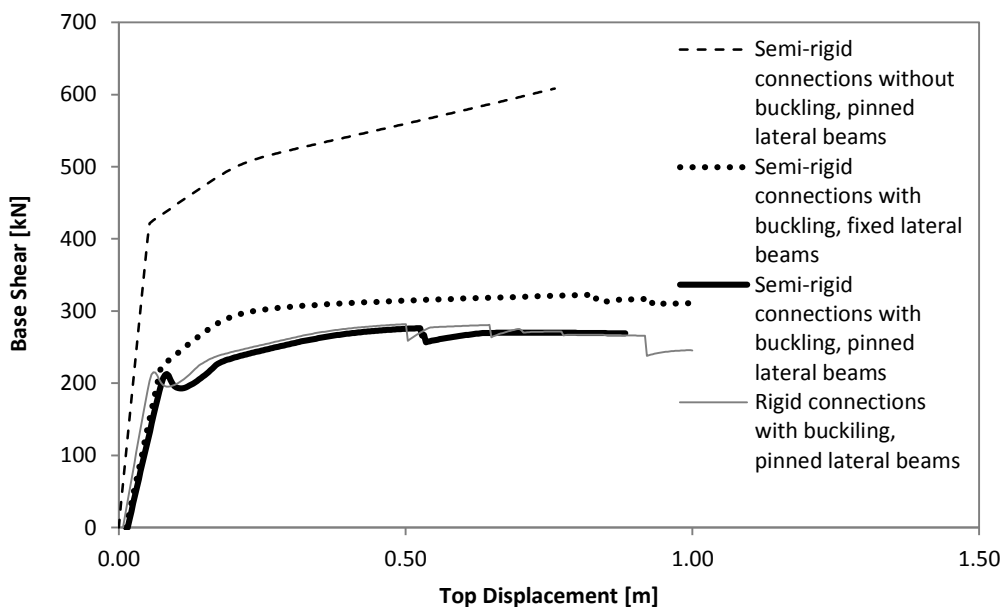


Figure 5.7: Pushover curves in the longitudinal direction under different modelling assumptions

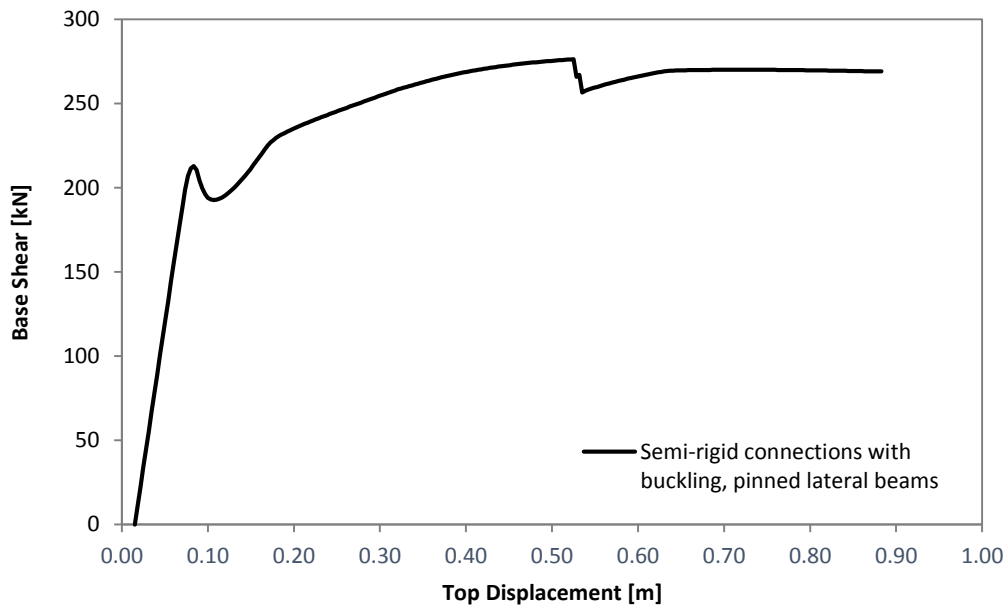


Figure 5.8: Selected pushover curve in the longitudinal direction

The deformed shape at ultimate displacement is shown in Figure 5.9, which shows that collapse occurs due to the buckling and the attainment of the ultimate rotational capacity of the columns.

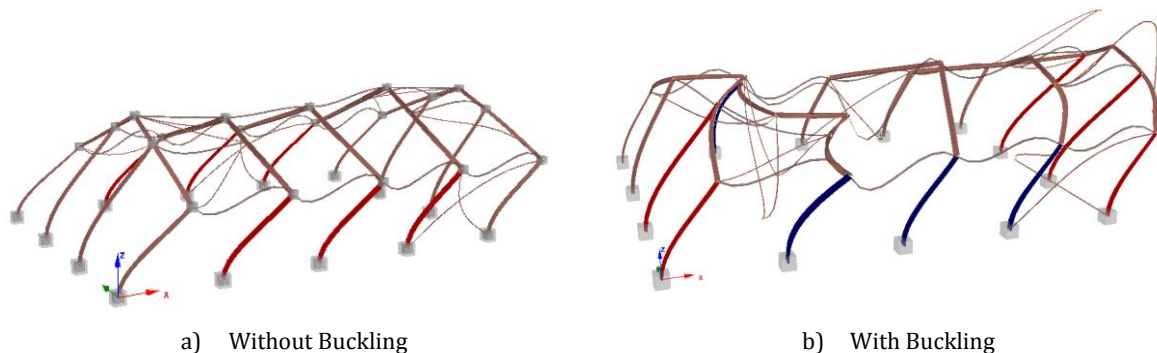


Figure 5.9: Deformed shape (long. direction) at ultimate displacement, showing the elements (in red and blue) that reach their rotational capacity

A comparison of the pushover curves in the transverse direction under different assumptions is shown in Figure 5.10. In the transverse direction, the connection flexibility and pinning (or not) of lateral beams also has an influence on the stiffness and strength. In this case the ultimate displacement is affected by the modelling of ultimate rotation of the connections and the attainment of the ultimate rotational capacity. The pushover curve with semi-rigid connections, pinned lateral beams, and modelling of ultimate rotation of the connections will be used for the fragility model (see Figure 5.11). The ultimate displacement is taken as the point at which the base shear drops by more than 20%.

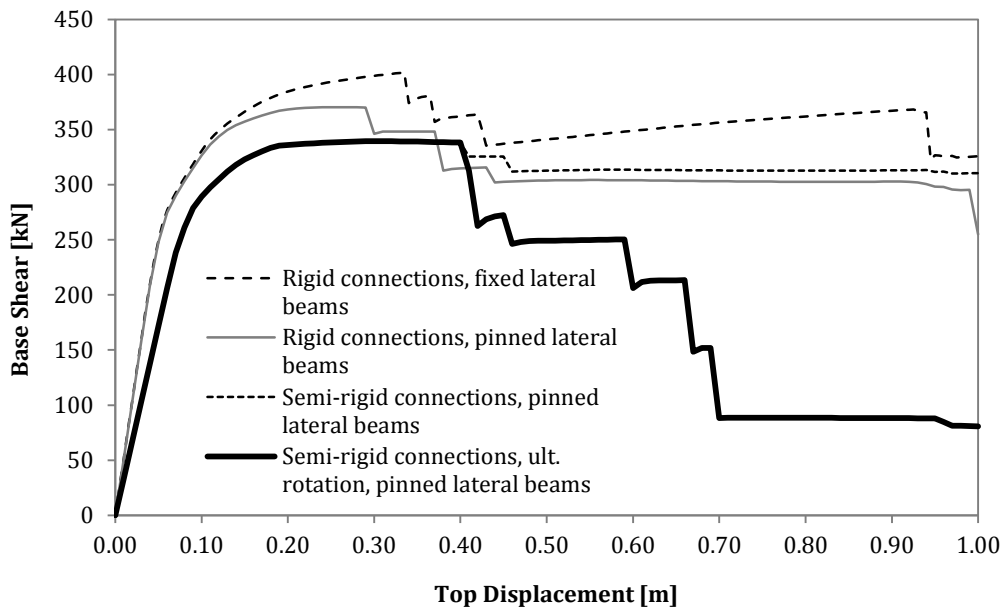


Figure 5.10: Pushover curves in the transverse direction under different modelling assumptions

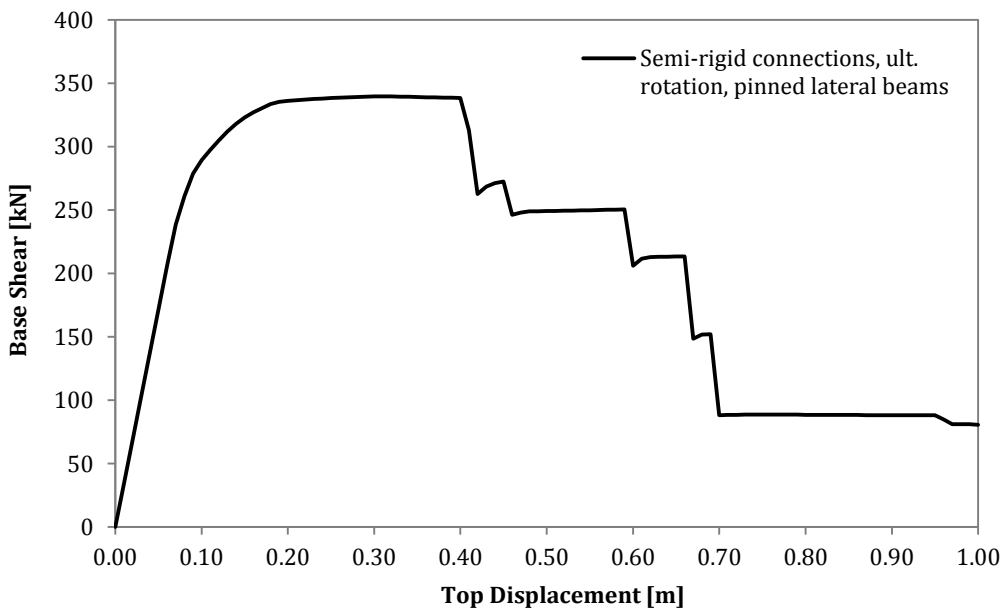


Figure 5.11: Selected pushover curve in the transverse direction

The deformed shape at ultimate displacement is shown in Figure 5.12, which shows that collapse occurs due to the failure of the connections and the attainment of the ultimate rotational capacity.

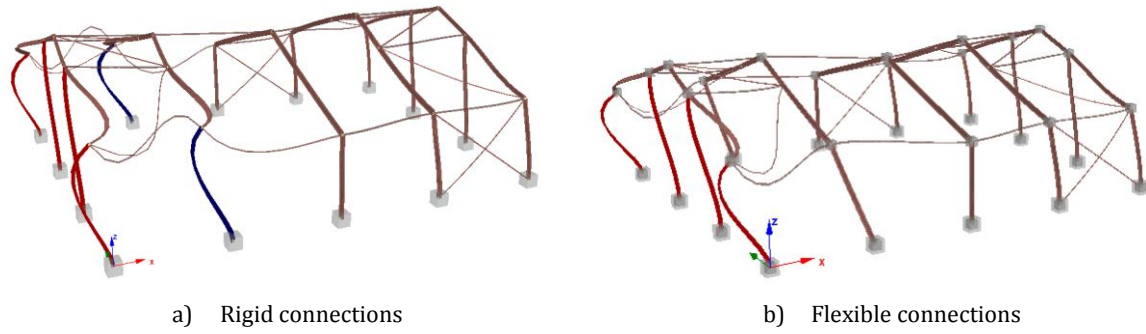


Figure 5.12: Deformed shape (trans. direction) at ultimate displacement, showing the elements (in red and blue) that reach their rotational capacity

6 Timber Agricultural Barns with URM walls (AGRI/INDU/COML-W-A)

6.1 General description and structural configuration

This building typology comprises old barns, typically used for agricultural purposes, which are constructed with a masonry perimeter fence covered by a lightweight wooden roof. Although the material properties have not been made available for this structure, it has been possible to construct a model based on the input provided by local engineers, attempting also to consider the effect of material deterioration and physical decay over time.

Figure 6.1 shows three global external views and two internal roof details that are typical for these construction typologies. The barn comprises the main body of the structure that is connected with other secondary internal and external structures.

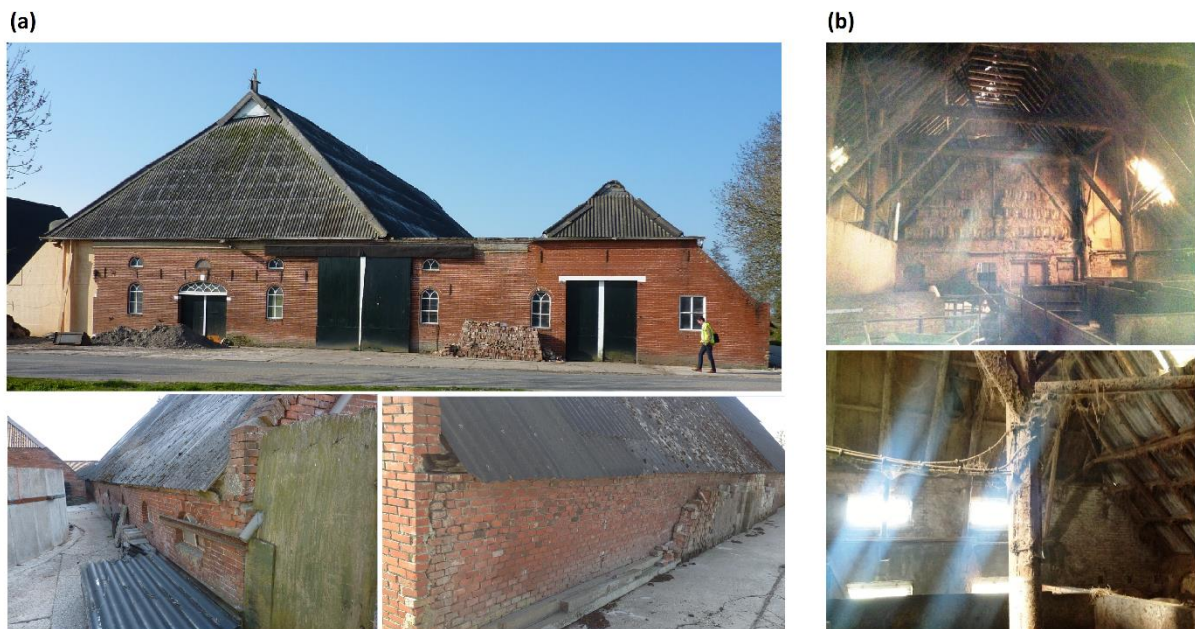


Figure 6.1: Timber URM Old Barn - (a) Front and Lateral external views; (b) Internal views of lightweight wooden roof and its load-bearing structure

According to local engineers, the following may be assumed:

- The timber most likely originated from oak trees.
- These structures were most likely erected more than 100 years ago.
- The masonry walls have probably been built later with respect to the wooden roof, whose function was initially the containment and the protection of animals. Thus, the roof was originally free-standing, but through the years, under its self-weight and deterioration, the roof was gradually supported by the masonry walls below.
- Decay of the structural elements is present, both for the wood and masonry (see Figure 6.2).



Figure 6.2: Timber URM Old Barn – Damage associated with decay over time

The building is 39.3 m long and 21 m wide at the ground level, with a maximum height of 12.2 m. Therefore, the overall footprint is 825.3 m². The index building has thus been produced based on the above input and adopting the geometrical details based on the available structural drawings for a real structure, summarised in the following tables and figures, i.e. masonry walls in longitudinal direction (Figure 6.3b), transverse façade (Figure 6.3a) and lightweight wooden roof elements (Figure 6.5).

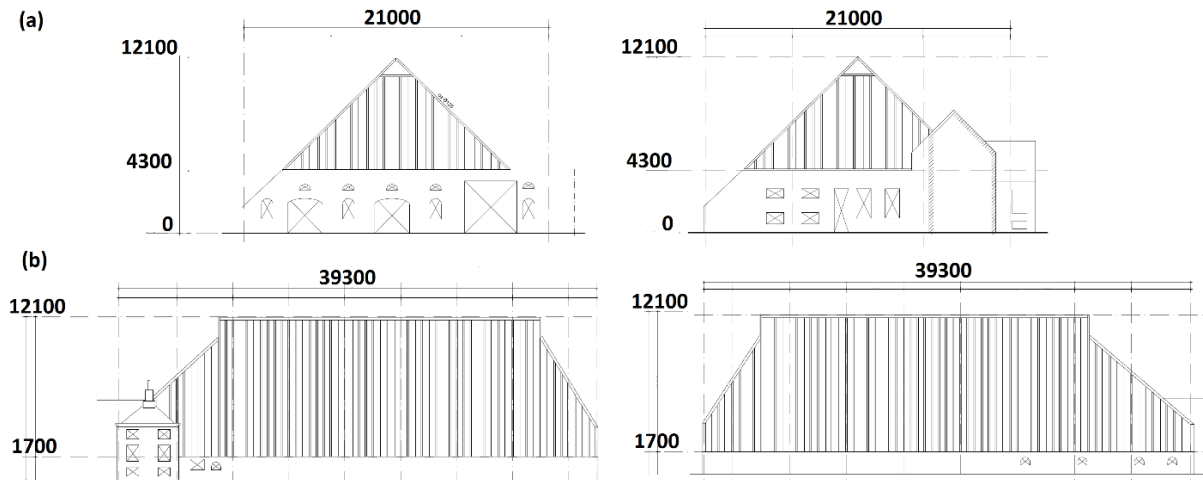


Figure 6.3: Timber URM Old Barn – Perspective Drawings

The walls in longitudinal direction have a 1.7 m height. The brick disposition, used to assemble and erect the walls, is shown in Figure 6.5. A decayed mortar layer between the bricks is considered.

Table 6.1: Timber URM Old Barn – Geometrical wall details in longitudinal direction

	Thickness	Length
Longitudinal Walls	0.23 m	39.3 m

The transverse front façade is composed of six different vertical and two different horizontal structural elements, while the transverse back façade is composed of six different vertical and three different horizontal structural elements, as shown in Figure 6.4.

The foundation system consists of piles fully-fixed at the base (but these have not currently been considered in the model).

Table 6.2: Timber URM Old Barn – Geometrical wall details in transverse direction

Façade	Vert. 1	Vert. 2	Vert.3	Vert.4	Vert. 5	Vert. 6	Vert. 7	Vert. 8	Vert. 9	Vert. 10	Vert. 11	Vert. 12
2	-	-	-	-	-	-	2.15x 0.23m	1.4x 0.23m	0.36x 0.23m	4.3x 0.23m	3.0x 0.23m	1.19x 0.23m
1	1.3x 0.23m	0.96x 0.23m	0.63x 0.23m	2.5x 0.23m	2.15x 0.23m	2.3x 0.23m	-	-	-	-	-	-

Façade	Horizontal 1	Horizontal 2	Horizontal 3	Horizontal 4	Horizontal 5
2	-	-	0.58 x 0.23 m	1.00 x 0.23 m	1.26 x 0.23 m
1	0.58 x 0.23 m	0.96 x 0.23 m	-	-	-

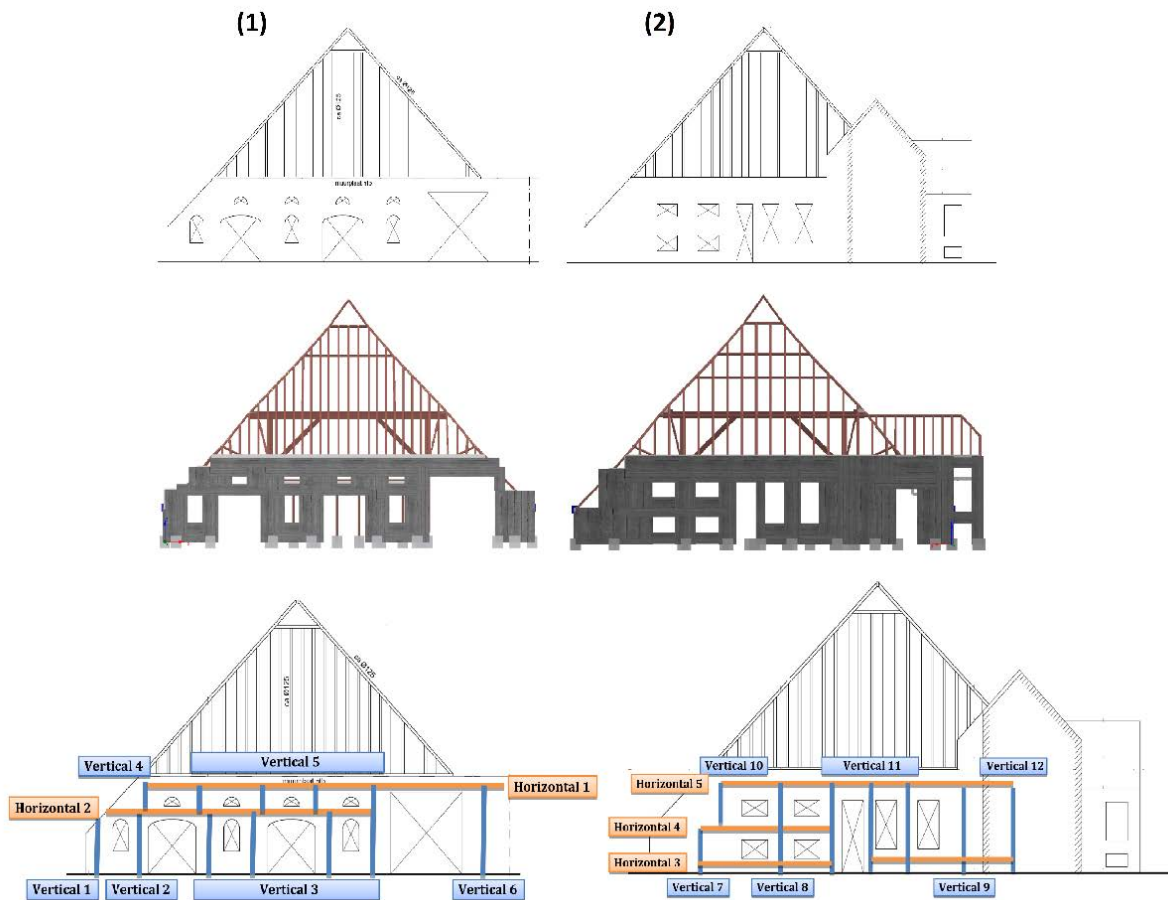


Figure 6.4: Timber URM Old Barn – Façade layout and structural elements in longitudinal direction

The following figure shows the element composition of the lightweight wooden roof and the connections between the barn covering and the masonry walls. The structural section shown in the figure represents a typical load-bearing resisting frame. This frame is repeated eight times in the longitudinal direction, with a distance of 4.6 m, in order to support the roof weight. The gabled roof elements are settled on a masonry horizontal beam called “muurplat”, on which these wooden elements have slightly slipped through the years. The modelling assumptions for this index building are further described in the next section.

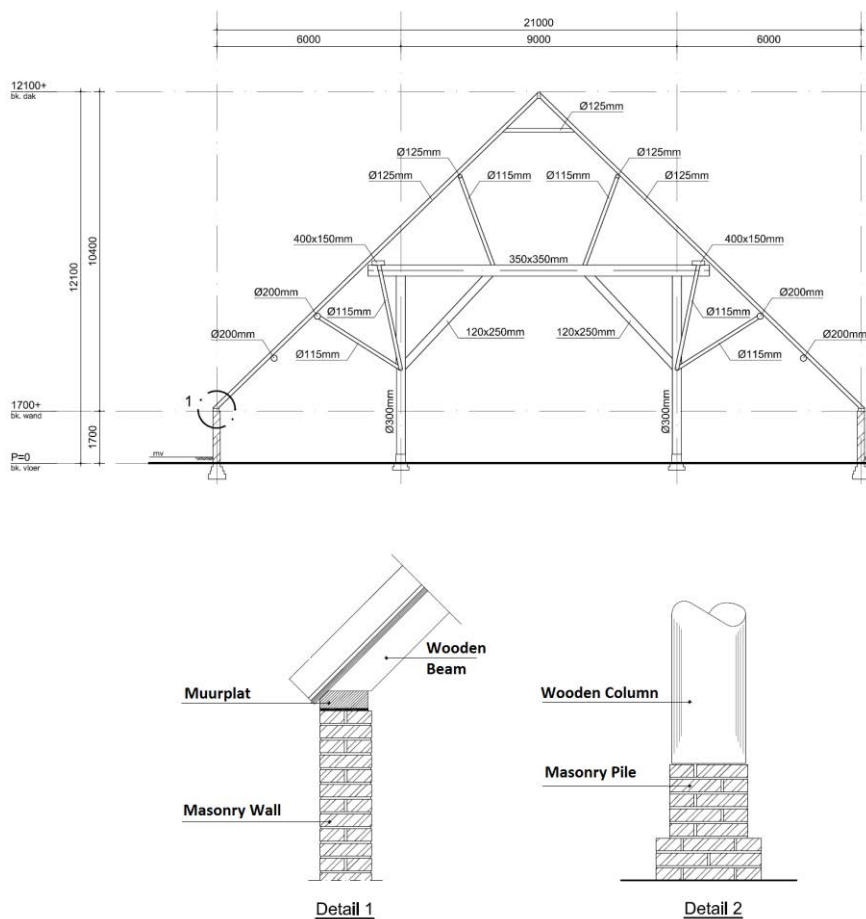


Figure 6.5: Timber URM Old Barn – Wooden elements and roof connection details

6.2 Modelling assumptions

The masonry structural elements have been modelled with force-based fibre-elements (infrmFB) with 5 integration sections (and 150 section fibres per section) with the structural analysis package SeismoStruct (Seismosoft, 2015). Equivalent-beam modelling has been used to represent the masonry walls. Due to the model dimensions and the large number of elements, the nonlinear analyses have been very time consuming. In order to reduce the computational effort, and considering that the global behaviour is governed by the roof-to-masonry interface, all wooden beams have been modelled through elastic frame elements with the properties given by the geometrical and material properties.

Materials

Without specific information about the material properties of these old barns and the details of structural decay, a conservative approach has been followed with what are judged to be lower bound properties for the masonry. The *bilinear steel* model has been employed for defining the deteriorated masonry. The material properties are listed in the following:

- Masonry: $E = 2.5 \text{ GPa}$; $f_y = 3.25 \text{ MPa}$; $\mu = 0$; $\varepsilon_{ult} = 0.1 \text{ m/m}$; $\gamma = 19 \text{ kN/m}^3$;

Loads

Taking into account the absence of interstorey floors and the inaccessibility of the roof, the loads have been calculated by the software using the self-weight of the elements, based on the definition of the material specific weights.

Other modelling assumptions

The interface between the masonry walls and the wooden roof has been modelled through springs (modelled with symmetric bilinear link elements). In order to evaluate the structural behaviour related to the adopted connection system, two different friction coefficients (20% and 40%) have been used to define the springs.

A screenshot of the model of the timber URM old barn building is presented in the following figure.

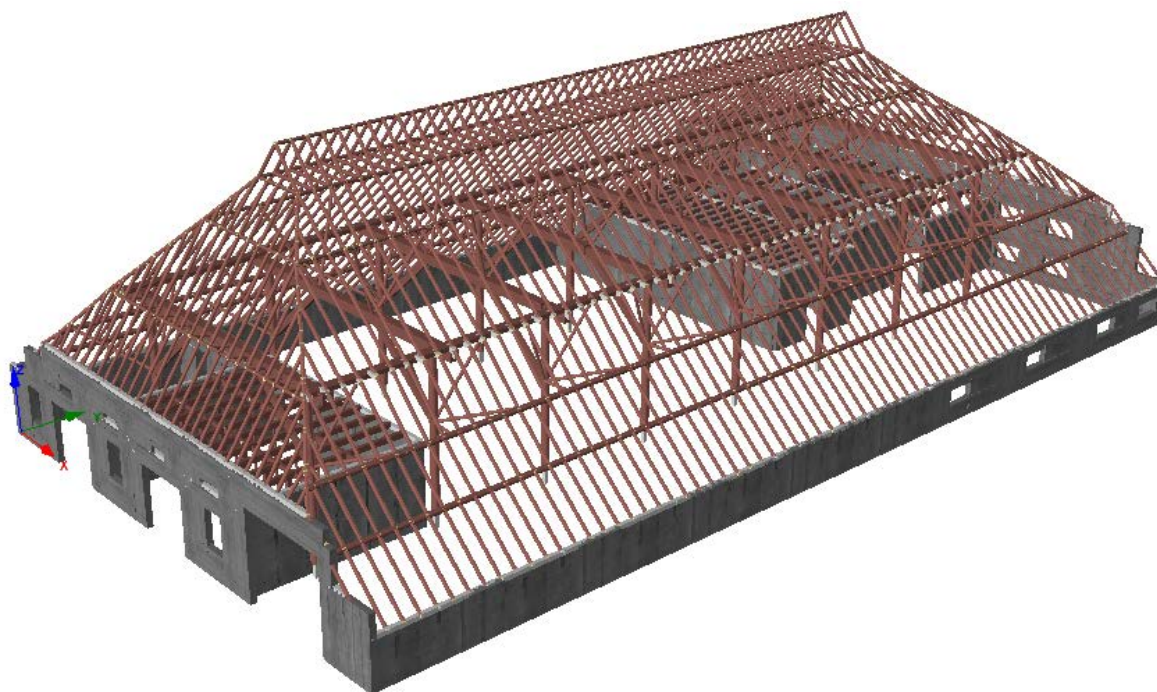


Figure 6.6: Timber URM Old Barn – SeismoStruct model

6.3 Numerical analyses and results

In order to evaluate the seismic response of the structure, a number of different cases have been investigated, summarized in the table below.

Table 6.3: Timber URM Old Barn – Analysis Cases

ANALYSES CASES	Longitudinal		Transverse	
	Friction Coefficient 20%	Friction Coefficient 40%	Friction Coefficient 20%	Friction Coefficient 40%
Façade Links	AGRI-W- A_long_FL20%	AGRI-W- A_long_FL40%	AGRI-W- A_trasv_FL20%	AGRI-W- A_trasv_FL40%
No Internal Structures	AGRI-W- A_long_NS20%	AGRI-W- A_long_NS40%	AGRI-W- A_trasv_NS20%	AGRI-W- A_trasv_NS40%
No Walls	AGRI-W-A_long_NW		AGRI-W-A_trasv_NW	

“Façade links (FL)” models consider the friction behaviour at the roof-wall interface (Figure 6.7a), while “No Internal Structures (NS)” models have the same properties of the first, without the internal structures (Figure 6.7b). The structure without the masonry walls has also been analysed (Figure 6.7c).

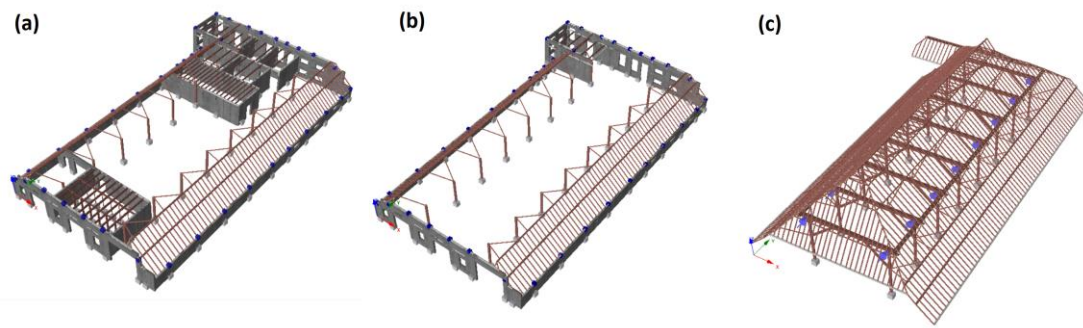


Figure 6.7: Timber URM Old Barn – Analysed Models

Eigenvalue analysis

An eigenvalue analysis has been undertaken as an initial check of the models and the results are displayed in the following table.

Table 6.4: Timber URM Old Barn – Eigenvalue Analyses

EIGENVALUE	First Longitudinal		First Transverse	
	Friction Coefficient 20%	Friction Coefficient 40%	Friction Coefficient 20%	Friction Coefficient 40%
Façade springs	0.38 s (32.13%)	0.34 s (34.18%)	0.34 s (23.76%)	0.30 s (24.31%)
No Internal Structures	0.34 s (35.61%)	0.30 s (35.68%)	0.45 s (61.81%)	0.42 s (62.31%)
No Walls	0.68 s (87.42%)		0.73 s (93.53%)	

Pushover analyses and sensitivity studies

Conventional force-based pushover analyses have been performed in each direction, using a triangular loading profile proportional to the masses. For this structure the entire load has been applied to the wooden frame connection joints, as shown in Figure 6.8, because these elements represent the load-bearing component of the chosen index building typology.

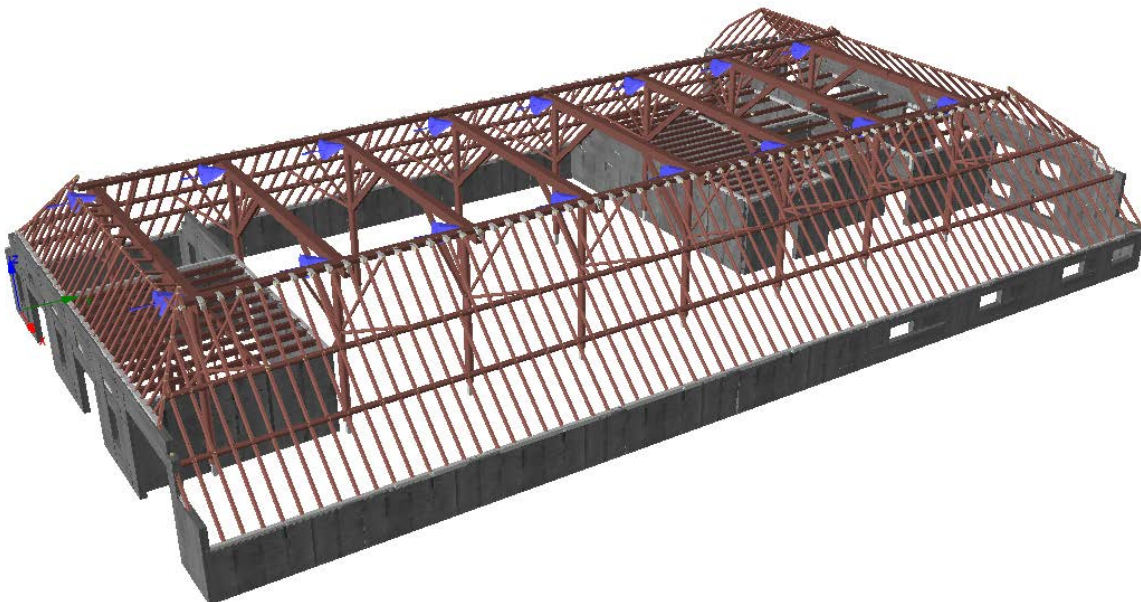


Figure 6.8: Timber URM Old Barn – application of pushover loads

In Figure 6.9, the various longitudinal pushover results are shown. The “No Walls” model is the most flexible and reaches the highest levels of ultimate deformation. However, this version of the model is not judged to be realistic. The removal of the internal structures reduces the base shear capacity and increases slightly the ultimate displacement capacity, whilst the reduction of the friction coefficient has a similar influence.

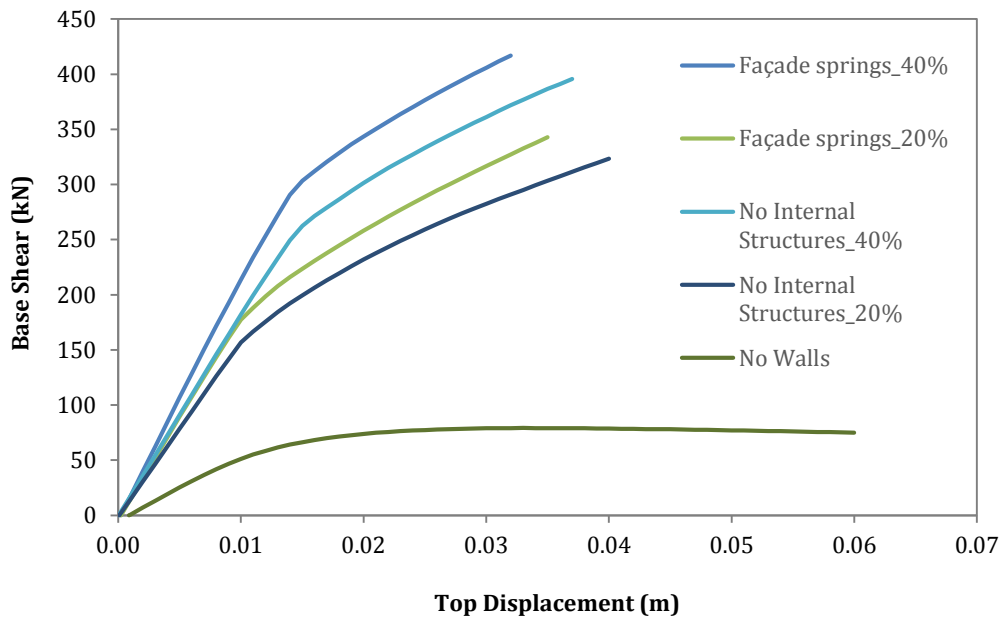


Figure 6.9: Timber URM Old Barn – Pushover curves in the longitudinal direction

The deformed shape at ultimate displacement in the longitudinal direction is shown in Figure 6.10, which displays the roof slipping over the masonry support, activating the shear reaction in the springs due to the adopted friction coefficient. The ultimate displacement is assumed to correspond to the collapse of the masonry walls.

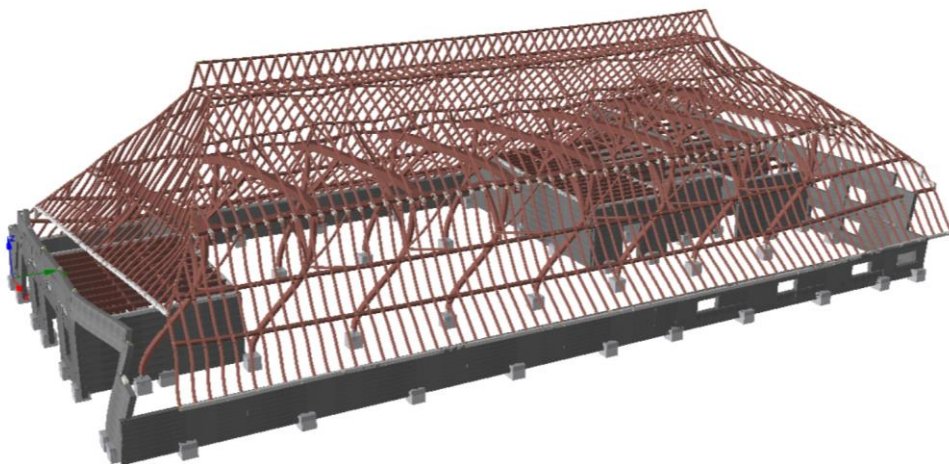


Figure 6.10: Timber URM Old Barn – Deformed shape at ultimate displacement (longitudinal direction)

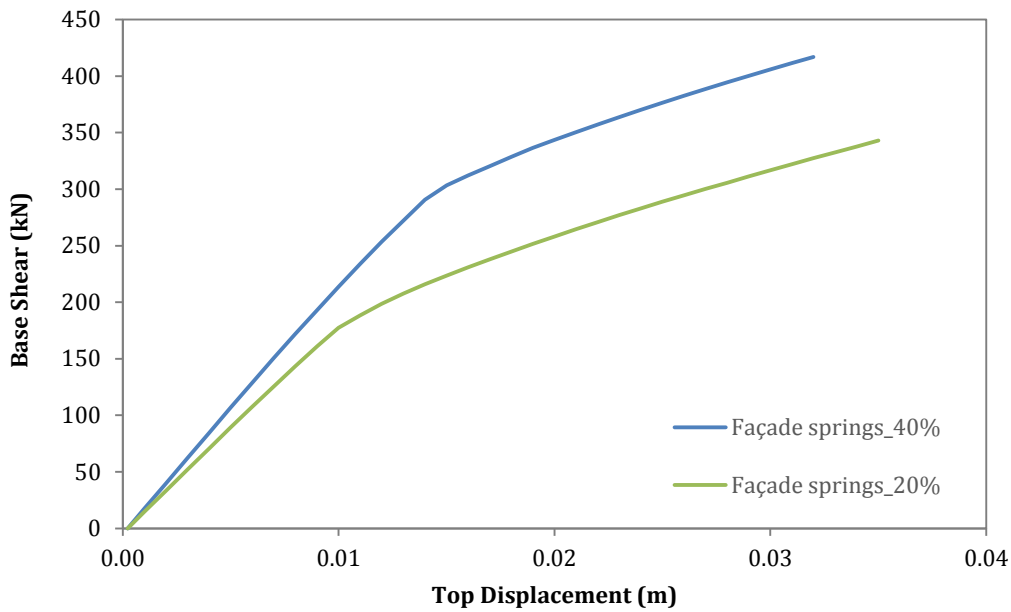


Figure 6.11: Timber URM Old Barn - Selected pushover curves in the longitudinal direction

In the transverse direction, as shown in Figure 6.12, the “Façade springs” and “No Internal Structures” group models coincide because the increase in shear force in the transverse direction due to internal structures is almost null.

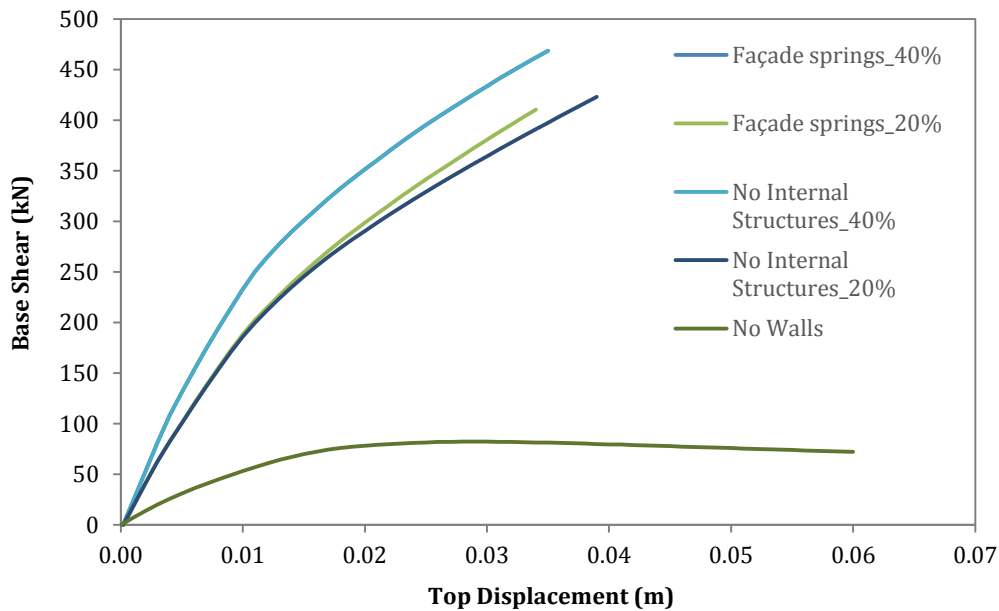


Figure 6.12: Timber URM Old Barn - Pushover curves in the transverse direction

The deformed shape at ultimate displacement in the transverse direction is shown in Figure 6.13. The ultimate displacement is assumed to correspond to the collapse of the masonry walls.

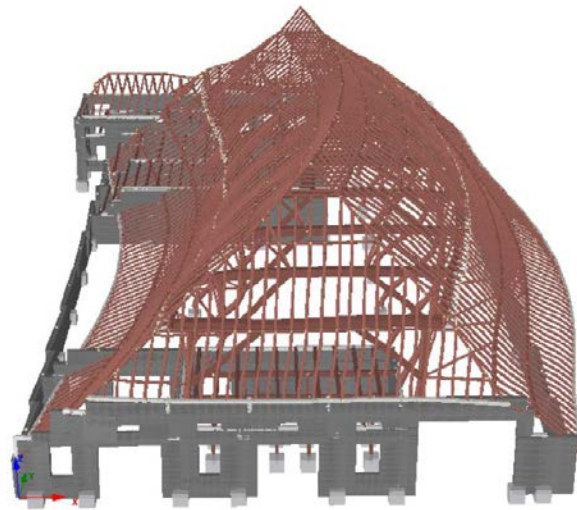


Figure 6.13: Timber URM Old Barn – Deformed shape at ultimate displacement (transverse direction)

Again, in the transverse direction the roof slips over the masonry support activating the shear reaction in the springs due to the adopted friction coefficient. In this direction, the change in friction coefficient influences the base shear capacity but has a minimal influence on the ultimate displacement.

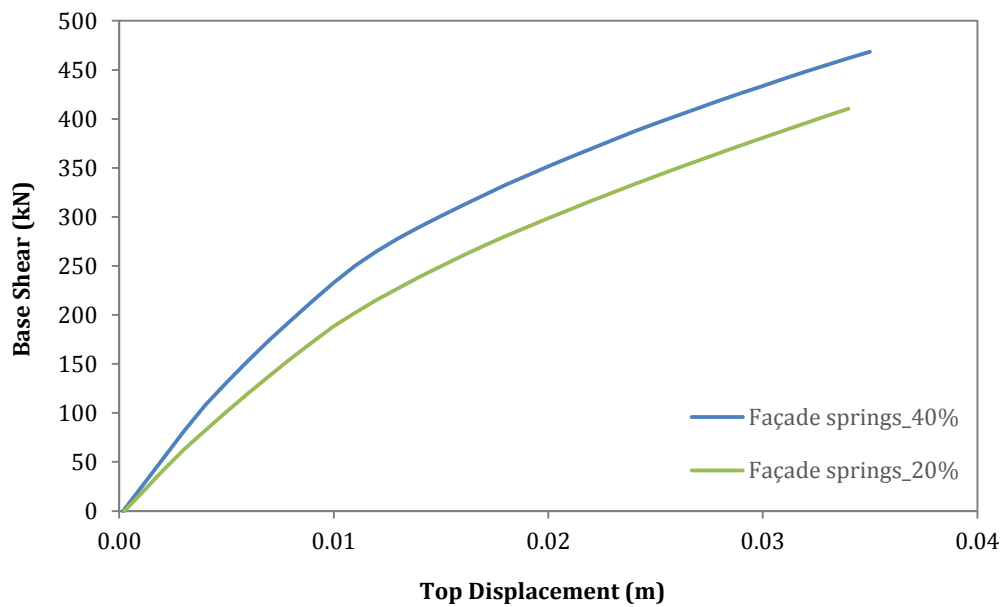


Figure 6.14: Timber URM Old Barn – Selected pushover curves in the transverse direction

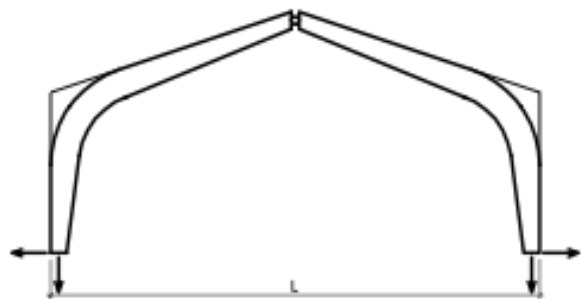
7 Glulam Portal Frame Buildings with Steel Stability Bracing (AGRI/INDU/COML-W-B1)

7.1 General description and structural configuration

Glued laminated timber (commonly referred to as glulam) is a form of structural timber that is made up of a number of layers of timber that are bonded together with durable, moisture-resistant structural adhesives. This structural timber is generally used to construct single-storey parallel portal frames, which are typically formed as pinned arches in the Netherlands, as shown in Figure 7.1b. The lateral resistance in the direction orthogonal to the portal frames is provided by either steel stability bracing (as described in this Chapter) or unreinforced masonry walls (as described in Chapter 8). The timber frame is generally bolted with steel plates to the concrete foundation.



(a)



(b)

Figure 7.1: (a) Glulam portal frame under construction, (b) common "arch" portal frame found in the Netherlands

A real index building was not available for this building typology, but a typical frame was dimensioned by Arup engineers (see Figure 7.2) and used to produce a structural model with typical material properties.

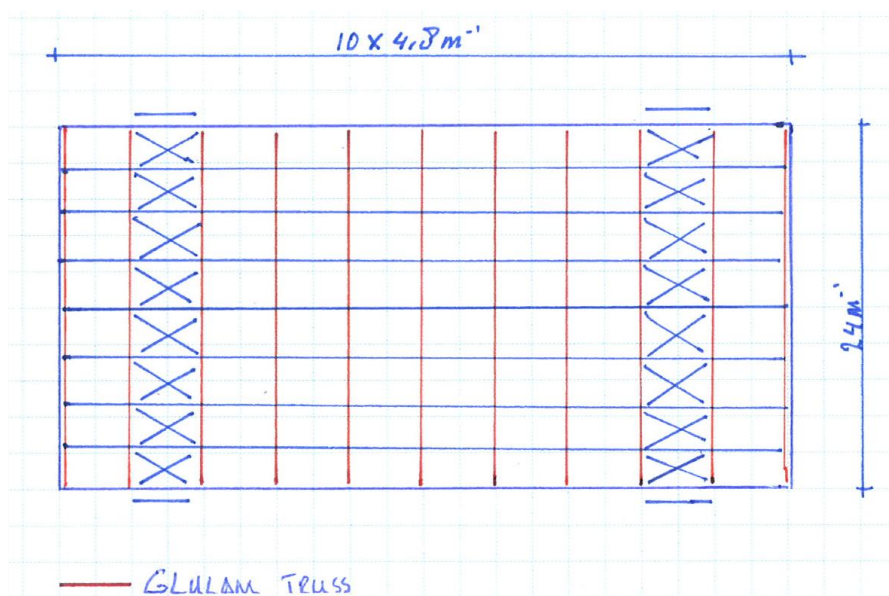


Figure 7.2: Dimensions of typical glulam frame building

The portal frames have been assumed to have a span of 24 m, and to be placed at a spacing of 4.8 m, whilst the section sizes have been dimensioned using the design guidance provided in Figure 7.3. The height to the apex has been taken as 6 m, with a height of the column (to the eave) of 4 m. The dimension h shown in Figure 7.3 has been calculated as 1 m with a thickness of the timber sections equal to 0.12 m. For this preliminary model, the steel lateral and roof bracing has been assumed to be the same as that used and described previously for the steel frame building (AGRI/INDU/COML-S-A/B), whilst only 5 of the frames shown in Figure 7.2 have been modelled (i.e. the same number of frames as the steel frame building).

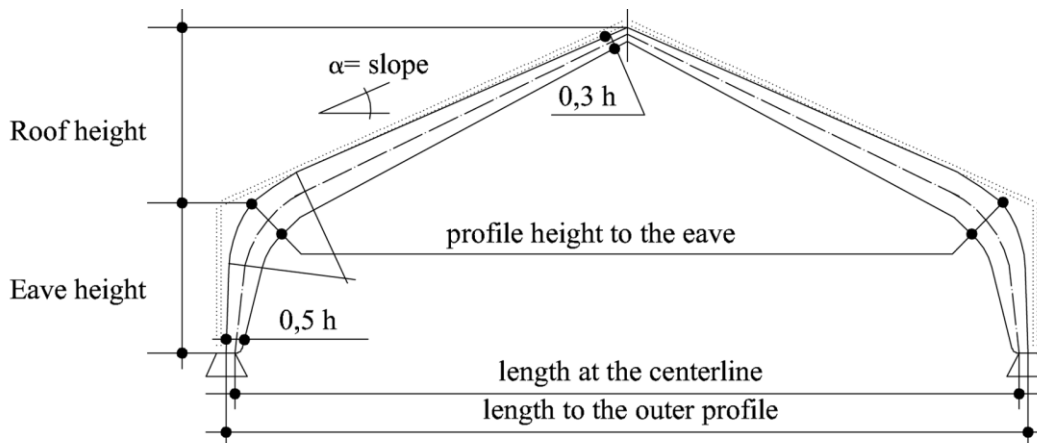


Figure 7.3: Dimensions of glulam frame sections

7.2 Modelling assumptions

The structural timber beam/column members, the steel lateral bracing (rectangular solid sections) and the roof bracing (L shaped solid sections) have all been modelled with 3D force-based inelastic fibre-elements (infrmFB) with 5 integration sections (each with 150 section fibres).

Materials

A bilinear stress-strain constitutive model has been used for both the timber and steel materials.

The average material properties for each constitutive model are listed below:

- Timber: $f_y = 30$ MPa; Young's Modulus = 12.6 GPa
- Steel: $f_y = 270$ MPa

Loads

The vertical loads assigned for the portal frame have been applied to each beam as permanent loads in terms of forces in the Z direction. Loads in addition to the self-weight for the roof are taken as 100% permanent load without considering the live load (given that it is inaccessible), based on the values given in Table 7.1.

Table 7.1: One storey glulam portal building – applied permanent loads (in addition to self-weight)

Load	Permanent Load [kN/m ²]	Live Load [kN/m ²]	Inter-column Length [m]	Total Distributed Load [kN/m]	
				Internal Frame	External Frame
Roof	0.5	0	4.8	2.4	1.2

Other modelling assumptions

In order to model the arch, the connections between the beams and columns of each portal frame have been fixed, whilst a semi-rigid connection has been modelled at the apex of the arch. Semi-rigid connections have also been added at the base of the section to model the steel connections connecting the timber posts to the concrete foundations. The properties of these semi-rigid connections have been based on the beam-column moment-rotation relationships reported previously for the steel frame (yield moment of 60 kNm, yield rotation of 0.01 rad, ultimate rotation of 0.1 rad).

Local buckling of the steel stability bracing and roof bracing has been modelled following the recommendations of Uriz et al. (2008) whereby each compression strut is modelled as two beam-column sections and an imperfection has been added midway by offsetting one of the nodes by 0.075% of the free brace length.

A screenshot of the glulam portal frame model with steel stability bracing is presented in the following figure.



Figure 7.4: AGRI/INDU/COML-W-B1 index building - Screenshot of the SeismoStruct model

7.3 Numerical analyses and results

Eigenvalue analysis

An eigenvalue analysis has been undertaken as an initial check of the model. The first mode period was found to be 0.48 s (with 95% modal mass) in the transverse (glulam portal) direction and 0.82 s (with 42% modal mass) in the longitudinal (steel braced) direction.

Pushover analyses

Given the simplicity of the structure, a conventional force-based pushover analysis with uniform lateral loads applied at the top of the columns has been undertaken in each direction. The results shown in Figure 7.5 show both the impact of buckling of the steel lateral bracing in the longitudinal direction, which reduces the base shear capacity of the structure, and the ultimate rotation capacity of the semi-rigid connections, which limits the ultimate displacement capacity. In the transverse direction, the base shear capacity is higher, whereas the ultimate displacement is limited by the ultimate rotation capacity of the semi-rigid connections at the base.

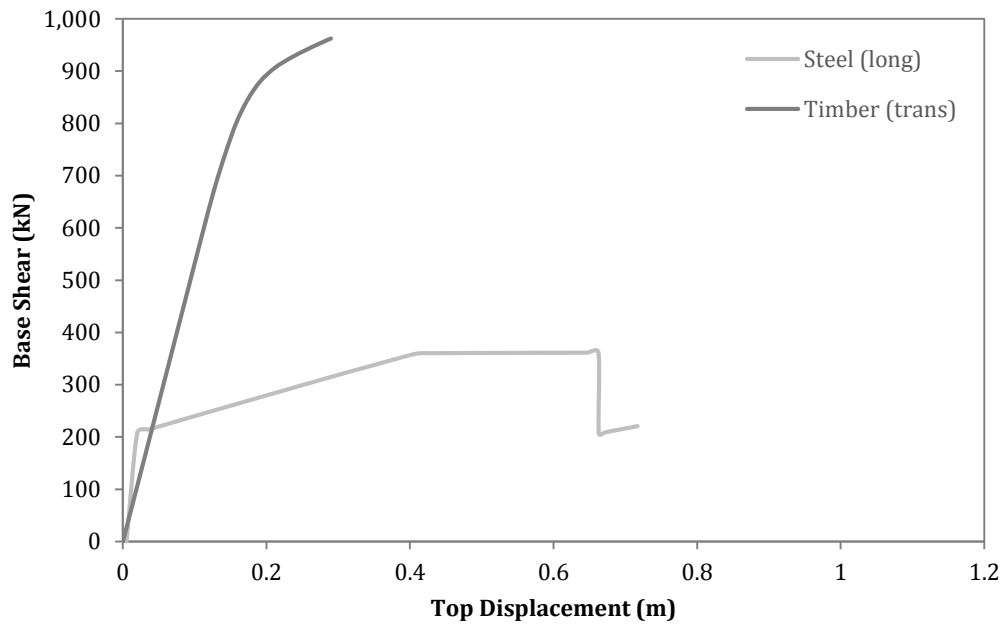


Figure 7.5: Pushover curves in the longitudinal and transverse directions

8 Glulam Portal Frame Buildings with URM Stability Walls (AGRI/INDU/COML-W-B2)

8.1 General description and structural configuration

There are two typologies of glulam portal frames within the Groningen exposure model, one with steel stability bracing (presented in Chapter 7) and the other with unreinforced masonry (URM) walls providing the lateral stability in the direction orthogonal to the portal frames (AGRI/INDU/COML-W-B2). The model described in Chapter 7 has been used here for AGRI/INDU/COML-W-B2, with the steel lateral bracing replaced with URM infill panels. The transverse direction is assumed to be the same as that presented previously in §7.3.

8.2 Modelling assumptions

The structural timber beam/column members and the roof bracing (L shaped solid sections) have been modelled with 3D force-based inelastic fibre-elements (infrmFB) with 5 integration sections (each with 150 section fibres).

The infill panels have been modelled using SeismoStruct's inelastic infill panel element (see Figure 8.1). They have been taken as 0.1 m thick, with a compression strut width calculated using the proposal of Liauw and Kwan (1984) and the contact length from Stafford Smith and Carter (1969), whilst all other parameters have been based on the lower bound default values suggested by the program.

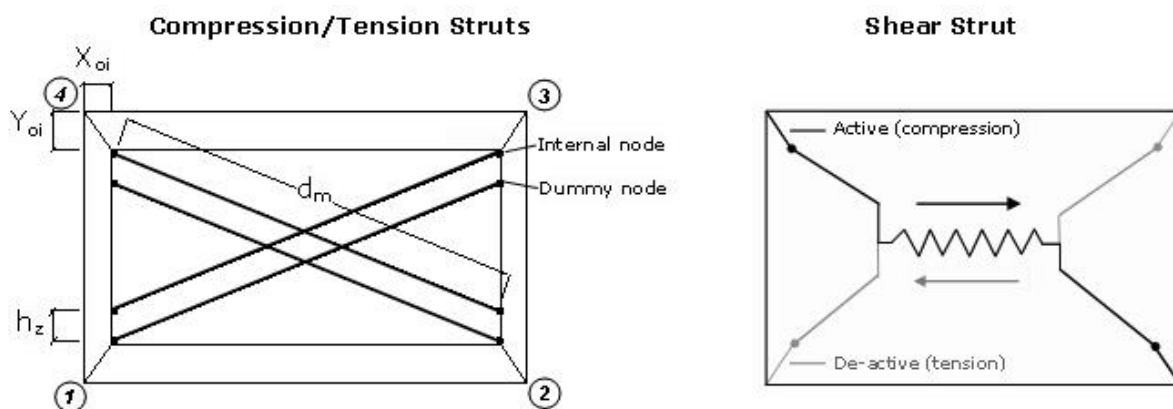


Figure 8.1: Inelastic infill panel model implemented in SeismoStruct

Materials

A bilinear stress-strain constitutive model has been used for both the timber and steel (roof bracing) materials, whilst the infill material properties have been provided as input to the infill panel element.

The average material properties for each constitutive model are listed below:

- Timber: $f_y = 30$ MPa; Young's Modulus = 12.6 GPa
- Steel: $f_y = 270$ MPa
- URM Infill: $f_c = 1$ MPa; Young's Modulus = $800 \times f_c$

Loads

The vertical loads assigned for the portal frame have been applied to each beam as permanent loads in terms of forces in the Z direction. Loads in addition to the self-weight for the roof are

taken as 100% permanent load without considering the live load (as the roof is inaccessible), based on the values given in Table 8.1.

Table 8.1: One storey glulam portal building - applied permanent loads (in addition to self-weight)

Load	Permanent Load [kN/m ²]	Live Load [kN/m ²]	Inter-column Length [m]	Total Distributed Load [kN/m]	
				Internal Frame	External Frame
Roof	0.5	0	4.8	2.4	1.2

A screenshot of the glulam portal frame model with URM stability walls is presented in the following figure.

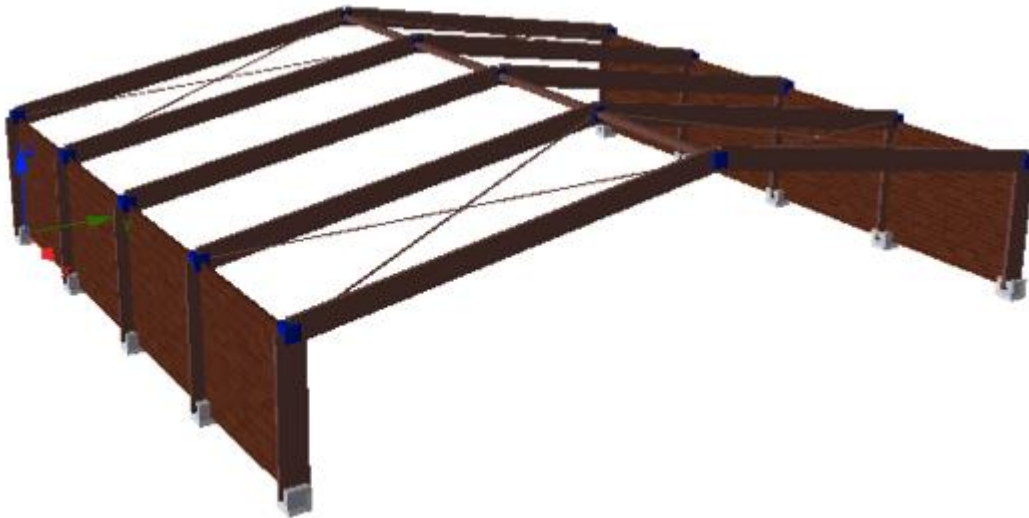


Figure 8.2: AGRI/INDU/COML-W-B2 index building - Screenshot of the SeismoStruct model

8.3 Numerical analyses and results

Eigenvalue analysis

An eigenvalue analysis has been undertaken as an initial check of the model. The first mode period was found to be 0.2 s (with 30% modal mass) in the longitudinal (URM infill wall) direction.

Pushover analyses

Given the simplicity of the structure, a conventional force-based pushover analysis with uniform lateral loads applied at the top of the columns has been undertaken in the longitudinal direction, whereas the pushover curve for the transverse direction has been carried out using the model presented in §7.3, without the infill panels.

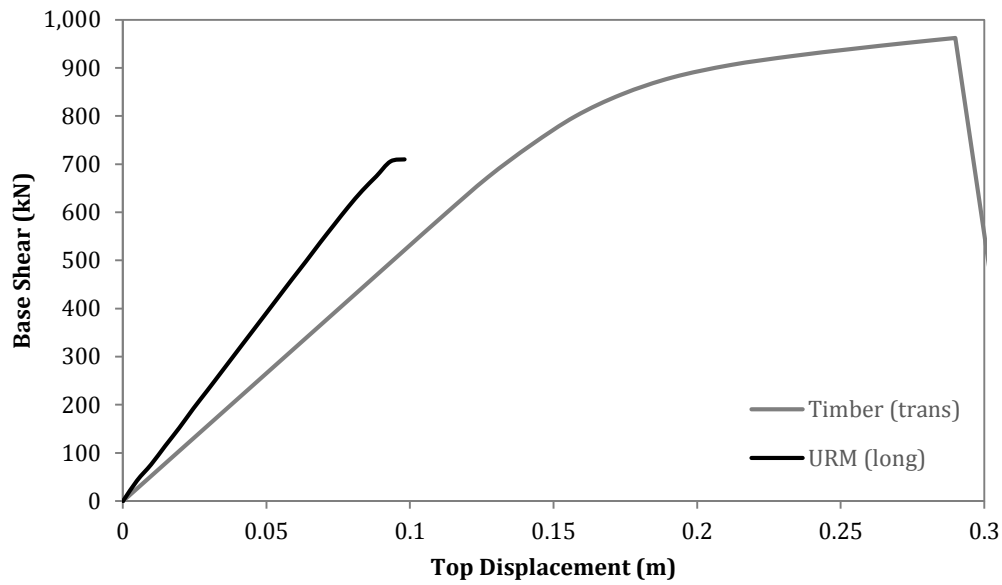


Figure 8.3: Pushover curves in the longitudinal and transverse directions

The results shown in Figure 8.3 show the influence of the stiff URM infill panels in the longitudinal direction, which lead to a high base shear capacity of the structure (compared to that obtained for the steel stability braced version), but limited ultimate displacement capacity when the infill panels exceed their lateral drift capacity. In the transverse direction, the base shear capacity is still higher, whereas the ultimate displacement is limited by the ultimate rotation capacity of the semi-rigid connections at the base.

9 Precast RC Portal Frame Industrial Buildings (AGRI/INDU/COML-RC-B1)

9.1 General description and structural configuration

Precast reinforced concrete (RC) single-storey portal frames are commonly used for industrial warehouses in Europe. For this typology it has not yet been possible to obtain a real index building from Groningen. However, given that these structures tend to follow similar construction practice across Europe, structural models that have been developed for Italian precast industrial buildings have been adopted here (the design assumptions behind these models will need to be checked in the next stages of the structural modelling work).

Figure 9.1 shows the most common structural system for these buildings, wherein a number of portal frames are placed in parallel whilst the roof (often with a concrete topping) provides the lateral resistance in the orthogonal direction. The beams shown in Figure 9.1b can either simply resting on the corbels of the column, or can be connected with steel dowels. Local engineers have confirmed that the use of steel dowels to connect the beam and column is common practice in the Netherlands, and so the connections shown in Figure 9.2 have been used in the numerical models.



Figure 9.1: Typical precast reinforced concrete portal frame

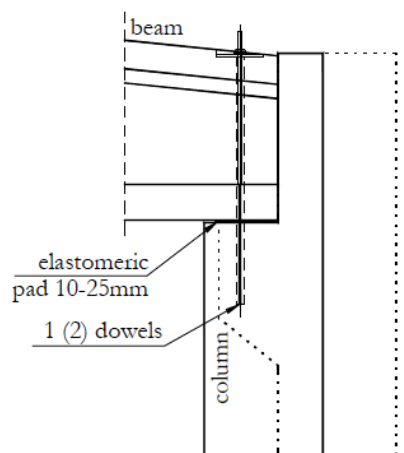


Figure 9.2: Beam-column steel dowel connection

The portal frame span and spacing of portal frames have been taken from a database of 650 Italian warehouses (Casotto et al., 2015), whilst the section sizes and reinforcement have been designed according to the 1996 Italian design code (DM, 1996).

9.2 Modelling assumptions

The structural column members have all been modelled with 3D force-based inelastic fibre-elements (infrmFB) with 4 integration sections (each with 220 section fibres). The beams have been modelled as elastic elements, and the roof has been modelled as a rigid diaphragm.

Materials

The *Mander et al. (1988) nonlinear* model has been used for the concrete and a *bilinear stress-strain constitutive* model has been used for the steel.

The average material properties for each constitutive model are listed below:

- Concrete C35/45: $f_c = 43$ MPa, $f_t = 0$ MPa
- Steel FeB500: $f_y = 575$ MPa

Loads

The vertical loads assigned for the portal frame have been applied to each column as lumped masses, using the values provided in the table below. Loads are taken as 100% permanent load plus 30% live load.

Table 9.1: Precast RC portal frame - assumed loads

Type of load	Roof
Permanent Load (roof weight and concrete topping)	3.7 [kN/m ²]
Portal beam self-weight	2.4 [kN/m]
Inter-column beam self-weight	3.8 – 8.55 [kN/m]
Live Load	0.5 [kN/m ²]

Other modelling assumptions

The beam-column connections have been modelled using multi-linear springs in SeismoStruct, allowing for the strength of the dowel connection followed by sliding until unseating of the beam to be modelled, which can occur in both directions.

A screenshot of the precast RC portal frame model is presented in the following figure.

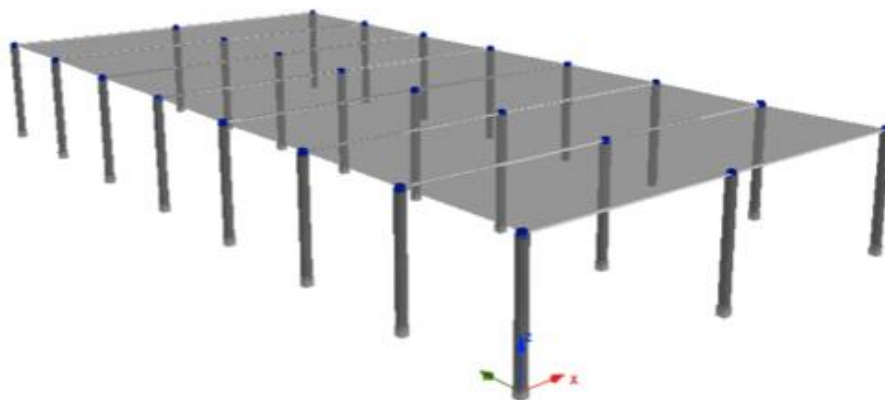


Figure 9.3: AGRI/INDU/COML-RC-B1 index building - Screenshot of the SeismoStruct model

9.3 Numerical analyses and results

Eigenvalue analysis

An eigenvalue analysis has been undertaken as an initial check of the model. The first mode period was found to be 1.1 s (with 100% modal mass) in both directions.

Pushover analyses and parametric studies

Given the simplicity of the structure, a conventional force-based pushover analysis with uniform lateral loads applied at the top of the columns has been undertaken in the both directions. Given the availability of the statistics of 650 industrial warehouses, it has been possible to vary the geometrical and material properties (using Monte Carlo simulation) to produce 100 individual models. The column reinforcement was calculated each time based on the specifications of the 1996 Italian design code and the applied masses were modified based on the geometry. The statistics used in the Monte Carlo simulation are summarised in Table 9.2.

Table 9.2: Random variables assumed in the parametric study

Random variable	Mean	CoV	Distribution	Reference
Beam length	14.9 m	30 %	Lognormal	Casotto et al. (2015)
Portal frame spacing	9 m	45%	Lognormal	Casotto et al. (2015)
Column height	6.5 m	25 %	Lognormal	Casotto et al. (2015)
C35/45 concrete compressive strength	43 MPa	15%	Normal	Judgment
FeB500 steel yield strength	575 MPa	8.5%	Normal	NEN 6008

The pushover curves for these 100 randomly generated buildings in both longitudinal and transverse directions are shown in the figures below. The ultimate displacement has been taken as either the point at which the connection fails and the beam unseats from the column, or the ultimate chord rotation capacity of the columns is reached (according to the formulae provided in Eurocode 8, Part 3 – CEN, 2005 – with all partial safety factors set to 1), whichever was found to be lower.

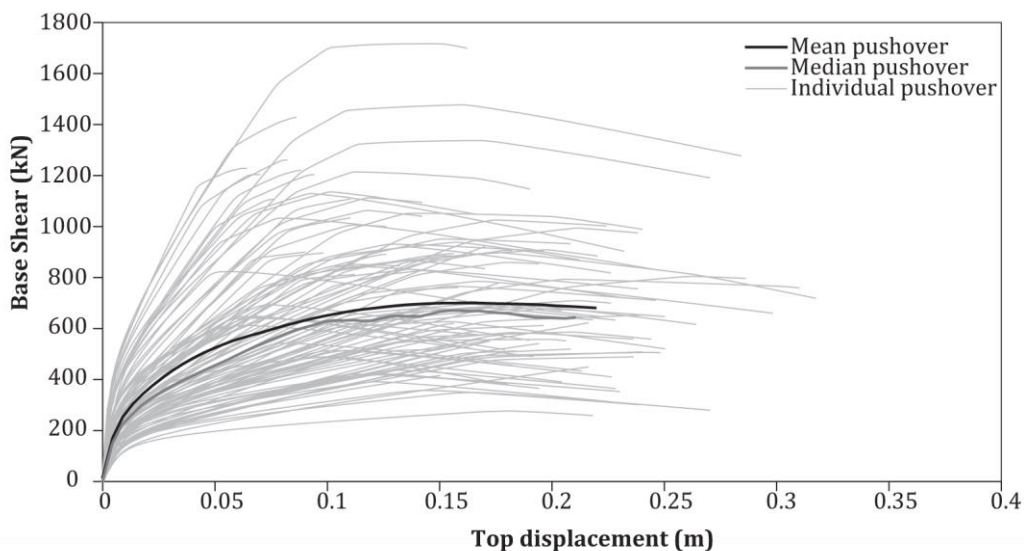


Figure 9.4: Pushover curves in the transverse direction

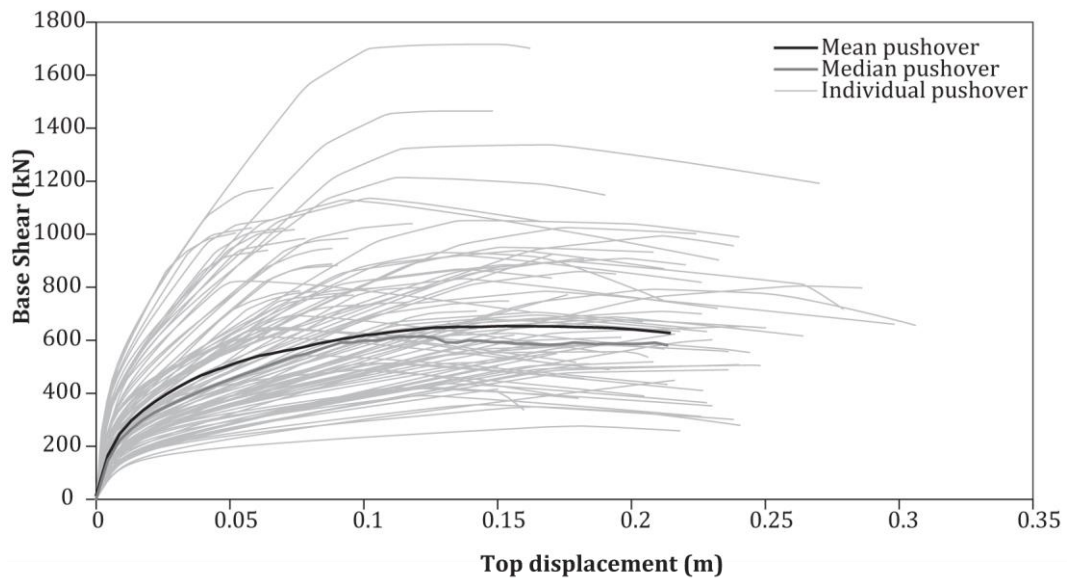


Figure 9.5: Pushover curves in the longitudinal direction

10 Cast-in-Place RC Portal Frame Industrial Buildings (AGRI/INDU/COML-RC-A)

10.1 General description and structural configuration

Reinforced concrete portal frames used for industrial warehouses in the Groningen region are also frequently cast-in-place (Figure 10.1). In this case the connections can be modelled as monolithic, and the beams are allowed to transmit moments to the columns. The same assumptions as those presented in the previous chapter, in terms of geometrical and material properties, have been assumed for this typology.



Figure 10.1: Cast-in-place industrial building from the Groningen region

10.2 Modelling assumptions

The structural column members have all been modelled with 3D force-based inelastic fibre-elements (infrmFB) with 4 integration sections (each with 220 section fibres). The beams have been modelled as elastic elements, the roof has been modelled as a rigid diaphragm, and the beam-column connections have been modelled as fixed.

Materials

The *Mander et al. (1988) nonlinear* model has been used for the concrete and a *bilinear stress-strain constitutive* model has been used for the steel.

The average material properties for each constitutive model are listed below:

- Concrete C35/45: $f_c = 43$ MPa, $f_t = 0$ MPa
- Steel FeB500: $f_y = 575$ MPa

Loads

The vertical loads assigned for the portal frame have been applied to each column as lumped masses, using the values provided in the table below. Loads are taken as 100% permanent load plus 30% live load.

Table 10.1: Cast-in-place RC portal frame – assumed loads

Type of load	Roof
Permanent Load (roof weight and concrete topping)	3.7 [kN/m ²]
Portal beam self-weight	2.4 [kN/m]
Inter-column beam self-weight	3.8 – 8.55 [kN/m]
Live Load	0.5 [kN/m ²]

A screenshot of the cast-in-place RC portal frame model is presented in the following figure.

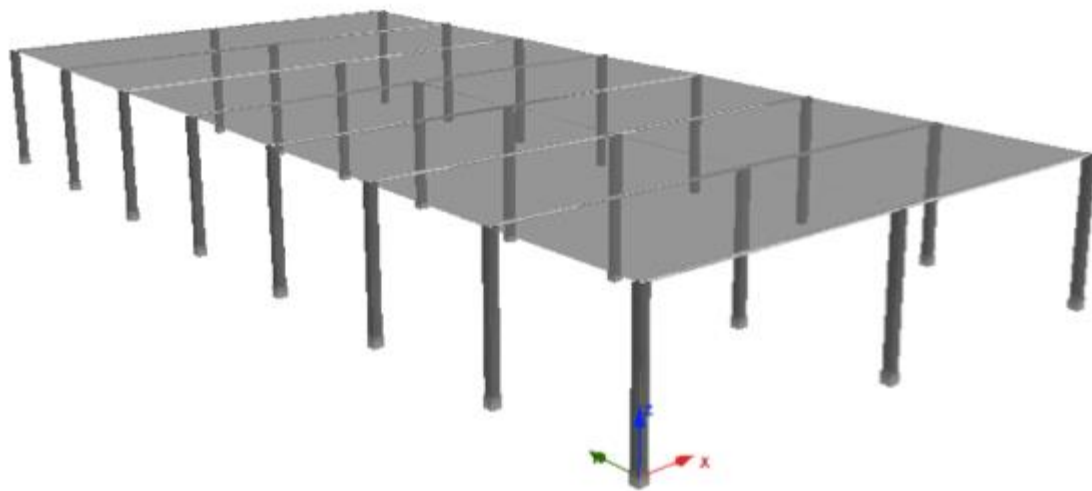


Figure 10.2: AGRI/INDU/COML-RC-A index building - Screenshot of the SeismoStruct model

10.3 Numerical analyses and results

Eigenvalue analysis

An eigenvalue analysis has been undertaken as an initial check of the model. The first mode period was found to be 0.42 s in the transverse direction and 0.81 s in the longitudinal direction.

Pushover analyses and parametric studies

Given the simplicity of the structure, a conventional force-based pushover analysis with uniform lateral loads applied at the top of the columns has been undertaken in the both directions. The same statistics presented in §9.3 have been used to generate 100 individual models, and the pushover curves in both longitudinal and transverse directions are presented in the figures below. The ultimate displacement has been taken as the point at which the ultimate chord rotation capacity of the columns is reached (according to the formulae provided in Eurocode 8, Part 3 – CEN, 2005 – with all partial safety factors set to 1).

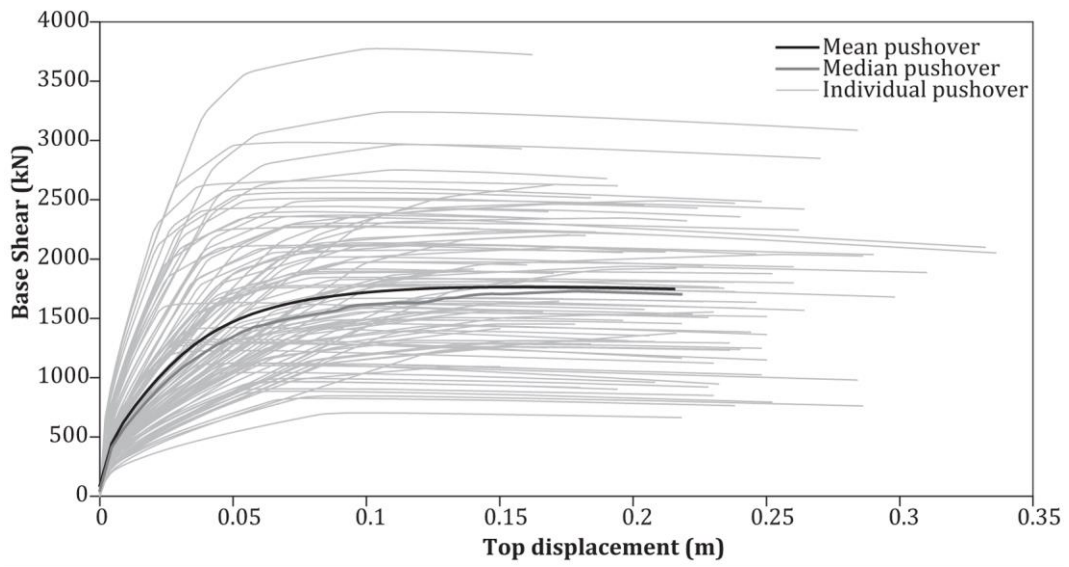


Figure 10.3: Pushover curves in the transverse direction

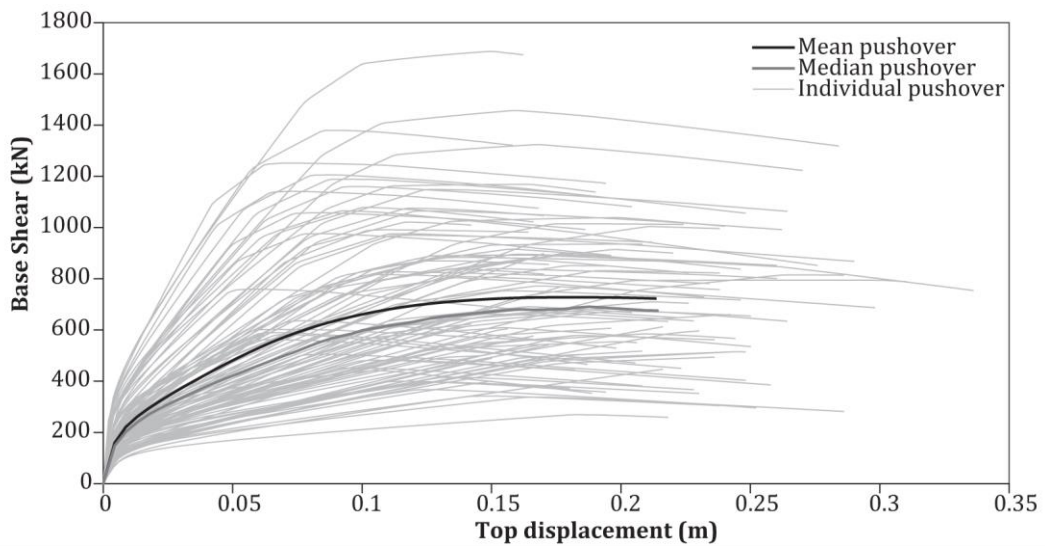


Figure 10.4: Pushover curves in the longitudinal direction

11 Steel Moment Frame Commercial Buildings (COMO-S-B-L4S)

11.1 General description and structural configuration

The building representing the COMO-S-B-L4S typology is a two-storey steel moment resisting frame building (see Figure 11.1 to Figure 11.5). Along the longitudinal direction there are ten frames: the external frames are comprised of three bays, each 4 m long (Figure 11.4a) and the internal frames are comprised of one bay, 12 m long (except for the frame 2 and 4 where there is one column in the middle bay at the first storey, as shown in Figure 11.4b). Along the transverse direction there are two frames, with one bay equal to 4 m long (Figure 11.5).

The structure plan dimensions are 36 m x 12 m and the total height of the structure is 6.6 m, with a higher height of the upper storey compared to the lower storey. The frames are constructed with HE and IPE columns, whilst composite HE beams have been employed for the slab.



Figure 11.1: Steel moment frame commercial building – external views (Google street view)

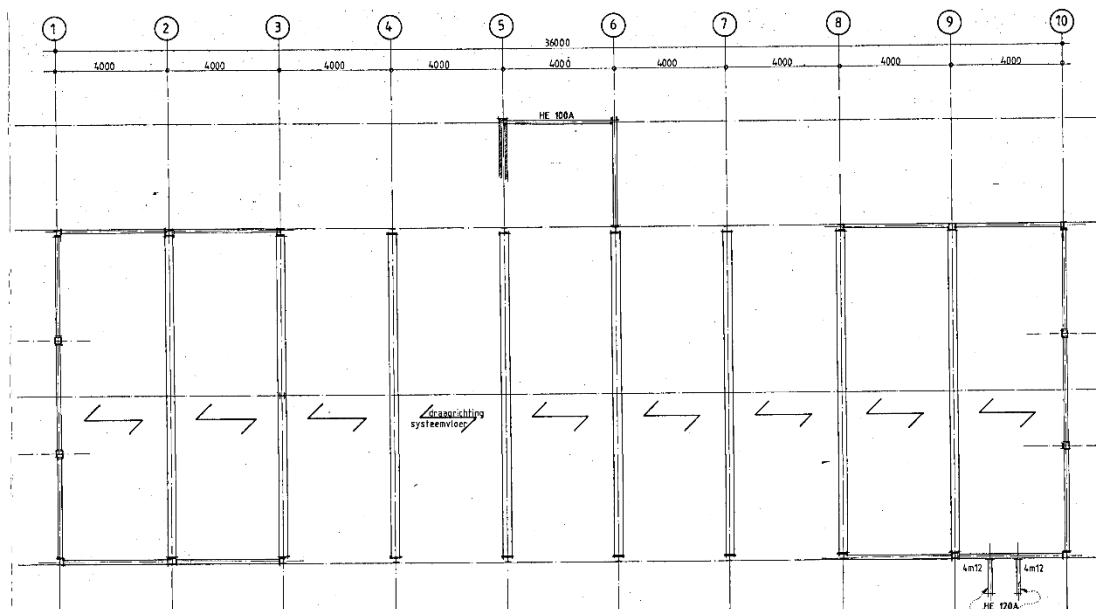


Figure 11.2: Steel moment frame commercial building – Plan view (ground floor)

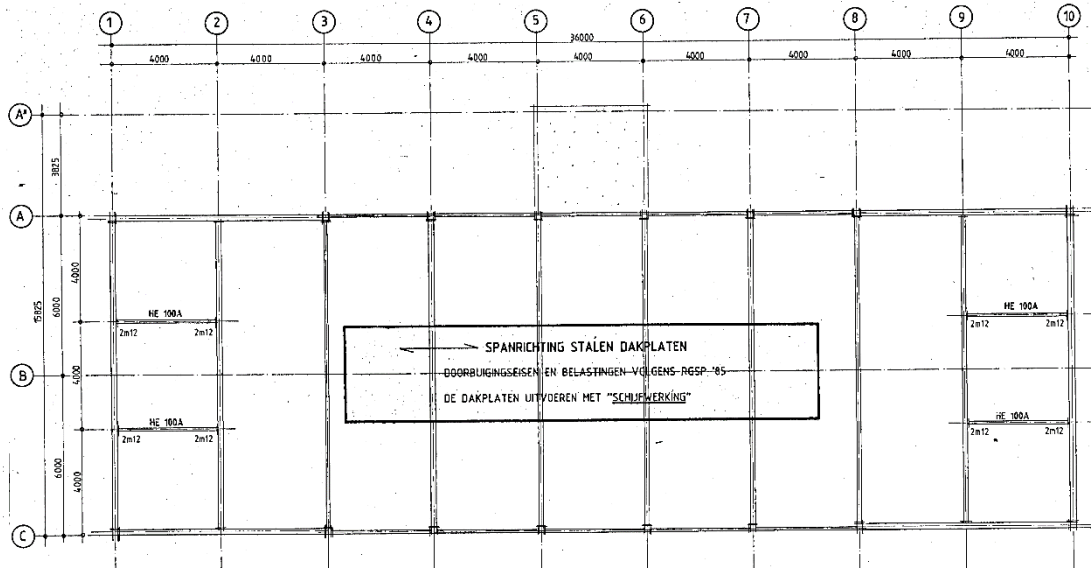


Figure 11.3: Steel moment frame commercial building – Plan view (roof)

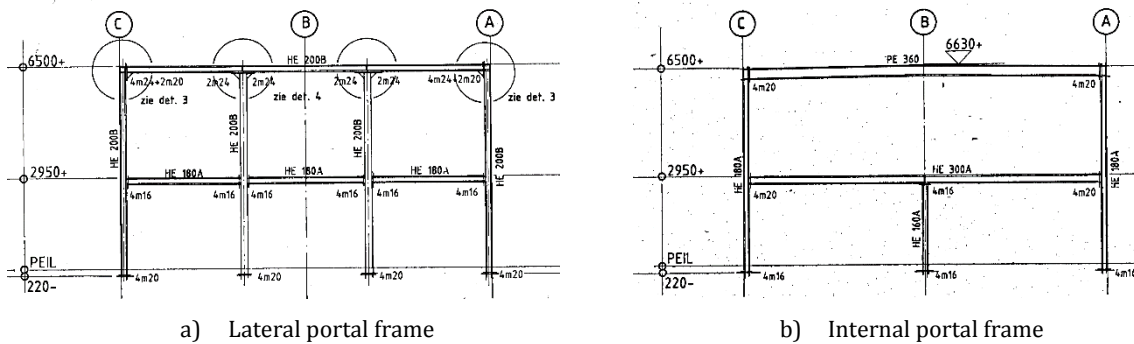


Figure 11.4: Steel moment frame commercial building – Portal frames (front view)

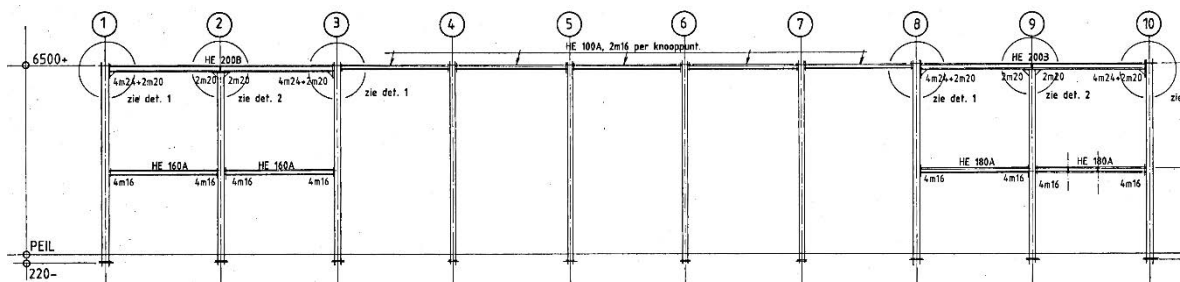


Figure 11.5: Steel moment frame commercial building – Lateral view

11.2 Modelling assumptions

The structure has been modelled using steel beam and column elements. Each structural member has been modelled through a 3D force-based inelastic frame element with 5 integration sections; the number of fibres used in the section equilibrium computations is set to 150.

Materials

A *bilinear* model has been employed for defining the steel material, with the properties listed in Table 11.1.

Table 11.1: Calibrating parameters for steel material

PARAMETERS	Steel
E (GPa)	200
f_y (MPa)	270
μ	0.1
γ (kN/m ³)	78

The *Mander et al. concrete* model has been employed for defining the concrete material properties used in the composite HE-sections for modelling the slabs, with the properties listed in Table 11.2.

Table 11.2: Calibrating parameters for concrete material

PARAMETERS	Concrete
f_c (MPa)	33
f_t (MPa)	3.3
E_c (GPa)	25.7
ϵ_c (m/m)	0.002
γ (kN/m ³)	24

Loads

The vertical loads assigned for the portal frame have been applied to each beam as permanent loads in terms of forces in the Z direction. Loads in addition to the self-weight for a typical level and for the roof are taken as 100% permanent load plus 30% live load, based on the values given in Table 11.3.

Table 11.3: Two storey steel building – applied permanent loads (in addition to self-weight)

Load	Permanent Load (G) [kN/m ²]	Live Load (Q) [kN/m ²]	G+0.3Q [kN/m ²]	Inter-column Length [m]	Total Distributed Load [kN/m]	
					Internal Frame	External Frame
1 st Storey	5.0	5.0	6.5	4	26	13
Roof	0.5	0	0.5	4	2	1

The slabs of the first storey have been modelled by introducing a rigid diaphragm. The building is assumed to be fixed at the base. A screenshot of the structural model is presented in the following figure.



Figure 11.6: Screenshot of the SeismoStruct model of the COMO-S-B-L4S index building

Performance criteria have been set in order to estimate the ultimate displacement capacity, setting the ultimate rotation capacity of each element to 8 times yielding rotation capacity (following the recommendations of Eurocode 8 Part 3 – CEN, 2005). Upon attainment of the rotation capacity of a given element, a residual strength of 80% is subsequently assigned.

11.3 Numerical analyses and results

Eigenvalue analysis

An eigenvalue analysis has been undertaken as an initial check of the model. The first mode period was found to be 0.89 s (with 81% modal mass) in the longitudinal direction and 0.40 s (with 96% modal mass).

Pushover analyses

Given the simplicity of the structure, conventional force-based pushover analysis has been undertaken in each direction. A comparison of the pushover curves in the longitudinal direction, with and without considering strength degradation due to ultimate rotational capacity, is shown in Figure 11.7; the same base shear is obtained, but the ultimate displacement is smaller when the aforementioned performance criterion is considered. In this case, the ultimate displacement is reduced by the attainment of the ultimate rotational capacity at around 0.4m.

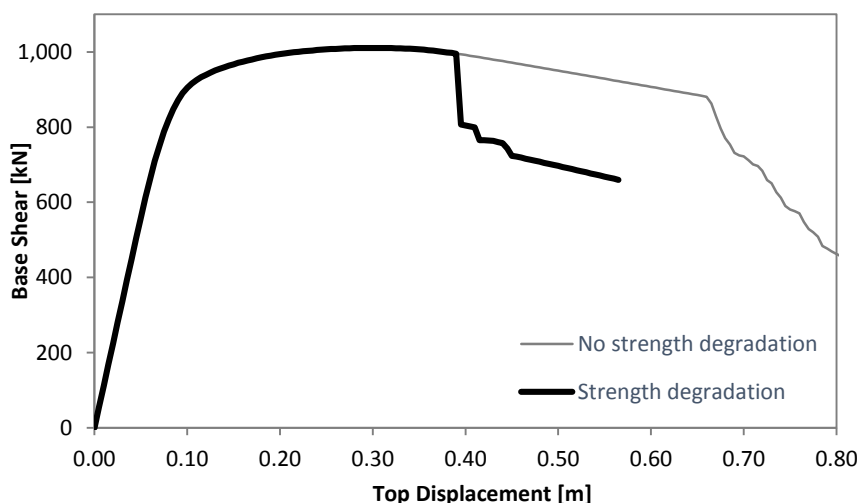


Figure 11.7: Pushover curve in the longitudinal direction considering performance criteria

The deformed shape at ultimate displacement is shown in Figure 11.8, which shows that collapse occurs due to the attainment of the rotational capacity of the columns.

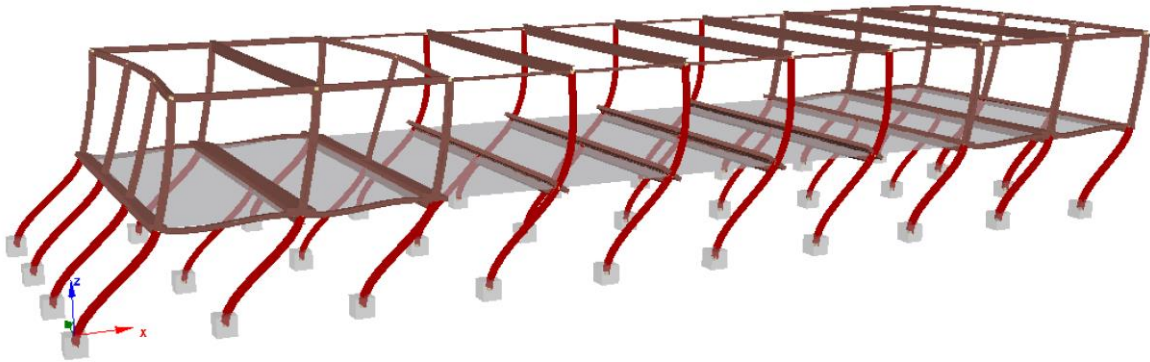


Figure 11.8: Deformed shape (long. direction) at ultimate displacement, showing the elements (in red) that reach their rotational capacity

Regarding the transverse direction, a comparison of the pushover curves, with and without considering aforementioned performance criterion, is shown in Figure 11.9; the same base shear is obtained, but the ultimate displacement is smaller when the performance criterion is considered. In this case, the ultimate displacement is reduced by the attainment of the rotational capacity, at around 0.3m.

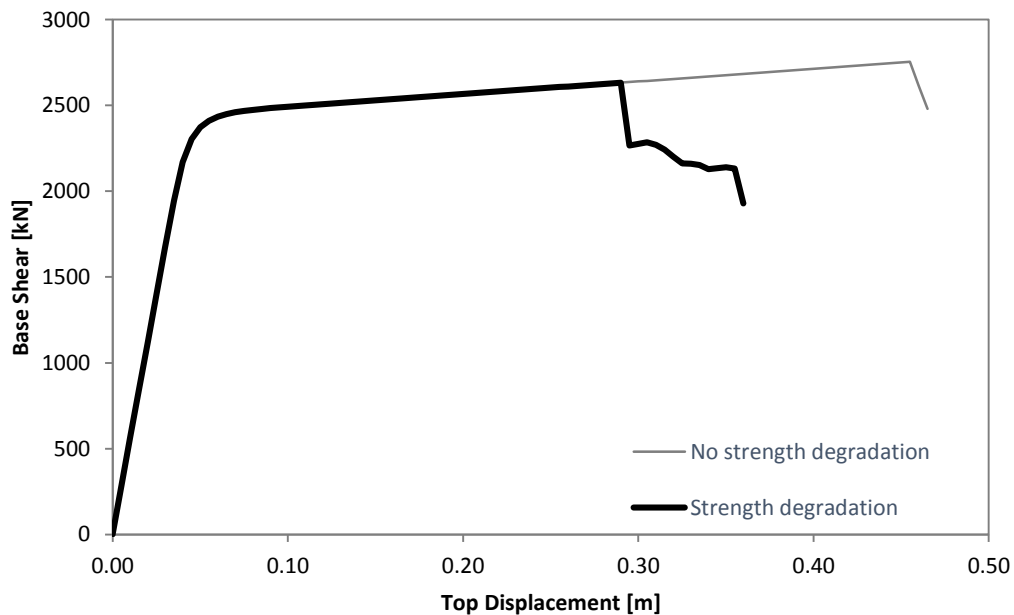


Figure 11.9: Pushover curve in the transverse direction considering performance criteria

The deformed shape at ultimate displacement is shown in Figure 11.10, which shows that collapse occurs due to the attainment of the rotational capacity of the columns.



Figure 11.10: Deformed shape (trans. direction) at ultimate displacement, showing the elements (in red) that reach their rotational capacity

Conclusions

This report has described the final results of the non-URM building modelling activities that have been directly implemented in the v2 fragility functions (Crowley et al., 2015).

With respect to the previous version of this report, in addition to only reporting those results used in the v2 fragility function development, the following updates and improvements have also been made:

- New software (Extreme Loading for Structures) has been used for the reinforced concrete tunnel/wall buildings, given the low displacement capacity that was found for these buildings in the previous version of this report. These new analyses confirmed that the shear capacity of these structures was previously being underestimated.
- A model for precast reinforced concrete terraced buildings has been calibrated using the results from the laboratory tests on precast panel connections (EUCENTRE, 2015).

Future developments in non-URM modelling are expected to focus on:

- validating the assumptions made in the models presented herein;
- running incremental nonlinear dynamic analysis to calibrate the hysteresis models used in SDOF systems, understand the potential variation in collapse mechanisms, and better calibrate the estimation of collapse debris and volume loss needed for the fatality models (see Crowley et al., 2015);
- modelling foundation flexibility/radiation and soil hysteresis damping for both shallow and piled foundations, for validation of the SDOF systems with soil-structure interaction used in the fragility function development (see Mosayk, 2015).

References

GENERAL

- Antoniou S, Pinho R. [2004] "Development and verification of a displacement-based adaptive pushover procedure," *Journal of Earthquake Engineering*, 8(5), 643–61.
- Casotto C., Silva V., Crowley H., Nascimbene R., Pinho R. [2015] "Seismic fragility of Italian RC precast industrial structures," *Engineering Structures*, DOI: 10.1016/j.engstruct.2015.02.034
- Crowley H., Pinho R., Polidoro B. and Stafford P. [2015] "Development of v2 Fragility and Consequence Functions for the Groningen Field," Internal Report submitted to NAM.
- EUCENTRE [2015] "Numerical and experimental evaluation of the seismic response of precast wall connections", Internal report submitted to NAM.
- Liauw T.C., Kwan K.H. [1984] "Nonlinear Behaviour of Non-Integral Infilled Frames," *Computers and Structures*, 18(3), 551-560.
- Mander, J.B., Priestley, M.J.N., Park, R. [1988] "Theoretical Stress-Strain Model for Confined Concrete," *Journal of Structural Engineering*, 114, 1804–1826.
- Meguro, K. and Tagel-Din, H. [2000] "Applied element method for structural analysis: Theory and application for linear materials". *Structural engineering/earthquake engineering*. (Japan: Japan Society of Civil Engineers (JSCE)) 17 (1): 21–35.
- Menegotto, M., Pinto, P.E. [1973] "Method of analysis for cyclically loaded RC plane frames including changes in geometry and non-elastic behaviour of elements under combined normal force and bending.," in: *IABSE Symposium on Resistance and Ultimate Deformability of Structures Acted on by Well Defined Repeated Loads - Final Report*.
- Mosayk (2015) "Report on soil-structure interaction (SSI) impedance functions for SDOF systems" Deliverable D3 report submitted to NAM.
- Stafford-Smith B., Carter C. [1969] "A Method for the Analysis of Infilled Frames," *Proceedings of the Institution of Civil Engineers*, London, England, 44, 31-38.
- Tagel-Din, H. and Meguro, K. [2000a] "Nonlinear simulation of RC structures using Applied Element Method," *Structural engineering/earthquake engineering*. (Japan: Japan Society of Civil Engineers (JSCE)) 17 (2): 137-148.
- Tagel-Din, H. and Meguro, K. [2000b] "Applied Element Method for dynamic large deformation analysis of structures," *Structural engineering/earthquake engineering*. (Japan: Japan Society of Civil Engineers (JSCE)) 17 (2): 215-224.
- Uriz P., Filipou F.C., Mahin S.A. [2008] "*Model for Cyclic Inelastic Buckling of Steel Braces*", *ASCE Journal of Structural Engineering*, 134(4).

CODES

- Decreto Ministeriale 16 gennaio 1996 [1996] "Norme tecniche per le costruzioni in zone sismiche," (in Italian).
- CEN [2005] Eurocode 8: Design of structures for earthquake resistance - Part 3: Assessment and retrofitting of buildings, EN 1998-3:2005, Comité Européen de Normalisation, Brussels

NEN 6008 [1991]. Steel for reinforced concrete. Nederlands Normalisatie Instituut. December 1991, pp. 26 (in Dutch).

Tempcoreit [2003] "Reinforced Concrete Design Tables", Italian Association of Tempcore Steel, Brescia, Italy. [in Italian]

TOOLS

Applied Science International [2010], Extreme Loading® for Structures (Version 3.1 B64).

Seismosoft [2015]. "*SeismoStruct v7 – A computer program for static and dynamic nonlinear analysis of framed structures*", available from <http://www.seismosoft.com>

MIDAS [2010]. "*Nonlinear and Detail FE Analysis System for Civil Structures – FEA Analysis and Algorithm Manual*", www.cspfea.net